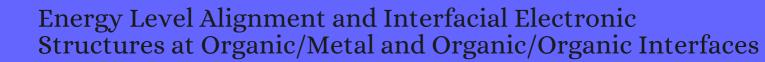
CITATION REPORT List of articles citing



DOI: 10.1002/(sici)1521-4095(199906)11:83.0.co;2-q Advanced Materials, 1999, 11, 605-625.

Source: https://exaly.com/paper-pdf/30619946/citation-report.pdf

Version: 2024-04-28

This report has been generated based on the citations recorded by exaly.com for the above article. For the latest version of this publication list, visit the link given above.

The third column is the impact factor (IF) of the journal, and the fourth column is the number of citations of the article.

#	Paper	IF	Citations
2313	Tuning the Crystal Packing and Semiconductor Electronic Properties of 7,7-Diazaisoindigo by Side-Chain Length and Halogenation.		
2312	MottSchottky Effect Leads to Alkyne Semihydrogenation over Pd-Nanocube@N-Doped Carbon.		
2311	Image force effects at contacts in organic light-emitting diodes. 1999 , 75, 3880-3882		28
2310	Analysis of scanning probe used for simultaneous measurement of tunneling current and surface potential. 1999 , 86, 7087-7093		21
2309	First synthesis and electronic properties of ring-alkynylated phenothiazines. 1999 , 40, 6563-6566		38
2308	Polymer band alignment at the interface with indium tin oxide: consequences for light emitting devices. 1999 , 310, 391-396		116
2307	Angle-resolved ultraviolet photoelectron spectroscopy and theoretical simulation of a well-ordered ultrathin film of tetratetracontane (nt 44H90) on Cu(100): Molecular orientation and intramolecular energy-band dispersion. 1999, 60, 9046-9060		52
2306	Electronic Structure of Organic/Metal Interfaces Studied by UPS and Kelvin Probe. 1999 , 582, 83		
2305	A New Alternative for the Low-Workfunction Electrode in Organic Devices. 1999 , 598, 23		1
2304	Photoemission Study of Metal-Deposited p-Sexiphenyl Film. 1999 , 598, 315		
2303	Electronic structure of hybrid interfaces of poly(9,9-dioctylfluorene). 2000, 321, 379-384		34
2302	Energy level alignment and band bending at model interfaces of organic electroluminescent devices. 2000 , 87-89, 61-65		53
2301	Organic electroluminescent devices using alkaline-earth fluorides as an electron injection layer. 2000 , 87-89, 1177-1179		30
2300	A low reflectivity multilayer cathode for organic light-emitting diodes. 2000 , 379, 195-198		20
2299	Interfacial charges and electric field distribution in organic hetero-layer light-emitting devices. 2000 , 1, 41-47		99
2298	Vacant electron state manifestations in the electron-beam-induced current spectra of macromolecular films. 2000 , 26, 1110-1113		1
2297	Introduction to the physics of organic electroluminescence. 2000 , 1, 381-402		2

(2000-2000)

2296	Blue light emitting polymers. 2000, 25, 1089-1139	388
2295	Space Charge Distribution and CapacitanceWoltage Characteristics of Metal/Polyimide Langmuir-Blodgett Film/Metal Structure. 2000 , 39, 1840-1844	3
2294	Ultraviolet Photoelectron Spectroscopy and Surface Potential of Econjugated Langmuir-Blodgett Films on Gold Metal Electrode. 2000 , 39, 5146-5150	14
2293	Efficiency peaks in the transient electroluminescence of multilayer organic light-emitting devices. 2000 , 76, 2170-2172	10
2292	Improved band alignment for hole injection by an interfacial layer in organic light emitting devices. 2000 , 77, 1093-1095	37
2291	Energy level alignment at the conjugated phenylenevinylene oligomer/metal interface. 2000 , 76, 2253-2255	37
2290	Energy level alignment in organic-based three-layer structures studied by photoelectron spectroscopy. 2000 , 88, 7187-7191	25
2289	Band alignment at the organic-inorganic interface. 2000 , 76, 927-929	42
2288	Influence of oxygen on band alignment at the organic/aluminum interface. 2000, 77, 1212-1214	24
2287	High resolution x-ray photoemission study of plasma oxidation of indium E inBxide thin film surfaces. 2000 , 88, 5180-5187	127
2286	LithiumQuinolate Complexes as Emitter and Interface Materials in Organic Light-Emitting Diodes. 2000 , 12, 3012-3019	111
2285	Determination of interface dipole and band bending at the Ag/tris (8-hydroxyquinolinato) gallium organic Schottky contact by ultraviolet photoemission spectroscopy. 2000 , 450, 142-152	73
2284	Investigation of band bending and charging phenomena in frontier orbital alignment measurements of para-quaterphenyl thin films grown on highly oriented pyrolytic graphite and SnS2. 2000 , 459, 349-364	34
2283	Surface Characterization and Modification of Indium Tin Oxide in Ultrahigh Vacuum. 2000 , 122, 1808-1809	114
2282	Importance of indium tin oxide surface acido basicity for charge injection into organic materials based light emitting diodes. 2000 , 87, 7973-7980	117
2281	Transient analysis of organic electrophosphorescence: I. Transient analysis of triplet energy transfer. 2000 , 62, 10958-10966	441
2280	Blue Light-Emitting Diodes Based on Dipyrazolopyridine Derivatives. 2000 , 12, 2788-2793	59
2279	Synthesis and Electronic Structure Investigations of #Bis(arylthio)oligothiophenes: Toward Understanding Wire-Linker Interactions in Molecular-Scale Electronic Materials. 2000 , 122, 6746-6753	88

2278	Electronic Structure at Organic/Metal Interfaces: Naphthalene/Cu(111). 2000, 104, 10332-10338	47
2277	Electroluminescence of Multicomponent Conjugated Polymers. 1. Roles of Polymer/Polymer Interfaces in Emission Enhancement and Voltage-Tunable Multicolor Emission in Semiconducting Polymer/Polymer Heterojunctions. 2000 , 33, 2069-2082	267
2276	Fabrication and Transport Properties of Single-Molecule-Thick Electrochemical Junctions. 2000 , 122, 5831-5840	152
2275	Organic semiconductors: fundamentals and applications. 2000 , 795-808	6
2274	Electronic Energy Levels in Individual Molecules, Thin Films, and Organic Heterojunctions of Substituted Phthalocyanines. 2001 , 105, 4791-4800	108
2273	Fine tuning work function of indium tin oxide by surface molecular design: Enhanced hole injection in organic electroluminescent devices. 2001 , 79, 272-274	182
2272	Lithium doping of semiconducting organic charge transport materials. 2001 , 89, 4986-4992	295
2271	Determination of energy barriers in organic light-emitting diodes by internal photoemission. 2001 , 89, 466-470	15
2270	Electronic Properties of Molecular Organic Semiconductor Thin Films. 2001 , 211-338	5
2269	Simulation of charge injection enhancements in organic light-emitting diodes. 2001 , 79, 4438-4440	28
2268	Mobility-dependent charge injection into an organic semiconductor. 2001 , 86, 3867-70	146
2267	A study of the conjugated Ooct-OPV5 oligomer/gold interface using photoelectron spectroscopy. 2001 , 482-485, 1186-1191	19
2266	Interface-limited injection in amorphous organic semiconductors. 2001 , 64,	334
2265	Polymers for opto-electronic applications: structure and morphology of thin films and their interfaces. 2001 , 122, 83-86	10
2264	Numerical model for injection and transport in multilayers OLEDs. 2001 , 122, 141-144	14
2263	Transient and steady-state behavior of space charges in multilayer organic light-emitting diodes. 2001 , 89, 4575-4586	226
2262	Ultraviolet photoelectron spectroscopy of thin films of new materials for multilayer organic light emitting diodes. 2001 , 482-485, 1205-1209	4
2261	Energy level alignment driven by electron affinity difference at 3,4,9,10-perylenetetracarboxylic dianhydride/n-GaAs(100) interfaces. 2001 , 79, 4124-4126	29

2260	Tuning of Au/n-GaAs Diodes with Highly Conjugated Molecules. 2001 , 105, 12011-12018	36
2259	Interfacial chemistry of Alq3 and LiF with reactive metals. 2001 , 89, 2756-2765	313
2258	Tailoring of self-assembled monolayer for polymer light-emitting diodes. 2001 , 79, 2109-2111	54
2257	The Reaction between Tetrakis(diethylamino)tin and Indium Tin Oxide. 2001 , 17, 5696-5702	12
2256	Adsorption of Polar Molecules on a Molecular Surface. 2001 , 105, 2881-2884	31
2255	Joint Experimental and Theoretical Characterization of the Electronic Structure of 4,4Ebis(N-m-tolyl-N-phenylamino)biphenyl (TPD) and Substituted Derivatives. 2001 , 105, 5206-5211	47
2254	Surface Modification of Indium Tin Oxide by Phenoxytin Complexes. 2001 , 17, 948-952	23
2253	Optical Spectroscopy during Growth of PTCDA-C60Complex Thin Films. 2001 , 105, 12076-12081	
2252	Comparison of ultraviolet photoelectron spectroscopy and scanning tunneling spectroscopy measurements on highly ordered ultrathin films of hexa-peri-hexabenzocoronene on Au(111). 2001 , 63,	49
2251	Charge Transfer and Recombination Kinetics at Electrodes of Molecular Semiconductors Investigated by Intensity Modulated Photocurrent Spectroscopy. 2001 , 105, 9524-9532	26
2250	INTERFACES IN ORGANIC LIGHT-EMITTING DEVICES. 2001 , 285-327	5
2249	Effects of Inserting Highly Polar Salts Between the Cathode and Active Layer of Bulk Heterojunction Photovoltaic Devices. 2001 , 665, 1	3
2248	Photo-Electron Spectroscopy Study of Energy Levels in Conjugated Oligomers. 2001 , 708, 261	1
2247	Chemical modification of indium-tin-oxide electrodes by surface molecular design. 2001 , 708, 3221	2
2246	Effect of doping of Li-complex on charge injection and transport in tris(8-quinolato) aluminum layer. 2001 ,	1
2245	PEEM and MEEM of chloroaluminum phthalocyanine ultrathin film on MoS2. 2001 , 114-116, 1025-1030	18
2244	Photoelectron spectroscopy of thin films of PEDOT P SS conjugated polymer blend: a mini-review and some new results. 2001 , 121, 1-17	353
2243	Electronic structures of TPD/metal interfaces studied by photoemission and Kelvin probe method. 2001 , 175-176, 407-411	30

2242	Growth of organic films on passivated semiconductor surfaces: gallium arsenide versus silicon. 2001 , 175-176, 326-331	22
2241	Electronic structure of organic/metal interfaces. 2001 , 393, 298-303	80
2240	A non-ideal bias dependence of the inner electric field in Au/Zn-phthalocyanine/Al photovoltaic cells studied by electroabsorption and photocurrent measurements. 2001 , 119, 357-361	11
2239	The role of interface states in controlling the electronic structure of Alq3/reactive metal contacts. 2001 , 2, 89-95	75
2238	The electronic structure of polymerthetal interfaces studied by ultraviolet photoelectron spectroscopy. 2001 , 34, 121-146	79
2237	Direct detection of low-concentration NO in physiological solutions by a new GaAs-based sensor. 2001 , 7, 1743-9	85
2236	The Optical Properties of Copper Phthalocyanine Ultrathin Films Deposited on Silver: An ATR Study. 2001 , 187, 641-649	
2235	Photoemission study of energy alignment at the metal/Alq3 interfaces. 2001 , 175-176, 412-418	45
2234	Device physics of organic light-emitting diodes based on molecular materials. 2001 , 2, 1-36	508
2233	Interface electronic structure of organic semiconductors with controlled doping levels. 2001 , 2, 97-104	234
2232	Photoelectron spectroscopy study of the energy level alignment at polymer/electrode interfaces in light emitting devices. 2001 , 1, 98-106	10
2231	The photovoltaic effect in poly(alkylthiophene) films on a silicon substrate. 2001 , 43, 397-400	
2230	Energy level line-up in polymer light-emitting diodes via electroabsorption spectroscopy. 2001 , 148, 74-80	10
2229	Electronic Structure of Ordered Langmuir-Blodgett Films of an Amphiphilic Derivative of 2,5-Diphenyl-1,3,4-Oxadiazole. 2001 , 121-135	4
2228	Analysis of Potential Distribution and Current Voltage Characteristic in Polyimide Langmuir Blodgett Films. 2001 , 40, 4575-4580	5
2227	Effect of Ionization Potential of Hole Transport Layer on Device Characteristics of Organic Light Emitting Diode with Oxygen Plasma Treated Indium Tin Oxide. 2001 , 40, 4720-4725	14
2226	Epitaxial growth and electronic structure of a C60 derivative prepared by using a solution spray technique. 2001 , 90, 209-212	9
2225	Determination of the orbital lineup at reactive organic semiconductor interfaces using photoemission spectroscopy. 2001 , 90, 1903-1910	19

2224	Band alignment in organic devices: Photoemission studies of model oligomers on In2O3. 2001 , 90, 270-275	11
2223	Photoemission study of frontier orbital alignment at a metal®rganic interface as a function of conjugation length of oligothiophene derivatives. 2001 , 78, 670-672	34
2222	Theory of electrical rectification in a molecular monolayer. 2001 , 64,	150
2221	Hole injection barriers at polymer anode/small molecule interfaces. 2001 , 79, 557-559	92
2220	Photoelectron spectroscopy of hybrid interfaces for light emitting diodes: Influence of the substrate work function. 2001 , 79, 3185-3187	6
2219	Controlled p-doping of zinc phthalocyanine by coevaporation with tetrafluorotetracyanoquinodimethane: A direct and inverse photoemission study. 2001 , 79, 4040-4042	307
2218	Origin of indium-[perylene-3,4,9,10-tetracarboxilic dianhydride] interface states studied by outermost surface spectroscopy using metastable atoms. 2001 , 63,	65
2217	Mechanisms of injection enhancement in organic light-emitting diodes through an Al/LiF electrode. 2001 , 89, 420-424	177
2216	Improving efficiency by balancing carrier transport in poly(9,9-dioctylfluorene) light-emitting diodes using tetraphenylporphyrin as a hole-trapping, emissive dopant. 2001 , 79, 3872-3874	57
2215	Electronic structure, diffusion, and p-doping at the Au/F16CuPc interface. 2001 , 90, 4549-4554	103
2214	Direct observation of Fermi-level pinning in Cs-doped CuPc film. 2001 , 79, 4148-4150	77
2213	Molecular engineering versus energy level alignment: Interface formation between oligothiophene derivatives and a metal substrate studied with photoemission spectroscopy. 2002 , 91, 5456-5461	21
2212	Vacuum level alignment in organic guest-host systems. 2002 , 92, 1598-1603	33
2211	Barrier lowering and reorientation of dipoles grafted at indium E inBxide/polymer interfaces. 2002 , 92, 992-996	12
2210	Interface between poly (9,9-dioctylfluorene) and alkali metals: cesium, potassium, sodium, and lithium. 2002 , 20, 911-918	12
2209	Adsorption site determination of a large Econjugated molecule by normal incidence x-ray standing waves: End-capped quaterthiophene on Ag(111). 2002 , 66,	27
2208	First-principles electronic structure study of Ti-PTCDA contacts. 2002 , 65,	25
2207	Spontaneous buildup of giant surface potential by vacuum deposition of Alq3 and its removal by visible light irradiation. 2002 , 92, 7306-7310	134

2206	Growth and interfacial studies of conjugated oligomer films on Si and SiO2 substrates. 2002 , 91, 4213-4219	26
2205	Energy level alignment at organic/metal interfaces: Dipole and ionization potential. 2002, 81, 2400-2402	138
2204	Low-energy electron transmission through organic monolayers: An estimation of the effective monolayer potential by an excess electron interference. 2002 , 92, 5203-5207	11
2203	Full characterization of the interface between the organic semiconductor copper phthalocyanine and gold. 2002 , 91, 4872-4878	217
2202	Electronic structure at the interface between metals and new materials for organic light emitting diodes. 2002 , 507-510, 666-671	4
2201	Semiconducting Block Copolymers for Self-Assembled Photovoltaic Devices. 2002 , 27, 456-460	42
2200	Growth, microstructure, charge transport, and transparency of random polycrystalline and heteroepitaxial metalorganic chemical vapor deposition-derived gallium-indium-oxide thin films. 2002 , 17, 3155-3162	25
2199	Grafting Molecular Properties onto Semiconductor Surfaces. 2002,	
2198	Controlling the work function of indium tin oxide: differentiating dipolar from local surface effects. 2002 , 124, 3192-3	75
2197	Physisorption-like Interaction at the Interfaces Formed by Pentacene and Samarium. 2002 , 106, 4192-4196	56
<i>,</i>	Physisorption-like Interaction at the Interfaces Formed by Pentacene and Samarium. 2002, 106, 4192-4196 Exchangelike effects for closed-shell adsorbates: interface dipole and work function. 2002, 89, 096104	56308
2196	Exchangelike effects for closed-shell adsorbates: interface dipole and work function. 2002 , 89, 096104	
2196	Exchangelike effects for closed-shell adsorbates: interface dipole and work function. 2002 , 89, 096104	308
2196 2195	Exchangelike effects for closed-shell adsorbates: interface dipole and work function. 2002 , 89, 096104 The origin of the open-circuit voltage in polyfluorene-based photovoltaic devices. 2002 , 92, 4266-4270	308
2196 2195 2194	Exchangelike effects for closed-shell adsorbates: interface dipole and work function. 2002 , 89, 096104 The origin of the open-circuit voltage in polyfluorene-based photovoltaic devices. 2002 , 92, 4266-4270 Effect of LiF/metal electrodes on the performance of plastic solar cells. 2002 , 80, 1288-1290 Orbital alignment at p-sexiphenyl and coronene/layered materials interfaces measured with	308 202 805
2196 2195 2194 2193	Exchangelike effects for closed-shell adsorbates: interface dipole and work function. 2002, 89, 096104 The origin of the open-circuit voltage in polyfluorene-based photovoltaic devices. 2002, 92, 4266-4270 Effect of LiF/metal electrodes on the performance of plastic solar cells. 2002, 80, 1288-1290 Orbital alignment at p-sexiphenyl and coronene/layered materials interfaces measured with photoemission spectroscopy. 2002, 91, 9095-9107 Thin-film solid-state electroluminescent devices based on tris(2,2'-bipyridine)ruthenium(II)	308 202 805
2196 2195 2194 2193 2192	Exchangelike effects for closed-shell adsorbates: interface dipole and work function. 2002, 89, 096104 The origin of the open-circuit voltage in polyfluorene-based photovoltaic devices. 2002, 92, 4266-4270 Effect of LiF/metal electrodes on the performance of plastic solar cells. 2002, 80, 1288-1290 Orbital alignment at p-sexiphenyl and coronene/layered materials interfaces measured with photoemission spectroscopy. 2002, 91, 9095-9107 Thin-film solid-state electroluminescent devices based on tris(2,2'-bipyridine)ruthenium(II) complexes. 2002, 124, 6090-8 Effective ionic charge polarization using typical supporting electrolyte and charge injection	308 202 805 44 236

(2002-2002)

218	The copper phthalocyanine/Au(100) interface studied using high resolution electron energy-loss spectroscopy. 2002 , 506, 333-338	68
218	Interface formation between thin Cu-phthalocyanine films and crystalline and oxidized silicon surfaces. 2002 , 128, 205-210	31
218	6 Progress in high work function TCO OLED anode alternatives and OLED nanopixelation. 2002 , 127, 29-35	65
218	Analysis of detrapping processes of aromatic 1,3,4-oxadiazoles with thermally stimulated luminescence. 2002 , 127, 181-184	3
218	Electronic structure of aromatic 1,3,4-oxadiazoles studied by ultraviolet photoelectron spectroscopy. 2002 , 127, 185-188	4
218	Examination of band bending at buckminsterfullerene (C60)/metal interfaces by the Kelvin probe method. 2002 , 92, 3784-3793	128
218	2 Strong chemical interaction between indium tin oxide and phthalocyanines. 2002 , 80, 2916-2918	40
218	1 Studies of Alq/Mg: Ag Interface in Organic Light-Emitting Diodes by XPS. 2002 , 725, 1	1
218	O Interfacial electrostatic phenomena in phthalocyanine Langmuir B lodgett films. 2002 , 198-200, 729-734	3
217	9 Recent progress of molecular organic electroluminescent materials and devices. 2002 , 39, 143-222	980
217	8 Electric signal transfer through nm-thick molecular bilayers. 2002 , 19, 339-343	9
217	Charge transfer processes in polymer light-emitting diodes. 2002 , 21, 259-264	11
217	6 Surprising electronic magnetic properties of close-packed organized organic layers. 2002 , 281, 305-309	38
217	5 Interfacial trap states in junctions of molecular semiconductors. 2002 , 285, 103-112	7
217	Determination of the electronic density of states at a nanostructured TiO2/Ru-dye/electrolyte interface by means of photoelectron spectroscopy. 2002 , 285, 157-165	54
217	The use of charge transfer interlayers to control hole injection in molecular organic light emitting diodes. 2002 , 410, 159-166	21
217	Electronic structure of partially fluorinated copper phthalocyanine (CuPCF4) and its interface to Au(). 2002 , 515, 491-498	120
217	Tuning Schottky barrier heights by organic modification of metal-semiconductor contacts. 2002 , 67, 101-113	28

2170	Electronic structure and current injection in zinc phthalocyanine doped with tetrafluorotetracyanoquinodimethane: Interface versus bulk effects. 2002 , 3, 53-63	237
2169	Interfaces in organic semiconductor devices. 2002 , 417, 101-106	37
2168	Structural studies on thin films of an unsubstituted oligo(para-phenylenevinylene). 2002 , 422, 104-111	12
2167	Prospects for electrically pumped organic lasers. 2002 , 66,	267
2166	Structure and Photoelectric Characteristics of Functional Polymers and of Compositions Based on Them. 2002 , 38, 88-108	17
2165	1,8-Naphthalimides in phosphorescent organic LEDs: the interplay between dopant, exciplex, and host emission. 2002 , 124, 9945-54	224
2164	Electroluminescence of Thin Films of Organic Compounds (Review). 2003, 70, 165-194	23
2163	Fluorination of copper phthalocyanines: Electronic structure and interface properties. 2003, 93, 9683-9692	141
2162	Interfacial chemistry of Sm with Alq3 and its implication to organic light-emitting devices. 2003 , 376, 90-95	16
2161	Interface modification of ITO thin films: organic photovoltaic cells. 2003 , 445, 342-352	171
2161 2160	Interface modification of ITO thin films: organic photovoltaic cells. 2003 , 445, 342-352 Hole injection from an ITO PEDT anode into the hole transporting layer of an OLED probed by bias induced absorption. 2003 , 4, 227-232	171 32
	Hole injection from an ITO PEDT anode into the hole transporting layer of an OLED probed by bias	
2160	Hole injection from an ITO PEDT anode into the hole transporting layer of an OLED probed by bias induced absorption. 2003 , 4, 227-232 Electronic charge distribution at interfaces between Cu-phthalocyanine films and semiconductor	32
2160 2159	Hole injection from an ITO PEDT anode into the hole transporting layer of an OLED probed by bias induced absorption. 2003, 4, 227-232 Electronic charge distribution at interfaces between Cu-phthalocyanine films and semiconductor surfaces. 2003, 532-535, 1004-1010 Low-energy molecular exciton in indium/perylene-3,4,9,10-tetracarboxylic dianhydride system	32
2160 2159 2158	Hole injection from an ITO PEDT anode into the hole transporting layer of an OLED probed by bias induced absorption. 2003, 4, 227-232 Electronic charge distribution at interfaces between Cu-phthalocyanine films and semiconductor surfaces. 2003, 532-535, 1004-1010 Low-energy molecular exciton in indium/perylene-3,4,9,10-tetracarboxylic dianhydride system observed by electronic energy loss spectroscopy. 2003, 212-213, 515-519 The effect of permanent dipole moments of adsorbates upon I-V characteristics of a bilayer tunneling junction between self-assembled monolayers on an Au(111) substrate and a gold tip.	3 ² 6 4
2160 2159 2158 2157	Hole injection from an ITO PEDT anode into the hole transporting layer of an OLED probed by bias induced absorption. 2003, 4, 227-232 Electronic charge distribution at interfaces between Cu-phthalocyanine films and semiconductor surfaces. 2003, 532-535, 1004-1010 Low-energy molecular exciton in indium/perylene-3,4,9,10-tetracarboxylic dianhydride system observed by electronic energy loss spectroscopy. 2003, 212-213, 515-519 The effect of permanent dipole moments of adsorbates upon I-V characteristics of a bilayer tunneling junction between self-assembled monolayers on an Au(111) substrate and a gold tip. 2003, 97, 27-33 Electronic structure and electrical properties of interfaces between metals and Etonjugated	3 ² 6 4
2160 2159 2158 2157 2156	Hole injection from an ITO PEDT anode into the hole transporting layer of an OLED probed by bias induced absorption. 2003, 4, 227-232 Electronic charge distribution at interfaces between Cu-phthalocyanine films and semiconductor surfaces. 2003, 532-535, 1004-1010 Low-energy molecular exciton in indium/perylene-3,4,9,10-tetracarboxylic dianhydride system observed by electronic energy loss spectroscopy. 2003, 212-213, 515-519 The effect of permanent dipole moments of adsorbates upon I-V characteristics of a bilayer tunneling junction between self-assembled monolayers on an Au(111) substrate and a gold tip. 2003, 97, 27-33 Electronic structure and electrical properties of interfaces between metals and Etonjugated molecular films. 2003, 41, 2529-2548 Supersonic molecular beam growth of thin films of organic materials: A novel approach to	3 ² 6 4 9 733

2152	Magnetism induced by the organization of self-assembled monolayers. 2003 , 118, 10372-10375	139
2151	Mixing of interface dipole and band bending at organic/metal interfaces in the case of exponentially distributed transport states. 2003 , 93, 6084-6089	47
2150	Photoelectrochemical Reactions at Phthalocyanine Electrodes. 2003 , 247-283	18
2149	Interface Dipoles Arising from Self-Assembled Monolayers on Gold: UVBhotoemission Studies of Alkanethiols and Partially Fluorinated Alkanethiols. 2003 , 107, 11690-11699	381
2148	New electronic and magnetic properties of monolayers of thiols on gold. 2003 , 43, 399-405	7
2147	Controlling Energy-Level Alignments at Carbon Nanotube/Au Contacts. 2003 , 3, 783-787	216
2146	Photoemission from Azobenzene Alkanethiol Self-Assembled Monolayers. 2003 , 107, 7768-7775	32
2145	Hot Microcontact Printing for Patterning ITO Surfaces. Methodology, Morphology, Microstructure, and OLED Charge Injection Barrier Imaging. 2003 , 19, 86-93	59
2144	Alternation between modes of electron transmission through organized organic layers. 2003, 68,	13
2143	Electron transmission through organized organic thin films. 2003 , 36, 291-9	28
2142	Photoelectron Spectroscopy to Probe the Mechanism of Electron Transfer through Oligo(phenylene vinylene) Bridges. 2003 , 107, 1170-1173	15
2141	MoleculeMetal Polarization at Rectifying GaAs Interfaces. 2003 , 107, 6360-6376	76
2140	Role of electrons in laser desorption/ionization mass spectrometry. 2003 , 75, 6063-7	82
2139	Unoccupied electronic states and energy level alignment at interfaces between Cu-phthalocyanine films and semiconductor surfaces. 2003 , 138, 119-123	20
2138	Controlling the work function of indium tin oxide: differentiating dipolar from local surface effects. 2003 , 138, 223-227	20
2137	Interface properties of organic materials investigated by using ultraviolet photoelectron spectroscopy. 2003 , 138, 131-134	2
2136	An X-ray photoelectron spectroscopy study of the interface formed between ITO and 4,4?-bis(4-dimethyl amino styryl)benzene based light emitting diode. 2003 , 138, 107-111	12
2135	Blue light-emitting devices based on 1,8-acridinedione derivatives. 2003 , 139, 347-353	33

2134	Simulation of organic light emitting diodes: influence of charges localized near the electrodes. 2003 , 139, 425-432	17
2133	Photoionization of Individual CdSe/CdS Core/Shell Nanocrystals on Silicon with 2-nm Oxide Depends on Surface Band Bending. 2003 , 3, 497-501	52
2132	Conjugated organic molecules on metal versus polymer electrodes: Demonstration of a key energy level alignment mechanism. 2003 , 82, 70-72	456
2131	Bisindolylmaleimides as Red Electroluminescence Materials. 2003 , 15, 4527-4532	52
2130	4 Electrical properties of organic materials. 2003 , 99, 87-125	35
2129	Close look at charge carrier injection in polymer field-effect transistors. 2003 , 94, 6129-6137	458
2128	MetalBrganic interface and charge injection in organic electronic devices. 2003, 21, 521-531	303
2127	Effect of electrical doping on molecular level alignment at organic@rganic heterojunctions. 2003 , 82, 4815-4817	76
2126	Enhanced hole injection in organic light-emitting diodes using a SAM-derivatised ultra-thin gold anode supported on ITO glass. 2003 , 13, 38-43	43
2125	Electronic line-up in light-emitting diodes with alkali-halide/metal cathodes. 2003, 93, 6159-6172	135
2124	Electronic interactions in codeposited films of naphthalene tetracarboxylic derivatives and metals. 2003 , 94, 3216-3221	14
2123	Electric field in phthalocyanine/perylene heterojunction solar cells studied by electroabsorption and photocurrent measurements. 2003 , 94, 2434-2439	26
2122	A robust ultrathin, transparent gold electrode tailored for hole injection into organic light-emitting diodes. 2003 , 13, 722-726	62
2121	Alignment of valence photoemission, x-ray absorption, and substrate density of states for an adsorbate on a semiconductor surface. 2003 , 67,	41
2120	Controlled p doping of the hole-transport molecular material N,N?-diphenyl-N,N?-bis(1-naphthyl)-1,1?-biphenyl-4,4?-diamine with tetrafluorotetracyanoquinodimethane. 2003 , 94, 359-366	244
2119	Hole-transport properties of a furan-containing oligoaryl. 2003 , 93, 5465-5471	67
2118	Molecular modification of an ionic semiconductor thetal interface: ZnO/molecule/Au diodes. 2003 , 82, 1051-1053	59
2117	Interplay between morphology, structure, and electronic properties at diindenoperylene-gold interfaces. 2003 , 68,	112

2116 Interface formation in K doped poly(dialkoxy-p-phenylene vinylene) light-emitting diodes. 2003, 94, 5756-57627

2115 Electronic structure of pentacene adsorbates on Au(111) surfaces. 2003 , 83, 4342-4344	19
2114 Liquid metals as electrodes in polymer light emitting diodes. 2003 , 93, 3299-3307	15
Transport of carriers in organic light-emitting devices fabricated with a p-phenylenevinylene-derivative copolymer. 2003 , 94, 2024-2027	12
The metallicity of aluminum and gold in contact with thin films of a urethane-substituted polythiophene. 2003 , 93, 3384-3388	6
2111 Band alignment on a nanoscopically patterned inorganic@rganic interface. 2003 , 83, 563-565	9
The origin of soft vibrational modes of alkanes adsorbed on Cu: An experimental and theoretical investigation. 2003 , 118, 5115-5131	33
Organic molecular films on gold versus conducting polymer: Influence of injection barrier height and morphology on current loltage characteristics. 2003 , 82, 2281-2283	91
2108 Lack of thermodynamic equilibrium in conjugated organic molecular thin films. 2003 , 67,	28
2107 Organic light-emitting diode materials. 2003,	2
2106 Nature of electrical contacts in a metaltholeculeBemiconductor system. 2003 , 21, 1928	45
2105 Electrical doping: the impact on interfaces of '-conjugated molecular films. 2003 , 15, S2757-S2770	62
2104 Electronic properties of interfaces between perylene derivatives and GaAs(001) surfaces. 2003 , 15, S26	79-S26928
$_{2103}$ Band mapping and frontier orbitals at the interface thin native SiO 2 /organics. 2003 ,	
2102 Evidence of electron and hole transfer in metal/CuPc interfaces. 2003,	4
Electronic interaction at molecule-metal interfaces: implication for molecule-based electronics. 2003 ,	1
Metal vs. Polymer Electrodes in Organic Devices: Energy Level Alignment, Hole Injection, and Structure. 2003 , 771, 361	4
Energy Level Alignment at Fullerene/Phthalocyanine Interface Studied by Electron Spectroscopies. 2093 , 771, 351	3

2098	Formation of a MgAu alloy Cathode by Photolithography and the Application for Organic Light-Emitting Diodes and Organic Field-effect Transistors. 2004 , 124, 1219-1223	3
2097	Organic Light-Emitting Diodes. 2004 , 1-5	
2096	Metalörganic interfaces at the nanoscale. 2004 , 15, 1818-1824	10
2095	Gate tunable electron injection in submicron pentacene transistors. 2004 , 15, 1023-1026	10
2094	Transparent low-work-function indium tin oxide electrode obtainedby molecular scale interface engineering. 2004 , 85, 1616-1618	55
2093	Inhomogeneous electronic structure of copper phthalocyanine film measured with microspot photoemission spectroscopy. 2004 , 85, 3584-3586	27
2092	Contact potential difference measurements of doped organic molecular thin films. 2004 , 22, 1488-1492	9
2091	Effects of FeCl3 doping on polymer-based thin film transistors. 2004 , 96, 454-458	31
2090	Sexithiophene films on clean and oxidized Si(111) surfaces: Growth and electronic structure. 2004 , 96, 2716-2724	37
2089	Hybrid nanocrystalline TiO2 solar cells with a fluorenethiophene copolymer as a sensitizer and hole conductor. 2004 , 95, 1473-1480	171
2088	Bipolar doping between a molecular organic donor-acceptor couple. 2004 , 69,	34
2087	Two-photon photoelectron spectroscopy of conjugated polymer thin films on gold. 2004 , 84, 76-78	18
2086	Enhancement of electron injection in organic light-emitting devices using an Ag/LiF cathode. 2004 , 95, 3828-3830	63
2085	Measurement of interface potential change and space charge region across metal/organic/metal structures using Kelvin probe force microscopy. 2004 , 85, 4148-4150	21
2084	Oxygen as a surfactant for Al contact metallization of organic layers. 2004 , 85, 585-587	10
2083	Effects of intrinsic layer thickness on solar cell parameters of organic p-i-n heterojunction photovoltaic cells. 2004 , 85, 6412-6414	54
2082	Impact of an interface dipole layer on molecular level alignment at an organic-conductor interface studied by ultraviolet photoemission spectroscopy. 2004 , 70,	145
2081	Synthesis and Electroluminescence of Metal 4-Styryl-8-hydroxyquinolates. 2004 , 51, 735-742	7

2080	Anode/organic interface modification by plasma polymerized fluorocarbon films. 2004 , 95, 4397-4403	41
2079	Effect of acidic and basic surface dipoles on the depletion layer of indium tin oxide as measured by in-plane conductance. 2004 , 84, 61-63	19
2078	Introduction to Organic Light-Emitting Devices. 2004 , 1-41	15
2077	Hybrid interfaces of conjugate polymers: Band edge alignment studied by ultraviolet photoelectron spectroscopy. 2004 , 19, 1917-1923	39
2076	CuPc/C60Solar CellsInfluence of the Indium Tin Oxide Substrate and Device Architecture on the Solar Cell Performance. 2004 , 43, 1305-1311	7
2075	Control of carrier density by self-assembled monolayers in organic field-effect transistors. 2004 , 3, 317-22	753
2074	Surface states at the nanoparticle-polymer matrix interface. 2004 , 30, 322-324	3
2073	Dipole formation at metal/PTCDA interfaces: Role of the Charge Neutrality Level. 2004 , 65, 802-808	210
2072	Donor-mediated band gap reduction in a homologous series of conjugated polymers. 2004 , 126, 16440-50	85
2071	Surface photovoltage of thin organic films studied by modulated photoelectron emission. 2004 , 552, 77-84	8
2070	Low- and high-frequency CIV characteristics of the contacts formed by sublimation of the nonpolymeric organic compound on p-type Si substrate. 2004 , 201, 3077-3086	17
2069	Efficient Electron Injection from a Bilayer Cathode Consisting of Aluminum and Alcohol-/Water-Soluble Conjugated Polymers. <i>Advanced Materials</i> , 2004 , 16, 1826-1830	391
2068	Reliable and reproducible determination of work function and ionization potentials of layers and surfaces relevant to organic light emitting diodes. 2004 , 5, 199-205	26
2067	HOMO-band fine structure of OTi- and Pb-phthalocyanine ultrathin films: effects of the electric dipole layer. 2004 , 137-140, 223-227	51
2066	Cross-section analysis of organic light-emitting diodes. 2004 , 101, 123-8	13
2065	The electronic properties of the interface between a thin conjugated oligomer film and SiO2/Si(111), studied by photoemission spectroscopies. 2004 , 459, 32-36	8
2064	Interface dipole at organic/metal interfaces and organic solar cells. 2004, 83, 147-168	49
2063	Adsorption structure and spin polarization of pentacene on a magnetized Fe(1 0 0) substrate: SPMDS and ERDA study. 2004 , 549, 97-102	20

2062	The interface between phthalocyanines and PEDOT:PSS: evidence for charge transfer and doping. 2004 , 566-568, 554-559	19
2061	Photoelectron fine structures of uppermost valence band for well-characterized ClAl-phthalocyanine ultrathin film: UPS and MAES study. 2004 , 566-568, 571-578	44
2060	Electronic structure of long-range ordered pentacene structures on the stepped Cu(119) surface. 2004 , 566-568, 613-617	18
2059	A photoemission study of the Ooct-OPV5/SiO2/Si(111) interface: Effect of the SiO2 interlayer thickness. 2004 , 569, 207-218	11
2058	Luminescence of molecules adsorbed on surfaces of wide gap materials. 2004 , 110, 275-283	8
2057	Consequences of twisting the aromatic core of N,N?-dimethylperylene-3,4,9,10-biscarboximide by chemical substitution for the electronic coupling and electric transport in thin films. 2004 , 5, 237-249	19
2056	Relation between morphology and work function of metals deposited on organic substrates. 2004 , 234, 333-340	21
2055	Direct interface states observation by total-current spectroscopy. 2004 , 239, 55-58	3
2054	An efficient organic light-emitting diode with silver electrodes. 2004 , 386, 128-131	60
2053	Influence of contact geometry and molecular derivatization on the interfacial interactions between gold and conjugated wires. 2004 , 387, 502-508	21
2052	Electronegativity and charge-injection barrier at organic/metal interfaces. 2004, 396, 92-96	32
2051	Interaction of caesium with poly(p-phenylene vinylene) surfaces. 2004 , 234, 120-125	Ο
2050	Thickness dependence of the LUMO position for phthalocyanines on hydrogen passivated silicon (111). 2004 , 234, 138-143	19
2049	Barrier formation at metalorganic interfaces: dipole formation and the charge neutrality level. 2004 , 234, 107-112	159
2048	Effect of MoleculeMolecule Interaction on the Electronic Properties of Molecularly Modified Si/SiOx Surfaces. 2004 , 108, 664-672	38
2047	Photoemission study of hole-injection enhancement in organic electroluminescent devices with Au/CFx anode. 2004 , 84, 73-75	24
2046	Evidence of nitric-oxide-induced surface band bending of indium tin oxide. 2004 , 95, 6273-6276	13
2045	Nanocrystalline metal electrodes for high-efficiency organic solar cells. 2004 , 85, 1832-1834	5

2044	Electronic structure of a silole derivative-magnesium thin film interface. 2004 , 95, 2832-2838	22
2043	High-Resolution Photoemission Study of Different NTCDA Monolayers on Ag(111): Bonding and Screening Influences on the Line Shapes 2004, 108, 14741-14748	56
2042	Patterned Redox Arrays of Polyarylamines III. Effect of Molecular Structure and Oxidation Potential on Film Morphology and Hole-Injection in Single-Layer Organic Diodes. 2004 , 16, 4711-4714	15
2041	Scanning tunneling spectroscopy on organic semiconductors: Experiment and model. 2004 , 70,	36
2040	Ambipolar Charge Injection and Transport in a Single Pentacene Monolayer Island. 2004 , 4, 2145-2150	60
2039	Interfacial Electronic Structure of Tris(8-hydroxyquinoline)aluminum (III) on Cu(111). 2004 , 16, 750-756	11
2038	Self-assembled monolayers of cobalt(II)- (4-tert-butylphenyl)-porphyrins: the influence of the electronic dipole on scanning tunneling microscopy images. 2004 , 126, 16951-8	36
2037	Building blocks for n-type molecular and polymeric electronics. Perfluoroalkyl- versus alkyl-functionalized oligothiophenes (nT; n = 2-6). Systematics of thin film microstructure, semiconductor performance, and modeling of majority charge injection in field-effect transistors.	305
2036	In situ spectroelectrochemistry of poly(N,N'-ethylenebis(salicylideneiminato)Cu(II)). 2004 , 76, 5918-23	14
2035	Electrochemical Characterization of Two Perylenetetracarboxylic Diimides: Langmuir B lodgett Films and Carbon Paste Electrodes. 2004 , 16, 358-364	28
2034	Charge Transport at Metal Molecule Interfaces: A Spectroscopic View. 2004 , 108, 8778-8793	115
2033	Threshold voltage shift in organic field effect transistors by dipole monolayers on the gate insulator. 2004 , 96, 6431-6438	475
2032	Carrier transport in multilayer organic photodetectors: II. Effects of anode preparation. 2004 , 95, 1869-1877	54
2031	Au-poly(3-hexylthiophene) contact behaviour at high resolution. 2004 , 145, 217-220	19
2030	Charge mobilities and luminescence characteristics of blue-light emitting bent carbazole trimers connected through vinylene linkers affect of nitrile substituents. 2004 , 145, 229-235	7
2029	Shifted transfer characteristics of organic thin film and single crystal FETs. 2004 , 146, 325-328	33
2028	VUV photoemission using synchrotron light: a tool for characterising surfaces and interfaces occurring in OLEDs. 2004 , 382, 179-186	9
2027	Organic solar cells: An overview. 2004 , 19, 1924-1945	2012

2026 An alternative method to build organic photodiodes. 2004 , 140, 281-286	21
2025 23.1: Efficient Electron Injection from Bilayer Cathode with High Work Function Metal. 2004 , 35, 892	
2024 Ballistic emission spectroscopy and imaging of a buried metal-organic interface. 2004 ,	
2023 Light-emitting materials based on liquid crystals. 2004 ,	1
Doping Effect of Tetrathianaphthacene Molecule in Organic Semiconductors on Their Interfacial Electronic Structures Studied by UV Photoemission Spectroscopy. 2005 , 44, 3760-3763	37
2021 61.2: Invited Paper: Structure and Electronic Structure of Organic Interfaces. 2005 , 36, 1752	
Chemisorption at interfaces between organic semiconductors and metals: role of the electron affinity. 2005 , 252, 77-80	8
2019 Polarization at the gold/pentacene interface. 2005 , 6, 85-91	229
2018 B and bendinglin copper phthalocyanine on hydrogen-passivated Si(111). 2005 , 6, 168-174	36
Luminescence and electroluminescence of bis (2-(benzimidazol-2-yl) quinolinato) zinc. Exciplex 2017 formation and energy transfer in mixed film of bis (2-(benzimidazol-2-yl) quinolinato) zinc and N,N?-bis-(1-naphthyl)-N,N?-diphenyl-1,1?-biphenyl-4,4?-diamine. 2005 , 737, 35-41	29
2016 High-efficiency electron injection cathode of Au for polymer light-emitting devices. 2005 , 6, 118-128	136
Size dependence investigations of hot electron cooling dynamics in metal/adsorbates nanoparticles. 2005 , 319, 409-421	17
n-Type doping effect on the electronic structure of organic semiconductor: doping of tetrathianaphthacene (TTN) into hexadecafluorophthalocyaninatozinc (F16ZnPc) by co-evaporation. 2005 , 144-147, 533-536	10
UPS fine structures of highest occupied band in vanadyl-phthalocyanine ultrathin film. 2005 , 144-147, 475-477	25
Photoemission microscopy for surface states of copper measured at different photoelectron energies. 2005 , 144-147, 1167-1169	3
Photoemission study of the sodium stearate/tris-(8-hydroxyquinoline) aluminum interface. 2005 , $144-147$, 925-928	2
2010 New organic discotic materials for photovoltaic conversion. 2005 , 85, 535-543	57
Ex-situ prepared films of 4-aminothiophenol on Au(1 1 1): photoemission, NEXAFS and STM measurements. 2005 , 580, 63-70	7

2008 Electronic properties of the interface between #dihexyl-quaterthiophene and gold. 2005 , 595, 165-171	20
2007 Influence of molecular conformation on organic/metal interface energetics. 2005 , 413, 390-395	66
Evidence for the atmospheric p-type doping of titanyl phthalocyanine thin film by oxygen observed as the change of interfacial electronic structure. 2005 , 414, 479-482	41
Energy level alignment at interfaces with pentacene: metals versus conducting polymers. 2005 , 244, 593-597	26
2004 Electronic properties of the organic semiconductor hetero-interface CuPc/C60. 2005 , 252, 143-147	21
2003 Flexible Conjugated Polymer-Based Plastic Solar Cells: From Basics to Applications. 2005 , 93, 1429-1439	126
Formation of MgAu alloy cathode by photolithography and its application to organic light-emitting diodes and organic field effect transistors. 2005 , 152, 37-42	6
Influence of molecular order on the local work function of nanographene architectures: a Kelvin-probe force microscopy study. 2005 , 6, 2371-5	35
2000 The Cooperative Molecular Field Effect. 2005 , 15, 1571-1578	150
Work Function Independent Hole-Injection Barriers Between Pentacene and Conducting Polymers. Advanced Materials, 2005 , 17, 330-335	111
Tuning of Metal Work Functions with Self-Assembled Monolayers. <i>Advanced Materials</i> , 2005 , 17, 621-625 ₂₄	599
1997 In-Situ Preparation and Analysis of Functional Oxides. 2005 , 7, 945-949	56
Ambipolar Field-Effect Transistor (FET) and Redox Characteristics of a Econjugated Thiophene/1,3,4-Thiadiazole CT-Type Copolymer. 2005 , 26, 1214-1217	67
1995 The first studies of a tetrathiafulvalene-sigma-acceptor molecular rectifier. 2005 , 11, 2914-22	99
Charge injection spectroscopy of Alq3 thin films deposited on bare and LiF-modified metal substrates. 2005 , 81, 222-228	10
Laser-based photoemission micro-spectroscopy for occupied and unoccupied states of inhomogeneous surfaces. 2005 , 593, 38-42	5
1992 Energetics of molecular interfaces. 2005 , 8, 32-41	290
1991 Soft lithography contacts to organics. 2005 , 8, 42-54	23

1990 Effects of Various Types of Doping on the Electronic Structure of Organic Interfaces. 2005, 871, 1

1989	Enhancement of Surface Potential Buildup and Decay of Tris(8-quinolinato)aluminum Film Deposited on Ultraviolet/Ozone-Treated Gold Electrodes. 2005 , 44, 1091-1094	5
1988	Investigation of the poly[2-methoxy-5-(2?-ethyl-hexyloxy)-1,4-phenylene vinylene]Indium tin oxide interface using photoemission spectroscopy. 2005 , 98, 023512	12
1987	Characterization of the interface dipole at the paraphenylenediamine-nickel interface: a joint theoretical and experimental study. 2005 , 122, 84712	22
1986	White organic light-emitting diode comprising of blue fluorescence and red phosphorescence. 2005 , 86, 113507	83
1985	Electronegativity model for barrier formation at metal/organic interfaces. 2005, 87, 252110	24
1984	Effect of metal chelate layer on electroluminescent and current-voltage characteristics. 2005 , 86, 202109	5
1983	Electronic structure and femtosecond electron transfer dynamics at noble metal/tris-(8-hydroxyquinoline) aluminum interfaces. 2005 , 71,	21
1982	Chemistry and electronic properties of a metal-organic semiconductor interface: In on CuPc. 2005 , 72,	40
1981	Metal-induced gap states in epitaxial organic-insulator/metal interfaces. 2005 , 72,	19
1980	Conducting polymer and hydrogenated amorphous silicon hybrid solar cells. 2005 , 87, 223504	63
1979	Investigation of dye-doped red emitting organic electroluminescent devices with metal-mirror microcavity structure. 2005 , 97, 103112	10
1978	Organic thin-film transistors with improved characteristics using lutetium bisphthalocyanine as a buffer layer. 2005 , 97, 026106	33
1977	Photoexcited carriers in organic light emitting materials and blended films observed by surface photovoltage spectroscopy. 2005 , 71,	9
1976	Switching in organic devices caused by nanoscale Schottky barrier patches. 2005 , 122, 204702	5
1975	Influence of the alkyl-chains length on the electronic structure and interface properties of 1,4-octasubstituted zinc phthalocyanines on gold. 2005 , 97, 073715	22
1974	Master equation approach to charge injection and transport in organic insulators. 2005 , 122, 124705	12
1973	CobaltpolypyrroleBobalt nanowire field-effect transistors. 2005 , 86, 213113	28

1972	Chemical reaction at the interface between pentacene and HfO2. 2005 , 72,	8
1971	Effect of thin iridium oxide on the formation of interface dipole in organic light-emitting diodes. 2005 , 87, 232105	21
1970	Photoelectron spectroscopic investigation of in-vacuum-prepared luminescent polymer thin films directly from solution. 2005 , 97, 024909	50
1969	Electronic structure of organic films in the first excited states determined using scanning tunneling spectroscopy: An experimental and theoretical study. 2005 , 72,	2
1968	Systematic Modification of Indium Tin Oxide to Enhance Diode Device Behavior. 2005 , 871, 1	1
1967	Fabrication of RR-P3HT-based TFTs using low-temperature PECVD silicon nitride passivation. 2005 , 871, 1	
1966	Determination of Interface Dipole Energy at the Interface of Ruthenium-Oxide-Coated Anode with Organic Material Using Synchrotron Radiation Photoemission Spectroscopy. 2005 , 8, H79	6
1965	Reversal of doping-induced energy level shift: Au on Cs-doped tris(8-hydroxyquinoline) aluminum. 2005 , 87, 051918	11
1964	Direct evidence of molecular aggregation and degradation mechanism of organic light-emitting diodes under joule heating: an STM and photoluminescence study. 2005 , 109, 1675-82	137
1963	Electronic properties of interfaces between different sexithiophenes and gold. 2005 , 97, 123712	37
1962	Electroluminescence of 2,4-bis(4-(2?-thiophene-yl)phenyl)thiophene in organic light-emitting field-effect transistors. 2005 , 86, 093505	54
1961	Spectroscopy of Emerging Materials. 2005,	1
1960	Highly efficient organic light-emitting diodes with hole injection layer of transition metal oxides. 2005 , 98, 093707	41
1959	Modeling electrical transport in blend heterojunction organic solar cells. 2005 , 97, 124901	76
1958	Effect of molecular binding to a semiconductor on metal/molecule/semiconductor junction behavior. 2005 , 109, 9622-30	34
1957	Electrical studies on the doping dependence and electrode effect of metalPANIhetal structures. 2005 , 38, 1437-1443	28
1956	Influence of Structure and C60Composition on Properties of Blends and Bilayers of Organic Donor-Acceptor Polymer/C60Photovoltaic Devices. 2005 , 44, 1296-1300	27
1955	Organization-induced charge redistribution in self-assembled organic monolayers on gold. 2005 , 109, 14064-73	53

1954	Origin of enhancement in open-circuit voltage by adding ZnO to nanocrystalline SnO2 in dye-sensitized solar cells. 2005 , 109, 17892-900	63
1953	The reaction of tetrakis(dimethylamido)titanium with self-assembled alkyltrichlorosilane monolayers possessing -OH, -NH2, and -CH3 terminal groups. 2005 , 127, 6300-10	58
1952	Covalently bound hole-injecting nanostructures. Systematics of molecular architecture, thickness, saturation, and electron-blocking characteristics on organic light-emitting diode luminance, turn-on voltage, and quantum efficiency. 2005 , 127, 10227-42	142
1951	Advanced surface modification of indium tin oxide for improved charge injection in organic devices. 2005 , 127, 10058-62	164
1950	Exciton dynamics at molecule-metal interfaces: C60Au(111). 2005 , 72,	50
1949	Energy level alignment at metal-octaethylporphyrin interfaces. 2005 , 109, 23558-63	15
1948	Photoemission studies of polythiophene and polyphenyl films produced via surface polymerization by ion-assisted deposition. 2005 , 109, 7134-40	34
1947	Electrostatic field and partial Fermi level pinning at the pentacene-SiO(2) interface. 2005, 109, 1834-8	43
1946	Direct measurement of surface complex loading and surface dipole and their effect on simple device behavior. 2005 , 109, 3966-70	20
1945	Electrical transport characteristics of single-layer organic devices from theory and experiment. 2005 , 98, 063709	27
1944	Efficient electron injection from bilayer cathode with aluminum as cathode. 2005 , 153, 197-200	9
1943	Electron transfer/transport at metal-molecule interfaces probed by femtosecond time-resolved two-photon photoemission: Heptane and fullerene on Au(111). 2005 , 45, 195-203	2
1942	Introduction. 2005 , 13, 123	4
1941	Determination of the electronic structure of self-assembled L-cysteine/Au interfaces using photoemission spectroscopy. 2005 , 21, 3551-8	39
1940	Toward the ideal organic light-emitting diode. The versatility and utility of interfacial tailoring by cross-linked siloxane interlayers. 2005 , 38, 632-43	231
1939	Inversion of the rectifying effect in diblock molecular diodes by protonation. 2005 , 127, 10456-7	130
1938	Metal Diffusion in Polymers and on Polymer Surfaces. 2005 , 333-363	1
1937	Charge injection barriers at a ribonucleic acid/inorganic material contact determined by photoemission spectroscopy. 2005 , 109, 748-56	6

(2006-2005)

1936	Origin of the interface dipole at interfaces between undoped organic semiconductors and metals. 2005 , 23, 1072-1077	76
1935	Organic heterojunction and its application for double channel field-effect transistors. 2005 , 87, 093507	164
1934	Effects of Deformation on Electric Conductivity in Al-Zr Alloys. 2005 , 475-479, 1743-1746	
1933	Transport of Low-Energy Electrons in Thin Organic Films. 2005, 427, 71/[383]-93/[405]	9
1932	Charge injection into cathode-doped amorphous organic semiconductors. 2005, 71,	55
1931	Energy level alignment at organic heterojunctions: Role of the charge neutrality level. 2005, 71,	242
1930	n-type carbon nanotube field-effect transistors fabricated by using Ca contact electrodes. 2005 , 86, 073105	132
1929	Metal Diffusion in Polymers and on Polymer Surfaces. 2005 , 333-363	6
1928	EPR studies on the organization of self-assembled spin-labeled organic monolayers adsorbed on GaAs. 2005 , 7, 524-9	15
1927	Control of cationic conjugated polymer performance in light emitting diodes by choice of counterion. 2006 , 128, 14422-3	181
1926	N4-Macrocyclic Metal Complexes. 2006 ,	96
1925	Molecular gap and energy level diagram for pentacene adsorbed on filled d-band metal surfaces. 2006 , 89, 152119	29
1924	Effect of intermolecular disorder on the intrachain charge transport in ladder-type poly(p-phenylenes). 2006 , 73,	45
1923	Green polyfluorene-conducting polymer interfaces: Energy level alignment and device performance. 2006 , 100, 024512	24
1922	Electronic and chemical properties of tin-doped indium oxide (ITO) surfaces and ITO/ZnPc interfaces studied in-situ by photoelectron spectroscopy. 2006 , 110, 4793-801	100
1921	Achieving fast oxygen response in individual 眍a2O3 nanowires by ultraviolet illumination. 2006 , 89, 112114	64
1920	Metal electrode effects on spin-orbital coupling and magnetoresistance in organic semiconductor devices. 2006 , 89, 203510	40
1919	A supersonic molecular beam study of the reaction of tetrakis(dimethylamido)titanium with self-assembled alkyltrichlorosilane monolayers. 2006 , 125, 34706	11

1918	Experimental estimation of the electric dipole moment and polarizability of titanyl phthalocyanine using ultraviolet photoelectron spectroscopy. 2006 , 73,	132
1917	Threshold voltage as a measure of molecular level shift in organic thin-film transistors. 2006 , 88, 043509	24
1916	Adsorption of pentacene on filled d-band metal surfaces: long-range ordering and adsorption energy. 2006 , 124, 154702	36
1915	New electronic and magnetic properties emerging from adsorption of organized organic layers. 2006 , 8, 2217-24	30
1914	Weak charge transfer between an acceptor molecule and metal surfaces enabling organic/metal energy level tuning. 2006 , 110, 21069-72	35
1913	Morphology selected molecular architecture: acridine carboxylic acid monolayers on Ag (111). 2006 , 110, 1271-6	14
1912	Development of Experimental Methods for Determining the Electronic Structure of Organic Materials. 2006 , 455, 145-181	23
1911	Substrate effects on the electronic properties of an organic/organic heterojunction. 2006 , 88, 232103	47
1910	New benchmark for water photooxidation by nanostructured alpha-Fe2O3 films. 2006, 128, 15714-21	1370
1909	Optical susceptibilities of supported indium tin oxide thin films. 2006 , 100, 113123	20
1908	Energy-Level Alignment at Interfaces Between Gold and Poly(3-hexylthiophene) Films with Two Different Molecular Structures. 2006 , 9, G317	36
1907	Modification of indium tin oxide films by alkanethiol and fatty acid self-assembled monolayers: a comparative study. 2006 , 22, 3118-24	39
1906	Electrode-molecular semiconductor contacts: Work-function-dependent hole injection barriers versus Fermi-level pinning. 2006 , 89, 162107	89
1905	Frontier Electronic Structures in Fluorinated Copper Phthalocyanine Thin Films Studied Using Ultraviolet and Inverse Photoemission Spectroscopies. 2006 , 455, 211-218	53
1904	How important is the interfacial chemical bond for electron transport through alkyl chain monolayers?. 2006 , 6, 2873-6	64
1903	Does the molecular orientation induce an electric dipole in Cu-phthalocyanine thin films?. 2006 , 99, 093705	97
1902	Spiro Compounds for Organic Electroluminescence and Related Applications. 2006, 83-142	100
1901	Electron transport through rectifying self-assembled monolayer diodes on silicon: Fermi-level pinning at the molecule-metal interface. 2006 , 110, 13947-58	73

(2006-2006)

1900	Lithium intercalation of phenyl-capped aniline dimers: a study by photoelectron spectroscopy and quantum chemical calculations. 2006 , 110, 19023-30	1
1899	Fermi level alignment in self-assembled molecular layers: the effect of coupling chemistry. 2006 , 110, 17138-44	36
1898	Study of alkyl organic monolayers with different molecular chain lengths directly attached to silicon. 2006 , 22, 9962-6	31
1897	Origin of the highest occupied band position in pentacene films from ultraviolet photoelectron spectroscopy: Hole stabilization versus band dispersion. 2006 , 73,	173
1896	Systematic Investigation of Nanoscale Adsorbate Effects at Organic Light-Emitting Diode Interfaces. Interfacial Structure Tharge Injection Duminance Relationships. 2006 , 18, 2431-2442	50
1895	Controlling charge injection in organic field-effect transistors using self-assembled monolayers. 2006 , 6, 1303-6	166
1894	Ab initio calculations of the reaction mechanisms for metal-nitride deposition from organo-metallic precursors onto functionalized self-assembled monolayers. 2006 , 128, 836-47	27
1893	Ion yields of thin MALDI samples: dependence on matrix and metal substrate and implications for models. 2006 , 110, 12728-33	25
1892	Luminescence quenching of tetracene films adsorbed on an ultrathin alumina AlOx layer on Ni3Al(111). 2006 , 74,	15
1891	Control of interchain contacts, solid-state fluorescence quantum yield, and charge transport of cationic conjugated polyelectrolytes by choice of anion. 2006 , 128, 16532-9	133
1890	Effects of electron transfer between TiO2 films and conducting substrates on the photocatalytic oxidation of organic pollutants. 2006 , 110, 13470-6	76
1889	Heteroepitaxy of organic-organic nanostructures. 2006 , 6, 1207-12	80
1888	Dependence of band offset and open-circuit voltage on the interfacial interaction between TiO2 and carboxylated polythiophenes. 2006 , 110, 3257-61	96
1887	Electron Transfer Mediated by Photosynthetic Reaction Center Proteins between Two Chemical-Modified Metal Electrodes. 2006 , 445, 291/[581]-296/[586]	10
1886	Screening and surface states in molecular monolayers adsorbed on silicon. 2006 , 110, 11496-503	3
1885	Role of molecular anchor groups in molecule-to-semiconductor electron transfer. 2006 , 110, 25383-91	92
1884	Electronic structure of Si(111)-bound alkyl monolayers: Theory and experiment. 2006, 74,	102
1883	Tuning the hole injection barrier at the organic/metal interface with self-assembled functionalized aromatic thiols. 2006 , 110, 26075-80	59

1882	Elimination of hole injection barriers by conducting polymer anodes in polyfluorene light-emitting diodes. 2006 , 74,	39
1881	Transparent, Plastic, Low-Work-Function Poly(3,4-ethylenedioxythiophene) Electrodes. 2006 , 18, 4246-4252	70
1880	The photovoltaic effect in a heterojunction of molybdenyl phthalocyanine and perylene dye. 2006 , 352, 4319-4324	9
1879	Energy level diagrams of C60/pentacene/Au and pentacene/C60/Au. 2006, 156, 32-37	85
1878	Thin organic layers for photography and electronic devices. 2006 , 2006, 1-8	2
1877	Decay process of a large surface potential of Alq3 films by heating. 2006 , 100, 053707	16
1876	High intra-chain hole mobility on molecular wires of ladder type poly(p-phenylenes). 2006 , 6336, 114	
1875	17.1: Invited Paper: Carrier Injection Barrier Formation at Metal/Organic Interfaces. 2006 , 37, 1095	
1874	UVBzone treated Au for air-stable, low hole injection barrier electrodes in organic electronics. 2006 , 100, 053701	90
1873	First-Principles Study of Molecule/Al Interfaces. 2006 , 47, 2701-2705	1
1872	A work function study of ultrathin alumina formation on Cu-9%Al(111) surface. 2006 , 38, 793-796	11
1871	Electrical properties of polypyrrole/p-InP structure. 2006 , 44, 1572-1579	8
1870	Influence of indium tin oxide treatment using UVBzone and argon plasma on the photovoltaic parameters of devices based on organic discotic materials. 2006 , 55, 601-607	23
1869	How to model the behaviour of organic photovoltaic cells. 2006 , 55, 583-600	329
1868	Controlling Au/n-GaAs junctions by partial molecular monolayers. 2006 , 203, 3438-3451	25
1867	Investigation of the surface potential formed in Alq3 films on metal surface by Kelvin probe and nonlinear optical measurement. 2006 , 6, 877-881	12
1866	Ultraviolet photoelectron spectroscopy investigation of interface formation in an indium E in oxide/fluorocarbon/organic semiconductor contact. 2006 , 252, 3806-3811	12
1865	Chemical bonding and electronic structures at magnesium/copper phthalocyanine interfaces. 2006 , 252, 3948-3952	25

(2006-2006)

1864	Improved electrical and optical properties of MEH-PPV light emitting diodes using Ba buffer layer and porphyrin. 2006 , 252, 3953-3955	8
1863	Effect of end groups on contact resistance of alkanethiol based metalfholeculefhetal junctions using current sensing AFM. 2006 , 252, 3956-3960	6
1862	Charge-transfer at silver/phthalocyanines interfaces. 2006 , 252, 5453-5456	18
1861	Energy level alignment between C60 and Al using ultraviolet photoelectron spectroscopy. 2006 , 252, 8015-8017	15
1860	Oxygen effects on the interfacial electronic structure of titanyl phthalocyanine film: p-Type doping, band bending and Fermi level alignment. 2006 , 325, 121-128	45
1859	Layer-selective epitaxial self-assembly of porphyrins on ultrathin insulators. 2006 , 417, 22-27	57
1858	Important role of molecular permanent dipoles of the Alq3/Al interface studied from first-principles. 2006 , 420, 523-528	37
1857	Negative capacitance caused by electron injection through interfacial states in organic light-emitting diodes. 2006 , 422, 184-191	149
1856	Enhanced electron injection into tris(8-hydroxyquinoline) aluminum (Alq3) thin films by tetrathianaphthacene (TTN) doping revealed by currentloltage characteristics. 2006 , 423, 170-173	14
1855	Evidence for electric field dependent dissociation of exciplexes in electron donor acceptor organic solid films. 2006 , 432, 110-115	21
1854	Photoemission study of the interface properties of aminothiophene derivatives in contact to Au as a function of conjugation length. 2006 , 7, 107-113	7
1853	Bottom contact ambipolar organic thin film transistor and organic inverter based on C60/pentacene heterostructure. 2006 , 7, 457-464	68
1852	Temperature dependence of the currentwoltage characteristics of the Al/Rhodamine-101/p-Si(100) contacts. 2006 , 252, 2209-2216	59
1851	Synthesis, characterization and electroluminescence of B(III) compounds: BPh2(2-(2-quinolyl)naphtho[b]imidazolato) and BPh2(2-(2-quinolyl)benzimidazolato). 2006 , 691, 1998-2004	25
1850	Molecular orientation dependent energy levels at interfaces with pentacene and pentacenequinone. 2006 , 7, 537-545	80
1849	Interfacial electronic states of an anthracene derivative deposited on a SiO2 /Si substrate. 2006 , 139, 153-156	3
1848	The electronic structure of the interface between thin conjugated oligomer films and inorganic substrates with different work function. 2006 , 600, 3987-3991	5
1847	Electronic and geometric structure of electro-optically active organic films and associated interfaces. 2006 , 514, 156-164	23

1846	Ultraviolet lightBzone treatment of poly(3,4-ethylenedioxy-thiophene)-based materials resulting in increased work functions. 2006 , 515, 2085-2090	35
1845	Surface versus bulk electronic/defect structures of transparent conducting oxides: I. Indium oxide and ITO. 2006 , 39, 3959-3968	117
1844	Controlling semiconductor/metal junction barriers by incomplete, nonideal molecular monolayers. 2006 , 128, 6854-69	95
1843	Core-shell and segmented polymer-metal composite nanostructures. 2006 , 6, 2166-71	124
1842	Electrophysical properties of nanocomposites based on poly(p-xylylene) and copper nanoparticles. 2006 , 48, 1157-1163	5
1841	Molecular dynamics method in studies of molecular film growth processes. 2006 , 47, 532-548	1
1840	The In2O3/CdTe interface: A possible contact for thin film solar cells?. 2006 , 82, 281-285	24
1839	Electronic structure of organic interfaces 🖟 case study on perylene derivatives. 2006 , 82, 457-470	27
1838	Interface electronic properties of oligothiophenes: the effect of chain length and chemical substituents. 2006 , 600, 3978-3981	13
1837	Organic/metal interfaces in self-assembled monolayers of conjugated thiols: A first-principles benchmark study. 2006 , 600, 4548-4562	122
1836	Doping-induced realignment of molecular levels at organicBrganic heterojunctions. 2006 , 325, 129-137	77
1835	Electronic properties of organic monolayers and molecular devices. 2006 , 67, 17-32	5
1834	Effect of electrode modification on organic photovoltaic devices. 2006 , 95, 94-98	15
1833	Efficient charge injection from the S2 photoexcited state of special-pair mimic porphyrin assemblies anchored on a titanium-modified ITO anode. 2006 , 12, 8123-35	23
1832	Structural and Electrostatic Complexity at a Pentacene/Insulator Interface. 2006, 16, 879-884	127
1831	Electronic Characterization of Organic Thin Films by Kelvin Probe Force Microscopy. <i>Advanced Materials</i> , 2006 , 18, 145-164	345
1830	A green top-emitting organic light-emitting device with improved luminance and efficiency. 2006 , 39, 3738-3741	5
1829	Photoemission study of tris(8-hydroxyquinoline) aluminum/aluminum oxide/tris(8-hydroxyquinoline) aluminum interface. 2006 , 100, 113706	6

(2006-2006)

1828	Improved morphology and charge carrier injection in pentacene field-effect transistors with thiol-treated electrodes. 2006 , 100, 114517	139
1827	Energy level alignment symmetry at Co/pentacene/Co interfaces. 2006 , 100, 093714	30
1826	The temperature dependence of currentwoltage characteristics of the Au/Polypyrrole/p-Si/Al heterojunctions. 2006 , 18, 2665-2676	44
1825	Modeling the Capacitance-Voltage Characteristics of Organic Schottky Diode in the Forward Bias. 2006 , 965, 1	
1824	The Electronic Structure and the Energy Level Alignment at the Interface Between Organic Molecules and Metals. 2006 , 965, 1	
1823	Bottom Contact Ambipolar Organic Thin Film Transistors Based on C60/Pentacene Heterostructure. 2006 , 965, 1	
1822	Surface Modifications using Thiol Self-Assembled Monolayers on Au Electrodes in Organic Field Effect Transistors. 2006 , 965, 1	
1821	Improving Electrical and Optical Characteristics of White Organic Light-Emitting Diodes by Using Double Buffer Layers. 2006 , 153, H68	6
1820	High-Performance Hole-Transport Polyurethanes for Light-Emitting Diodes Applications. 2006 , 18, 4121-4129	20
1819	Electrical characterization of Fermi level pinning in metal/3,4,9,10 perylenetetracarboxylic dianhydride interfaces. 2006 , 89, 222114	15
1818	Evidence of the C60th contact formation after thermal treatment. 2006 , 88, 151103	7
1817	Current Characteristics of Pristine and Tetrathianaphthacene-Doped Tris(8-Hydroxyquinoline) Aluminum (ALQ3) Thin Films. 2006 , 455, 339-346	1
1816	Intermolecular and interlayer interactions in copper phthalocyanine films as measured with microspot photoemission spectroscopy. 2006 , 89, 202116	26
1815	Energetics at Au top and bottom contacts on conjugated polymers. 2006 , 88, 193504	83
1814	Current-voltage and capacitance-voltage characteristics of Sn/rhodamine-101Ē-Si and Sn/rhodamine-101Ē-Si Schottky barrier diodes. 2006 , 100, 074505	98
1813	Influence of alkyl chain substitution on sexithienyl-metal interface morphology and energetics. 2006 , 88, 203109	24
1812	Photophysics of Charge Carrier Generation. 2006 , 455, 183-191	
1811	Morphology, interfacial electronic structure, and optical properties of oligothiophenes grown on ZnSe(100) by molecular beam deposition. 2006 , 73,	9

1810	Roughness-induced energetic disorder at the metal/organic interface. 2006 , 73,	7
1809	Site-selective adsorption of naphthalene-tetracarboxylic-dianhydride on Ag(110): First-principles calculations. 2006 , 73,	32
1808	Surface states, surface potentials, and segregation at surfaces of tin-doped In2O3. 2006, 73,	163
1807	Hot electrons at metal-organic interface: Time-resolved two-photon photoemission study of phenol on Ag(111). 2006 , 24, 1454-1459	6
1806	High-efficiency polymer light-emitting diodes based on poly[2-methoxy-5-(2-ethylhexyloxy)-1,4-phenylene vinylene] with plasma-polymerized CHF3-modified indium tin oxide as an anode. 2006 , 88, 033512	22
1805	Improved n-type organic transistors by introducing organic heterojunction buffer layer under source/drain electrodes. 2006 , 89, 053510	47
1804	Effects of metal penetration into organic semiconductors on the electrical properties of organic thin film transistors. 2006 , 89, 132101	84
1803	Molecular monolayer modification of the cathode in organic light-emitting diodes. 2006 , 89, 223511	15
1802	True dipole at the indium tin oxide/organic semiconductor interface. 2006 , 89, 262110	4
1801	Electronic properties of the organic semiconductor interfaces CuPct 60 and C60t uPc. 2006, 99, 053704	72
1800	Energetic disorder at the metal-organic semiconductor interface. 2006 , 73,	13
1799	SCANNING TUNNELING SPECTROSCOPY (STS). 2006 , 305-350	17
1798	Electronic structure of C60 on Au(887). 2006 , 125, 144719	33
1797	THE ORGANIC LED SURFACE: A SYNCHROTRON RADIATION PHOTOEMISSION STUDY. 2007 , 14, 377-385	3
1796	p-n Type Heterostructures Based on N,N?-Dimethyl Perylene-Tetracarboxylic Acid Diimide. 2007 , 467, 107-122	8
1795	REVERSAL OF DOPING INDUCED ENERGY LEVEL SHIFT IN ORGANIC SEMICONDUCTORS. 2007 , 06, 125-129	1
1794	Electronic Structure of Bathocuproine on Metal Studied by Ultraviolet Photoemission Spectroscopy. 2007 , 46, 2692-2695	42
1793	In Situ Analysis of Hole Injection Barrier of O[sub 2] Plasma-Treated Au with Pentacene Using Photoemission Spectroscopy. 2007 , 10, H104	13

(2007-2007)

1792	poly[2-methoxy-5-(2-ethyl-hexyloxy)-p-phenylene vinylene] on gold studied using two-photon photoemission spectroscopy. 2007 , 126, 174901	7
1791	The effect of self-assembled monolayers on polarization-dependent two-photon photoemission and on the angular distribution of the photoelectrons. 2007 , 127, 121102	2
1790	Modification of Ionization Potential of Poly(ethylene dioxythiophene):Poly(styrene sulfonate) Film by Acid or Base Treatment. 2007 , 46, 7427-7431	2
1789	Characteristics of Organic Light Emitting Diodes with Tetrakis(Ethylmethylamino) Hafnium Treated Indium Tin Oxide. 2007 , 46, L461-L464	4
1788	Covalent bonding and hole-electron Coulomb interaction U in C(60) on Be(0001) surfaces. 2007 , 19, 176009	6
1787	The effects of chemical doping with F4TCNQ in carbon nanotube field-effect transistors studied by the transmission-line-model technique. 2007 , 18, 415202	47
1786	Ultra-thin fluoropolymer buffer layer as an anode stabilizer of organic light emitting devices. 2007 , 40, 4466-4470	2
1785	Improved temperature characteristics of single-wall carbon nanotube single electron transistors using carboxymethylcellulose dispersant. 2007 , 91, 263511	3
1784	On validity of the Schottky-Mott rule in organic semiconductors: Sexithiophene on various substrates. 2007 , 101, 103712	28
1783	Suppression of rectification at metalMott insulator interfaces. 2007 , 76,	18
1782	Annealing effects on interfacial electronic structures and photoexcitation kinetics of regioregular poly(3-hexylthiophene) film on gold. 2007 , 90, 171901	14
1781	Illumination induced charge separation at tetraphenyl-porphyrin/metal oxide interfaces. 2007 , 102, 053705	11
1780	Tuning hole injection and charge recombination with self-assembled monolayer on silver anode in top-emitting organic light-emitting diodes. 2007 , 90, 241104	17
1779	Modulated charge separation at tetraphenyl porphyrin/Au interfaces. 2007 , 90, 142103	10
1778	Scanning gate microscopy of copper phthalocyanine field effect transistors. 2007 , 91, 192113	9
1777	Efficient laser textured nanocrystalline silicon-polymer bilayer solar cells. 2007 , 90, 203514	21
1776	Orbital alignment at poly[2-methoxy-5-(2?-ethylhexyloxy)-p-phenylene vinylene interfaces. 2007 , 102, 023710	9
1775	Thickness-dependent energy level alignment of rubrene adsorbed on Au(111). 2007 , 90, 132121	35

1774	Photoemission study of oxygen and Au modification of doped copper phthalocyanine. 2007 , 102, 043703	18
1773	Effects of the permanent dipoles of self-assembled monolayer-treated insulator surfaces on the field-effect mobility of a pentacene thin-film transistor. 2007 , 90, 132104	83
1772	Tuning of electrical characteristics in networked carbon nanotube field-effect transistors using thiolated molecules. 2007 , 91, 103515	20
1771	Changing band offsets in copper phthalocyanine to copolymer poly(vinylidene fluoride with trifluoroethylene) heterojunctions. 2007 , 90, 242907	25
1770	Photoemission study of the electronic structures of tris-(8-hydroxyquinoline) aluminum/Li2OAl interfaces. 2007 , 91, 122101	6
1769	Control of the electrode work function and active layer morphology via surface modification of indium tin oxide for high efficiency organic photovoltaics. 2007 , 91, 112111	203
1768	Alignment of energy levels at the Alq3🛘a0.7Sr0.3MnO3 interface for organic spintronic devices. 2007 , 76,	73
1767	Interfacial electronic structure of N,N?-bis(1-naphthyl)-N,N?-diphenyl-1,1?-biphenyl-4,4?-diamine/copper phthalocyanine:C60 composite/Au studied by ultraviolet photoemission spectroscopy. 2007 , 91, 052102	17
1766	Enhanced thermal stability in organic light-emitting diodes through nanocomposite buffer layers at the anode/organic interface. 2007 , 101, 033522	26
1765	Copper phthalocyanine buffer layer to enhance the charge injection in organic thin-film transistors. 2007 , 90, 073504	54
1764	Light-induced charge separation in thin tetraphenyl-porphyrin layers deposited on Au. 2007, 75,	14
1763	Operation of a reversed pentacene-fullerene discrete heterojunction photovoltaic device. 2007 , 90, 113505	55
1762	Electronic structure and charge injection at interface between electrode and liquid-crystalline semiconductor. 2007 , 101, 024505	6
1761	Electronic Structure at Tetratetracontane/Au(111) Interface. 2007 , 1029, 1	
1760	Efficient Hole-Injection in Highly Transparent Organic Thin-Film Transistors. 2007, 10, H186	17
1759	Magnetic and Magnetotransport Properties in Nanogranular Co/C60-Co Film with High Magnetoresistance. 2007 , 48, 754-758	9
1758	Chemically Modified Oxide Electrodes. 2007,	4
1757	Charge Injection and Transport in Organic Nanofibers. 2007 , 61, 565-569	3

1756	AgX Photography: Present and Future. 2007 , 51, 110	7
1755	Study of the influence of the molecular organization on single-layer OLEDs[performances. 2007 , 157, 91-97	16
1754	Origin of charge transfer complex resulting in Ohmic contact at the C60/Cu interface. 2007, 157, 160-164	12
1753	CurrentIIoltage characteristics of Al/Rhodamine-101/n-GaAs and Cu/Rhodamine-101/n-GaAs rectifier contacts. 2007 , 157, 679-683	23
1752	Conformational adaptation and selective adatom capturing of tetrapyridyl-porphyrin molecules on a copper (111) surface. 2007 , 129, 11279-85	112
1751	Schottky contact on a ZnO (0001) single crystal with conducting polymer. 2007, 91, 142113	108
1750	Polymer Solar Cells. 2007 , 1-86	25
1749	Carbon nanotubes grown on In2O3:Sn glass as large area electrodes for organic photovoltaics. 2007 , 90, 023105	64
1748	Imaging photoelectron transmission through self-assembled monolayers: the work-function of alkanethiols coated gold. 2007 , 23, 6156-62	17
1747	Atmospheric effect of air, N2, O2, and water vapor on the ionization energy of titanyl phthalocyanine thin film studied by photoemission yield spectroscopy. 2007 , 102, 103704	54
1746	Surface transfer doping of diamond (100) by tetrafluoro-tetracyanoquinodimethane. 2007 , 129, 8084-5	93
1745	Surface transfer p-type doping of epitaxial graphene. 2007 , 129, 10418-22	517
1744	Kelvin Probe Force Microscopy of Semiconductors. 2007 , 663-689	5
1743	Spontaneous charge transfer at organic-organic homointerfaces to establish thermodynamic equilibrium. 2007 , 90, 122113	24
1742	Fixed p-i-n junction polymer light-emitting electrochemical cells based on charged self-assembled monolayers. 2007 , 90, 103508	20
1741	Novel Room Temperature Wiring Process of Ag Nanoparticle Paste. 2007,	6
1740	Density functional theory studies of reaction mechanisms for titanium alkylamide incorporation onto functionalized aromatic self-assembled monolayers. 2007 , 17, 3927	1
1739	Photophysical, electrochemical, and crystallographic investigation of conjugated fluoreno azomethines and their precursors. 2007 , 17, 2801-2811	33

1738	Electrical characterization of metal/pentacene contacts. 2007 , 101, 014510	72
1737	Electronic states of a single layer of pentacene: standing-up and flat-lying configurations. 2007 , 111, 12454-7	29
1736	1-Phenyl-1-propyne on Cu(111): TOFMS TPD, XPS, UPS, and 2PPE Studies. 2007 , 23, 12185-91	12
1735	Effects of Interfacial Organic Layers on Nucleation, Growth, and Morphological Evolution in Atomic Layer Thin Film Deposition. 2007 , 111, 11045-11058	34
1734	Phenyl Isocyanide on Cu(111): Bonding and Interfacial Energy Level Alignment. 2007, 111, 7816-7825	10
1733	Localized current injection and submicron organic light-emitting device on a pyramidal atomic force microscopy tip. 2007 , 7, 3645-9	11
1732	Phenylacetylene on Cu(111): Adsorption Geometry, Interfacial Electronic Structures and Thermal Chemistry. 2007 , 111, 5101-5110	23
1731	Ion motion in conjugated polyelectrolyte electron transporting layers. 2007 , 129, 10976-7	152
1730	Tuning of metal work function with organic carboxylates and its application in top-emitting electroluminescent devices. 2007 , 23, 7090-5	11
1729	Electrostatic properties of adsorbed polar molecules: opposite behavior of a single molecule and a molecular monolayer. 2007 , 129, 2989-97	57
1728	Copper-Doped Indium Tin Oxide Electrode for Organic Light-Emitting Devices. 2007, 46, 1640-1642	3
1727	Self-consistent analytical solution of a problem of charge-carrier injection at a conductor/insulator interface. 2007 , 75,	50
1726	The influence of the molecular dipole on the electronic structure of isomeric icosahedral dicarbadodecaborane and phosphacarbadodecaborane molecular films. 2007 , 111, 7009-16	36
1725	Novel organic materials through control of multichromophore interactions. 2007 , 72, 8615-35	159
1724	Nanostructured copper phthalocyanine-sensitized multiwall carbon nanotube films. 2007, 23, 6424-30	91
1723	Electronic structure at highly ordered organic/metal interfaces: Pentacene on Cu(110). 2007, 76,	89
1722	Adsorption of benzene on coinage metals: a theoretical analysis using wavefunction-based methods. 2007 , 111, 12778-84	37
1721	Effect of molecule-substrate interaction on thin-film structures and molecular orientation of pentacene on silver and gold. 2007 , 23, 8336-42	44

1720	Size-selective supramolecular chemistry in a hydrocarbon nanoring. 2007 , 129, 8440-2	86
1719	Influence of the electrode work function on the energy level alignment at organic-organic interfaces. 2007 , 91, 202108	64
1718	Influence of silanol groups on the electrical performance of organic thin-film transistors utilizing organosiloxane-based organicIhorganic hybrid dielectrics. 2007 , 18, 025204	17
1717	Modification of BaTiO3 thin films: adjustment of the effective surface work function. 2007 , 17, 4563	54
1716	A Highly Conjugated p- and n-Type Polythiophenoazomethine: 'Synthesis, Spectroscopic, and Electrochemical Investigation. 2007 , 40, 1792-1795	58
1715	Organometallic Complexes for Optoelectronic Applications. 2007 , 101-194	43
1714	Electronic structures of organic/organic heterojunctions: From vacuum level alignment to Fermi level pinning. 2007 , 101, 064504	92
1713	Electrical Contacts to Organic Molecular Films by Metal Evaporation: Effect of Contacting Details. 2007 , 111, 2318-2329	65
1712	Toward control of the metal-organic interfacial electronic structure in molecular electronics: a first-principles study on self-assembled monolayers of pi-conjugated molecules on noble metals. 2007 , 7, 932-40	244
1711	Interaction of Cobalt(II) Tetraarylporphyrins with a Ag(111) Surface Studied with Photoelectron Spectroscopy. 2007 , 111, 3090-3098	171
1710	Spectroscopic evidence of strong Interorbital interaction in a lead-phthalocyanine bilayer film attributed to the dimer nanostructure. 2007 , 75,	46
1709	Control of Surfaces and Interfaces in Organic Thin-Film Transistors. 2007 , 28, 242-248	1
1708	Adsorption Structure and Work Function of Succinic Acid on Cu(110) Surface. 2007, 28, 525-531	3
1707	Structural and Electronic Properties of the First Monolayers of Spin-Cast Poly(fluorene)-Based Conjugated- Polymer Films. 2007 , 17, 1093-1105	16
1706	A Kelvin Probe Force Microscopy Study of the Photogeneration of Surface Charges in All-Thiophene Photovoltaic Blends. 2007 , 17, 472-478	66
1705	Surface-Transfer Doping of Organic Semiconductors Using Functionalized Self-Assembled Monolayers. 2007 , 17, 1339-1344	53
1704	Depolarization Effects in Self-Assembled Monolayers: A Quantum-Chemical Insight. 2007 , 17, 1143-1148	96
1703	The Role of the Ionization Potential in Vacuum-Level Alignment at Organic Semiconductor Interfaces. <i>Advanced Materials</i> , 2007 , 19, 665-668	118

1702	Charge-Injection Barriers at Realistic Metal/Organic Interfaces: Metals Become Faceless. <i>Advanced Materials</i> , 2007 , 19, 754-756	24	41
1701	Ambipolar Transport in Organic Conjugated Materials. <i>Advanced Materials</i> , 2007 , 19, 1791-1799	24	253
1700	Electrostatic Properties of Ideal and Non-ideal Polar Organic Monolayers: Implications for Electronic Devices. <i>Advanced Materials</i> , 2007 , 19, 4103-4117	24	212
1699	Interface Fermi level pinning at contacts between PEDOT: PSS and molecular organic semiconductors. 2007 , 8, 386-90		30
1698	Organic electronic devices and their functional interfaces. 2007 , 8, 1438-55		663
1697	Characteristics of photoexcitations and interfacial energy levels of regioregular poly(3-hexythiophene-2,5-diyl) on gold. 2007 , 8, 1937-42		12
1696	Molecular level alignment and work function change of dimethyldisulfide physisorbed thin films on Au(1 1 1). 2007 , 601, 2592-2596		5
1695	AdsorbateBubstrate bonding and the growth of naphthalene thin films on Ag(1 1 1). 2007, 601, 2307-23	314	11
1694	Device relevant organic films and interfaces: A surface science approach. 2007 , 601, 5683-5689		27
1693	A unified model for metal/organic interfaces: IDIS, pillowleffect and molecular permanent dipoles. 2007 , 254, 378-382		29
1692	Hole-injection from a polar mono-molecular layer derivatised ultra-thin gold electrode into a triphenylamine derivative. 2007 , 434, 82-85		5
1691	Regiorandom poly(3-hexylthiophene) on gold: Interfacial electronic structures and photoexcitation kinetics. 2007 , 436, 228-232		10
1690	Effective anchoring energy in dipolar organic film on metals surfaces. 2007, 438, 244-248		5
1689	Oxygen effect on the interfacial electronic structure of C60 film studied by ultraviolet photoelectron spectroscopy. 2007 , 441, 63-67		42
1688	Novel method for room temperature sintering of Ag nanoparticle paste in air. 2007, 441, 305-308		114
1687	Photoexcitation quenching and interfacial electronic structures of photo-oxidized MEH-PPV film on gold studied using two-photon photoemission spectroscopy. 2007 , 444, 125-129		2
1686	Occupied and unoccupied electronic states of benzene adsorbed Cu(110) surface. 2007 , 445, 198-202		10
1685	Electron spectra of a self-assembled monolayer on gold: Inverse photoemission and two-photon photoemission spectroscopy. 2007 , 446, 359-364		12

1684	Photoemission study of direct hole injection into Alq3 by PEDOT:PSS polymer anode. 2007 , 446, 317-322	15
1683	Energy level alignment between sexithiophene and buckminsterfullerene films. 2007, 448, 65-69	24
1682	Photoemission microspectroscopy and imaging of bilayer islands formed in monolayer titanyl phthalocyanine films. 2007 , 449, 319-322	14
1681	Internal electric fields in vacuum-evaporated organic films as studied by electroabsorption spectroscopy. 2007 , 334, 216-223	5
1680	Induced Density of States model for weakly-interacting organic semiconductor interfaces. 2007 , 8, 241-248	128
1679	Energy level alignment and morphology of interfaces between molecular and polymeric organic semiconductors. 2007 , 8, 606-614	104
1678	New hole-transport polyurethanes applied to polymer light-emitting diodes. 2007 , 43, 4279-4288	10
1677	Energy level alignment regimes at hybrid organic@rganic and inorganic@rganic interfaces. 2007 , 8, 14-20	124
1676	The electronic band alignment on nanoscopically patterned substrates. 2007, 8, 63-68	35
1675	Novel approach for energy band diagram and barrier heights in metal/organic structures. 2007 , 8, 382-388	2
1674	The electronic structure of Ni-phthalocyanine/metal interfaces studied by X-ray and ultraviolet photoelectron spectroscopy. 2007 , 8, 522-528	58
1673	Energy level alignment and interface states at Bexithiophene/Ag interfaces. 2007, 8, 625-630	23
1672	Scanning probe microscopy investigation of self-organized perylenetetracarboxdiimide nanostructures at surfaces: structural and electronic properties. 2007 , 3, 161-7	25
1671	Thermal, photophysical, and electrochemical characterization of a conjugated polyazomethine prepared by anodic electropolymerization of a thiophenoazomethine co-monomer. 2007 , 61, 5102-5106	27
1670	Formation of organic films on the indium arsenide surface. 2007 , 52, 235-238	
1669	Influence of the substrate properties on the electronic structure of organic film-inorganic substrate interfaces. 2007 , 52, 1163-1168	4
1668	Consistent experimental determination of the charge neutrality level and the pillow effect at metal/organic interfaces. 2007 , 91, 244103	11
1667	Energy level alignment at metal/organic semiconductor interfaces: "pillow" effect, induced density of interface states, and charge neutrality level. 2007 , 126, 144703	167

1666	Electronic structure of hybrid interfaces for polymer-based electronics. 2007 , 19, 183202	102
1665	Electron and ambipolar transport in organic field-effect transistors. 2007 , 107, 1296-323	1846
1664	Assessment of density-functional models for organic molecular semiconductors: The role of Hartreeflock exchange in charge-transfer processes. 2007 , 331, 321-331	59
1663	Electronic structure of 1 ML NTCDA/Ag(1 1 1) studied by photoemission spectroscopy. 2007 , 601, 4013-4017	50
1662	Probing the interaction at the C60BiC nanomesh interface. 2007 , 601, 2994-3002	8
1661	Interactions at tetraphenyl-porphyrin/InP interfaces observed by surface photovoltage spectroscopy. 2008 , 254, 3255-3261	19
1660	Adsorption structure and work function of dicarboxylic acid on Cu(110) surface. 2008 , 254, 7835-7837	6
1659	Investigation of top-emitting organic light-emitting devices with highly saturated color employing metal-mirror structure. 2008 , 29, 250-253	O
1658	Surface potential measurement of organic photo-diode consisting of fullerene/copper phthalocyanine double layered device. 2008 , 516, 2562-2567	12
1657	Interfacial analysis and properties of regioregular poly(3-hexyl thiophene) spin-coated on an indium tin oxide-coated glass substrate. 2008 , 43, 5599-5604	16
1656	Electrical characteristics and inhomogeneous barrier analysis of aniline green/p-Si heterojunctions. 2008 , 19, 986-991	15
1655	Energy band and electron-vibration coupling in organic thin films: photoelectron spectroscopy as a powerful tool for studying the charge transport. 2008 , 92, 495-504	46
1654	Bond cutting in K-doped tris(8-hydroxyquinoline) aluminium. 2008 , 15, 519-24	1
1653	Fine structure of the electrostatic energetic disorder at the interface between disordered organic material and metal electrode. 2008 , 5, 750-754	3
1652	Electronic structure investigation of nickel phthalocyanine thin film interfaces with inorganic and organic substrates. 2008 , 5, 3708-3711	3
1651	Molecular beam deposition and characterization of thin organic films on metals for applications in organic electronics. 2008 , 205, 497-510	47
1650	Interface electronic structures of zinc oxide and metals: First-principle study. 2008 , 205, 1929-1933	21
1649	Alignment of the energy levels and charge injection barriers at interfaces for spin injection: La0.7Sr0.3MnO3 in contact with organic semiconductors. 2008 , 245, 799-803	4

(2008-2008)

1648	Intermolecular band dispersion in highly ordered monolayer and multilayer films of pentacene on Cu(110). 2008 , 245, 793-798		32
1647	Effect of dopant concentration on charge transport in crosslinkable polymers. 2008 , 245, 814-819		8
1646	The larger acenes: versatile organic semiconductors. 2008 , 47, 452-83		1666
1645	Reversible phototuning of ferromagnetism at Au-S interfaces at room temperature. 2008 , 47, 160-3		67
1644	Self-assembled Electroactive Phosphonic Acids on ITO: Maximizing Hole-Injection in Polymer Light-Emitting Diodes. 2008 , 18, 3964-3971		85
1643	Origin of Carrier Types in Intrinsic Organic Semiconductors. <i>Advanced Materials</i> , 2008 , 20, 2084-2089	24	16
1642	Water-Soluble Polyfluorenes as an Electron Injecting Layer in PLEDs for Extremely High Quantum Efficiency. <i>Advanced Materials</i> , 2008 , 20, 1624-1629	24	78
1641	Heterogeneous Interfacial Properties of Ink-Jet-Printed Silver Nanoparticulate Electrode and Organic Semiconductor. <i>Advanced Materials</i> , 2008 , 20, NA-NA	24	12
1640	Self-Organized Buffer Layers in Organic Solar Cells. Advanced Materials, 2008, 20, 2211-2216	24	229
1639	Recent Applications of Conjugated Polyelectrolytes in Optoelectronic Devices. <i>Advanced Materials</i> , 2008 , 20, 3793-3810	24	336
1638	Dipolar Chromophore Functional Layers in Organic Field Effect Transistors. <i>Advanced Materials</i> , 2008 , 20, NA-NA	24	6
1637	HBere Acene: vielseitige organische Halbleiter. 2008 , 120, 460-492		449
1636	Reversible Phototuning of Ferromagnetism at Auß Interfaces at Room Temperature. 2008, 120, 166-16	9	14
1635	PTCDA on Au(1 1 1), Ag(1 1 1) and Cu(1 1 1): Correlation of interface charge transfer to bonding distance. 2008 , 9, 111-118		206
1634	Low and small resistance hole-injection barrier for NPB realized by wide-gap p-type degenerate semiconductor, LaCuOSe:Mg. 2008 , 9, 890-894		28
1633	Injection of charge into the archetype organic hole transporting material TPD at the electrical contacts with ITO and Al. 2008 , 9, 883-889		6
1632	Self-assembled monolayers mediated charge injection for high performance bottom-contact poly(3,3???-didodecylquaterthiophene) thin-film transistors. 2008 , 9, 936-943		25
1631	Electron spectroscopy of functional organic thin films: Deep insights into valence electronic structure in relation to charge transport property. 2008 , 83, 490-557		230

1630	Kelvin Probe measurements of polymer coated gold substrates: Mechanism studies. 2008, 134, 266-272	7
1629	ElectronNibration interactions in carrier-transport material: Vibronic coupling density analysis in TPD. 2008 , 458, 152-156	36
1628	Organic heterojunction ambipolar field effect transistors with asymmetric source and drain electrodes. 2008 , 516, 2758-2761	4
1627	Organic tunneling devices and field effect transistors using polycrystalline naphthalene diimine frameworks. 2008 , 516, 3436-3440	2
1626	Effect of insertion of a thin bathocuproine layer at Au/Znphthalocyanine interface on energy level alignment and morphology. 2008 , 516, 1006-1011	5
1625	Improved performances in a top-emitting green organic light-emitting device with light magnification. 2008 , 516, 3364-3367	6
1624	Different approaches to adjusting band offsets at intermolecular interfaces. 2008 , 254, 4238-4244	14
1623	Dual enhancing properties of LiF with varying positions inside organic light-emitting devices. 2008 , 9, 30-38	17
1622	Lower hole-injection barrier between pentacene and a 1-hexadecanethiol-modified gold substrate with a lowered work function. 2008 , 9, 21-29	42
1621	Effect of interfacial layer thickness on the formation of interface dipole in metal/tris(8-hydroxyquinoline) aluminum interface. 2008 , 9, 678-686	11
1620	Manganite/Alq3 interfaces investigated by impedance spectroscopy technique. 2008, 9, 911-915	6
1619	A role of metal d-band in the interfacial electronic structure at organic/metal interface: PTCDA on Au, Ag and Cu. 2008 , 9, 783-789	20
1618	Electronic properties of the interface between the organic semiconductor Bexithiophene and polycrystalline palladium. 2008 , 9, 767-774	8
1618 1617		137
	polycrystalline palladium. 2008, 9, 767-774 The role of molybdenum oxide as anode interfacial modification in the improvement of efficiency	
1617	polycrystalline palladium. 2008, 9, 767-774 The role of molybdenum oxide as anode interfacial modification in the improvement of efficiency and stability in organic light-emitting diodes. 2008, 9, 985-993 Modeling the electrical characteristics of TIPS-pentacene thin-film transistors: Effect of contact	137
1617 1616	polycrystalline palladium. 2008, 9, 767-774 The role of molybdenum oxide as anode interfacial modification in the improvement of efficiency and stability in organic light-emitting diodes. 2008, 9, 985-993 Modeling the electrical characteristics of TIPS-pentacene thin-film transistors: Effect of contact barrier, field-dependent mobility, and traps. 2008, 9, 1026-1031 Organic light-emitting devices (OLEDs) and OLED-based chemical and biological sensors: an	137 64

(2008-2008)

1612	Analytical model for the open-circuit voltage and its associated resistance in organic planar heterojunction solar cells. 2008 , 77,	181
1611	X-ray diffraction study of the molecular propolis films deposited from an alcohol solution onto the cleavage surfaces of layered V2VI3 compounds. 2008 , 53, 1215-1221	3
1610	Orientation-dependent ionization energies and interface dipoles in ordered molecular assemblies. 2008 , 7, 326-32	512
1609	Indium Tin Oxide Modified by Au and Vanadium Pentoxide as an Efficient Anode for Organic Light-Emitting Devices. 2008 , 55, 2517-2520	17
1608	Resonant two-photon photoemission study of electronically excited states at the lead phthalocyanine/graphite interface. 2008 , 77,	24
1607	Mechanism of hole accumulation at ₽NPD/Alq 3 interface studied by displacement current measurement. 2008 ,	7
1606	Effect of ZnO Processing on the Photovoltage of ZnO/Poly(3-hexylthiophene) Solar Cells. 2008 , 112, 9544-9547	109
1605	Poly[2-methoxy-5-(2?-ethyl-hexyloxy)-p-phenylene vinylene] (MEH-PPV)/poly(3-hexylthiophene-2,5-diyl) (P3HT) heterolayer film on gold: two-photon photoemission spectroscopy. 2008 , 20, 215204	2
1604	Change in Molecular Conformation of Dibenzo-Crown Ether Induced by Weak MoleculeBubstrate Interaction. 2008 , 112, 4643-4648	17
1603	Tailoring the Work Function of Gold Surface by Controlling Coverage and Disorder of Polar Molecular Monolayers. 2008 , 112, 12988-12992	46
1602	PEDOT-Type Materials in Organic Solar Cells. 211-242	3
1601	Reversible work function changes induced by photoisomerization of asymmetric azobenzene dithiol self-assembled monolayers on gold. 2008 , 93, 083109	41
1600	Hole-transporting hydrazones. 2008, 37, 770-88	141
1599	Energy levels at interfaces between metals and conjugated organic molecules. 2008, 20, 184008	131
1598	The interface energetics of self-assembled monolayers on metals. 2008, 41, 721-9	340
1597	Ballistic electron microscopy of nanographene layers. 2008 , 8, 4259-64	10
1596	Electronic potential of a chemisorption interface. 2008, 78,	61
1595	Temperature dependent Schottky barrier height and Fermi level pinning on Au/HBC/GaAs diodes. 2008 , 92, 153309	5

1594	Electronic coupling in organic-inorganic semiconductor hybrid structures with type-II energy level alignment. 2008 , 77,	26
1593	Electrical characteristics of single-component ambipolar organic field-effect transistors and effects of air exposure on them. 2008 , 103, 094509	46
1592	Accurate calculation of transport properties for organic molecular semiconductors with spin-component scaled MP2 and modern density functional theory methods. 2008 , 129, 024103	38
1591	Organic light emitting diodes using a Ga:ZnO anode. 2008 , 92, 193304	95
1590	Reverse bias capacitanceNoltage characteristics of Al/polyaniline/p-Si/Al structure as a function of temperature. 2008 , 354, 4991-4995	18
1589	Electronic structures of 8-hydroquinolatolithium on Au substrate: The organic electron injection layer having semiconducting properties. 2008 , 158, 984-987	7
1588	Electronic structure of copper phthalocyanine: a comparative density functional theory study. 2008 , 128, 164107	143
1587	Semiconductor junction gas sensors. 2008 , 108, 367-99	198
1586	Microscopic mechanism of dipole layer formation at the pentacene/Si interface. 2008, 78,	4
1585	Molecular Orientation-Dependent Ionization Potential of Organic Thin Films. 2008, 20, 7017-7021	140
1584	Theoretical Characterization of the Indium Tin Oxide Surface and of Its Binding Sites for Adsorption of Phosphonic Acid Monolayers. 2008 , 20, 5131-5133	120
1583	Spectroscopy of C60single molecules: the role of screening on energy level alignment. 2008 , 20, 184001	78
1582	Nanostructured organic-inorganic photodiodes with high rectification ratio. 2008 , 19, 495202	35
1581	Contact resistance and electrode material dependence of air-stable n-channel organic field-effect transistors using dimethyldicyanoquinonediimine (DMDCNQI). 2008 , 18, 4165	33
1580	The use of size-selective excitation to study photocurrent through junctions containing single-size and multi-size arrays of colloidal CdSe quantum dots. 2008 , 130, 83-92	41
1579	Analyzing Bipolar Carrier Transport Characteristics of Diarylamino-Substituted Heterocyclic Compounds in Organic Light-Emitting Diodes by Probing Electroluminescence Spectra. 2008 , 20, 4439-4446	64
1578	Molecularly controlled metal-semiconductor junctions on silicon surface: a dipole effect. 2008 , 24, 11300-6	47
1577	Single-Layered Films of Diblock Copolymer Micelles Containing Quantum Dots and Fluorescent Dyes and Their Fluorescence Resonance Energy Transfer. 2008 , 20, 4185-4187	22

(2008-2008)

1576	Investigation of Corrosion-Inhibiting Aniline Oligomer Thin Films on Iron Using Photoelectron Spectroscopy. 2008 , 112, 18991-19004	14
1575	Evolution of the Electronic Structure at the Interface between a Thin Film of Halogenated Phthalocyanine and the Ag(111) Surface. 2008 , 112, 8654-8661	12
1574	Physical and Electronic Structure Effects of Embedded Dipoles in Self-Assembled Monolayers: Characterization of Mid-Chain Ester Functionalized Alkanethiols on Au{111}. 2008 , 112, 10842-10854	55
1573	Selective metal deposition on photoswitchable molecular surfaces. 2008 , 130, 10740-7	63
1572	Variable density effect of self-assembled polarizable monolayers on the electronic properties of silicon. 2008 , 130, 4158-65	42
1571	Gas-surface reactions between pentakis(dimethylamido)tantalum and surface grown hyperbranched polyglycidol films. 2008 , 24, 8610-9	6
1570	Abnormal charge injection behavior at metal-organic interfaces. 2008, 78,	17
1569	Adsorption-induced intramolecular dipole: correlating molecular conformation and interface electronic structure. 2008 , 130, 7300-4	138
1568	Interface-Induced Spin and Dipole Ordering of the Copper Spin 1/2 Molecule: Bis(4-cyano-2,2,6,6-tetramethyl-3,5-heptanedionato)copper(II). 2008 , 112, 13656-13662	5
1567	Characterization of transparent conducting oxide surfaces using self-assembled electroactive monolayers. 2008 , 24, 5755-65	30
1566	Energy level alignments at tris(8-hydroquinoline) aluminum/8-hydroquinolatolithium/aluminum interfaces. 2008 , 92, 093304	13
1565	Bottom-contact poly(3,3'''-didodecylquaterthiophene) thin-film transistors with gold source-drain electrodes modified by alkanethiol monolayers. 2008 , 24, 11889-94	9
1564	Odd-even effects in self-assembled monolayers of omega-(biphenyl-4-yl)alkanethiols: a first-principles study. 2008 , 24, 474-82	69
1563	Electronic properties of conjugated polyelectrolyte thin films. 2008, 130, 10042-3	110
1562	Charge Transfer and Polarization Screening at Organic/Metal Interfaces: Distinguishing between the First Layer and Thin Films. 2008 , 112, 5703-5706	28
1561	Structure and Electrical Bistability of a New Class of Diphenyl-bithiophenes: A Combined Theoretical and Experimental Study. 2008 , 112, 18628-18637	7
1560	Low-Temperature Scanning Tunneling Microscopy and Near-Edge X-ray Absorption Fine Structure Investigations of Molecular Orientation of Copper(II) Phthalocyanine Thin Films at Organic Heterojunction Interfaces. 2008 , 112, 5036-5042	59
1559	Interfacial Electronic Properties of Thiophene and Sexithiophene Adsorbed on a Fluorinated Alkanethiol Monolayer. 2008 , 112, 1174-1182	21

1558	Tailoring the Electron Affinity and Electron Emission of Diamond (100) 2 🗈 by Surface Functionalization Using an Organic Semiconductor. 2008 , 20, 6871-6879	13
1557	Air-Stable, Cross-Linkable, Hole-Injecting/Transporting Interlayers for Improved Charge Injection in Organic Light-Emitting Diodes. 2008 , 20, 4873-4882	30
1556	Size-dependent charge collection in junctions containing single-size and multi-size arrays of colloidal CdSe quantum dots. 2008 , 130, 74-82	54
1555	Tuning of Ag work functions by self-assembled monolayers of aromatic thiols for an efficient hole injection for solution processed triisopropylsilylethynyl pentacene organic thin film transistors. 2008 , 92, 143311	218
1554	Energy level alignment at organic semiconductor/metal interfaces: effect of polar self-assembled monolayers at the interface. 2008 , 128, 074705	37
1553	Reducing the Metal Work Function beyond Pauli Pushback: A Computational Investigation of Tetrathiafulvalene and Viologen on Coinage Metal Surfaces. 2008 , 112, 20357-20365	42
1552	Molecular Conformation, Organizational Chirality, and Iron Metalation of meso-Tetramesitylporphyrins on Copper(100). 2008 , 112, 8988-8994	64
1551	TipBample Interactions in Kelvin Probe Force Microscopy: Quantitative Measurement of the Local Surface Potential. 2008 , 112, 17368-17377	52
1550	Tuning the ionization energy of organic semiconductor films: the role of intramolecular polar bonds. 2008 , 130, 12870-1	145
1549	A theoretical view on self-assembled monolayers in organic electronic devices. 2008,	6
1548	STRUCTURAL AND ELECTRONIC PROPERTIES OF METAL-DOPED ORGANIC SEMICONDUCTORS. 2008 , 22, 1609-1631	2
1547	First-principles theoretical study of Alq3Al interfaces: origin of the interfacial dipole. 2008 , 128, 244704	48
1546	Electronic structure of the indium tin oxide/nanocrystalline anatase (TiO2)/ruthenium-dye interfaces in dye-sensitized solar cells. 2008 , 104, 073714	23
1545	Effect of Self-Assembled Monolayer on Electroluminescence Properties of Organic Light-Emitting Diodes. 2008 , 47, 455-459	24
1544	A high-resolution near-edge x-ray absorption fine structure investigation of the molecular orientation in the pentacene/poly(3,4-ethylenedioxythiophene):poly(styrenesulfonate) pentacene/system. 2008 , 128, 014705	20
1543	Temperature dependence of conformation, chemical state, and metal-directed assembly of tetrapyridyl-porphyrin on Cu(111). 2008 , 129, 214702	82
1542	Electronic structure of single-walled carbon nanotubes on ultrathin insulating films. 2008, 93, 233104	10
1541	A New Conducting Polymer Electrode for Organic Electroluminescence Devices. 2008 , 25, 3052-3055	4

1540	Electron injection into organic semiconductor devices from high work function cathodes. 2008 , 105, 12730-5	123
1539	Interface dipole formation of different ZnPcCl(8) phases on Ag(111) observed by Kelvin probe force microscopy. 2008 , 19, 305501	16
1538	Reducing the contact resistance of bottom-contact pentacene thin-film transistors by employing a MoOx carrier injection layer. 2008 , 92, 013301	117
1537	Interface electronic states and molecular structure of a triarylamine based hole conductor on rutile TiO2(110). 2008 , 128, 184709	18
1536	Degradation studies on high-voltage-driven organic light-emitting device using in situ on-operation method with scanning photoelectron microscopy. 2008 , 93, 133310	6
1535	Bias-induced doping engineering with ionic adsorbates on single-walled carbon nanotube thin film transistors. 2008 , 10, 113013	3
1534	Fabrication and electrical properties of organic-on-inorganic Schottky devices. 2008 , 20, 215210	20
1533	Performance Enhancement of Organic Thin-Film Transistors with C60/Au Bilayer Electrode. 2008 , 47, 5668-5671	8
1532	Characterization of Organic/Metal Interfaces Using Angle-Resolved X-ray Photoelectron Spectroscopy. 2008 , 47, 1393-1396	3
1531	Ballistic emission microscopy studies on metal-molecule interfaces. 2008 , 20, 374113	3
1530	Oxygen-Related Degradation Mechanisms for On- and Off-States of Perfluoropentacene Thin-Film Transistors. 2008 , 47, 3643-3646	24
1529	Ultraviolet Photoemission Study of Interaction between Bathocuproine and Calcium. 2008, 47, 1397-1399	12
1528	Electronic and vibronic interactions at weakly bound organic interfaces: The case of pentacene on graphite. 2008 , 78,	29
1527	Adsorption and bonding mechanism of a N,N?-di(n-butyl)quinacridone monolayer studied by density functional theory including semiempirical dispersion corrections. 2008 , 78,	3
1526	Excimer-based red/near-infrared organic light-emitting diodes with very high quantum efficiency. 2008 , 92, 113302	80
1525	Structural and electronic properties of pentacene-fullerene heterojunctions. 2008 , 104, 114518	89
1524	Energy level alignment and injection barriers at spin injection contacts between La0.7Sr0.3MnO3 and organic semiconductors. 2008 , 92, 023302	20
1523	Direct observation of the electronic states of single crystalline rubrene under ambient condition by photoelectron yield spectroscopy. 2008 , 93, 173305	67

1522	Comment on Schottky contact on a ZnO (0001) single crystal with conducting polymer[[Appl. Phys. Lett. 91, 142113 (2007)]. 2008 , 92, 046101	8
1521	Integer charge transfer at the tetrakis(dimethylamino)ethylene/Au interface. 2008, 92, 163302	40
1520	Characterization of copper selenide thin film hole-injection layers deposited at room temperature for use with p-type organic semiconductors. 2008 , 104, 113723	14
1519	Interfacial reactions between indium tin oxide and triphenylamine tetramer layers induced by photoirradiation. 2008 , 103, 093543	5
1518	Slope parameters at metal-organic interfaces. 2008 , 93, 093502	9
1517	Contact resistance of dibenzotetrathiafulvalene-based organic transistors with metal and organic electrodes. 2008 , 92, 023305	62
1516	Solution-processed carbon electrodes for organic field-effect transistors. 2008 , 93, 213303	25
1515	Energy level alignment and chemical interaction at Alq3/Co interfaces for organic spintronic devices. 2008 , 78,	89
1514	Gold work function reduction by 2.2eV with an air-stable molecular donor layer. 2008, 93, 243303	71
1513	Unified model for the injection and transport of charge in organic diodes. 2008 , 103, 064504	27
1512	Charge-carrier induced barrier-height reduction at organic heterojunction. 2008, 78,	26
1511	Absence of spin transport in the organic semiconductor Alq3. 2008, 77,	95
1510	Reproducible Single-molecule Conductance Measurements of 1,4-Benzenedithiol with Break Junction Methods by Diluting It in a Thin Insulating Monolayer. 2008 , 37, 408-409	5
1509	Bipolar charge-carrier injection in semiconductor/insulator/conductor heterostructures: Self-consistent consideration. 2008 , 104, 073719	8
1508	Vacuum sublimed #dihexylsexithiophene thin films: Correlating electronic structure and molecular orientation. 2008 , 104, 033717	19
1507	P-222: Solution-Processed Red-Emission Oligofluorene Electrophosphorescent Diodes. 2008 , 39, 2039	
1506	Scanning gate study of organic thin-film field-effect transistor. 2008 , 109, 012007	2
1505	. 2008,	223

1504	(Tetrathiafulvalene)(tetracyanoquinodimethane) as a Contact Material for n-Channel and Ambipolar Organic Transistors. 2008 , 1, 051801	10
1503	Giant magnetoresistance in ferromagnet/organic semiconductor/ferromagnet heterojunctions. 2009 , 80,	97
1502	Interfacial electronic properties of pentacene tuned by a molecular monolayer of C60. 2009, 80,	20
1501	Towards an accurate description of the electronic properties of the biphenylthiol/gold interface: the role of exact exchange. 2009 , 131, 234101	23
1500	Low-density band-gap states in pentacene thin films probed with ultrahigh-sensitivity ultraviolet photoelectron spectroscopy. 2009 , 95, 183303	120
1499	Critical evaluation of band bending determination in organic films from photoemission measurements. 2009 , 27, 1178-1182	9
1498	Electrical properties of GaN/poly(3-hexylthiophene) interfaces. 2009 , 106, 013713	7
1497	Spontaneous buildup of surface potential with a thin film of a zwitterionic molecule giving noncentrosymmetric crystal structure. 2009 , 95, 182901	4
1496	Effect of phosphonic acid surface modifiers on the work function of indium tin oxide and on the charge injection barrier into organic single-layer diodes. 2009 , 105, 074511	29
1495	Electronegativity equalization model for interface barrier formation at reactive metal/organic contacts. 2009 , 95, 173303	3
1494	Controlling energy level offsets in organic/organic heterostructures using intramolecular polar bonds. 2009 , 94, 033304	53
1493	Selectively patterned highly conductive poly(3,4-ethylenedioxythiophene)-tosylate electrodes for high performance organic field-effect transistors. 2009 , 95, 233509	7
1492	F4TCNQ on Cu, Ag, and Au as prototypical example for a strong organic acceptor on coinage metals. 2009 , 79,	108
1491	Organic thin-film solar cells with a Cu anode: Improvement of the photovoltaic properties on aging in air. 2009 , 106, 064510	7
1490	Transfer-arm evaporator cell for rapid loading and deposition of organic thin films. 2009, 80, 125101	12
1489	The thermal-field emission model for carrier injection characteristics of an organic field effect transistor. 2009 , 94, 073303	3
1488	Surface chemistry and surface electronic properties of ZnO single crystals and nanorods. 2009, 27, 328-335	22
1487	Influence of ionization energy change on valence band offset in organic p-n junction. 2009 , 95, 113306	7

1486	Interfacial electronic structure of a hybrid organic-inorganic optical upconverter device: The role of interface states. 2009 , 105, 083706	14
1485	Electronic structures of Ba-on-Alq3 interfaces and device characteristics of organic light-emitting diodes based on these interfaces. 2009 , 105, 083705	5
1484	Role of delta-hole-doped interfaces at Ohmic contacts to organic semiconductors. 2009 , 103, 036601	29
1483	Direct measurement of electric field screening in light emitting diodes with conjugated polyelectrolyte electron injecting/transport layers. 2009 , 94, 033301	29
1482	Interdiffusion of molecular acceptors through organic layers to metal substrates mimics doping-related energy level shifts. 2009 , 95, 093305	41
1481	Interface dipole at metal-organic interfaces: Contribution of metal induced interface states. 2009 , 94, 113304	24
1480	Light-Emitting Characteristics of Organic Light-Emitting Diodes with Ba/Al Cathode and Effect of Ba Thickness by Measuring their Built-in Potential. 2009 , 48, 122102	3
1479	Enhanced open-circuit voltage in polymer solar cells. 2009 , 95, 043301	115
1478	Interfacial properties of the K-doped C60: CuPc heterojunctions. 2009 ,	
1477	ELECTROLUMINESCENT PROPERTIES OF CERTAIN POLYAROMATIC COMPOUNDS: PART 2DRGANIC EMITTERS. 2009 , 29, 139-159	15
1476	Increase in Open-Circuit Voltage and Improved Stability of Organic Solar Cells by Inserting a Molybdenum Trioxide Buffer Layer. 2009 , 1154, 1	
1475	Visualization of bias-dependent potential barriers using scanning gate microscopy in copper-phthalocyanine field-effect transistor. 2009 , 27, 785	4
1474	Level alignment of gap state at organic-metal interface. 2009 , 106, 043715	10
1473	Interfacial electronic structure of copper phthalocyanine on a gold surface studied by synchrotron radiation photoemission. 2009 , 106, 113716	7
1472	High-barrier rectifying contacts on undoped ZnO films with (NH4)2Sxtreatment owing to Fermi-level pinning. 2009 , 42, 075308	14
1471	Study of the electronic structure at the interface between fluorene-1-carboxylic acid molecules and Cu(110). 2009 , 21, 355005	1
1470	Fully solution-processed organic solar cells on metal foil substrates. 2009,	1
1469	Electron Transport Properties and Dielectric Breakdown of Alkyl Monolayers Chemisorbed on a Highly Doped n-Type Si(111) Surface. 2009 , 48, 055003	9

1468	Density functional theory calculations and the induced density of interface states model for noble metals/C60 interfaces. 2009 , 27, 2008	4
1467	Molecular orientation and electronic structure of 11,11,12,12-tetracyanonaphtho-2,6-quinodimethane vacuum-deposited on metal substrates: Charge transfer, complexation, and potassium doping. 2009 , 105, 023703	10
1466	Interface properties of a Li3PO4/Al cathode in organic light emitting diodes. 2009, 105, 124517	7
1465	Charge transfer at polymer-electrode interfaces: The effect of energetic disorder and thermal injection on band bending and open-circuit voltage. 2009 , 106, 034507	75
1464	Photoelectron spectroscopy study of systematically varied doping concentrations in an organic semiconductor layer using a molecular p-dopant. 2009 , 106, 103711	117
1463	Substrate effects on the interface electronic properties of organic photovoltaic devices with an inverted C60/CuPc junction. 2009 , 106, 114501	15
1462	Adsorption of cobalt (II) octaethylporphyrin and 2H-octaethylporphyrin on Ag(111): new insight into the surface coordinative bond. 2009 , 11, 125004	68
1461	Tungsten oxide doped N,N?-di(naphthalen-1-yl)-N,N?-diphenyl-benzidine as hole injection layer for high performance organic light-emitting diodes. 2009 , 105, 084518	19
1460	Charge transfer between acenes and PbS nanocrystals. 2009 , 20, 195205	8
1459	Structural and photo-physical properties of spin-coated poly(3-hexylthiophene) thin films. 2009 , 116, 279-283	59
1458	Energy Level Alignment and Interactions at Potential Contacts for Spin Injection into Organic Semiconductors. 2009 , 11, 285-290	7
1457	Quantum-Chemical Characterization of the Origin of Dipole Formation at Molecular Organic/Organic Interfaces. 2009 , 19, 624-633	59
1456	Hole Injection in a Model Fluorene Triarylamine Copolymer. 2009 , 19, 304-310	32
1455	Organic Photovoltaic Cells Based On Solvent-Annealed, Textured Titanyl Phthalocyanine/C60 Heterojunctions. 2009 , 19, 1913-1921	110
1454	Controlling Electron and Hole Charge Injection in Ambipolar Organic Field-Effect Transistors by Self-Assembled Monolayers. 2009 , 19, 2407-2415	195
1453	Nanoscale Phase Separation and High Photovoltaic Efficiency in Solution-Processed, Small-Molecule Bulk Heterojunction Solar Cells. 2009 , 19, 3063-3069	841
1452	Origins of Improved Hole-Injection Efficiency by the Deposition of MoO3 on the Polymeric Semiconductor Poly(dioctylfluorene-alt-benzothiadiazole). 2009 , 19, 3746-3752	95
1451	Intrinsic Surface Dipoles Control the Energy Levels of Conjugated Polymers. 2009 , 19, 3874-3879	59

1450	Electronic Structure and Geminate Pair Energetics at Organic Organic Interfaces: The Case of Pentacene/C60 Heterojunctions. 2009 , 19, 3809-3814		204
1449	Electronic Properties at Gold/Conjugated-Polyelectrolyte Interfaces. Advanced Materials, 2009, 21, 100	16 <u>21</u> 1011	l 119
1448	Solvent effects on the architecture and performance of polymer white-light-emitting diodes with conjugated oligoelectrolyte electron-transport layers. <i>Advanced Materials</i> , 2009 , 21, 584-8	24	47
1447	Energy-Level Alignment at Organic/Metal and Organic/Organic Interfaces. <i>Advanced Materials</i> , 2009 , 21, 1450-1472	24	1269
1446	Single-Layer Pentacene Field-Effect Transistors Using Electrodes Modified With Self-assembled Monolayers. <i>Advanced Materials</i> , 2009 , 21, 4109-4114	24	92
1445	Patterned Graphene Electrodes from Solution-Processed Graphite Oxide Films for Organic Field-Effect Transistors. <i>Advanced Materials</i> , 2009 , 21, 3488-3491	24	323
1444	Organic Single-Crystal Schottky Gate Transistors. <i>Advanced Materials</i> , 2009 , 21, 3689-3693	24	36
1443	Oxidized gold thin films: an effective material for high-performance flexible organic optoelectronics. <i>Advanced Materials</i> , 2010 , 22, 2037-40	24	42
1442	Exciton binding energies in conjugated polyelectrolyte films. 2009 , 10, 1023-7		28
1441	A high molecular weight donor for electron injection interlayers on metal electrodes. 2009 , 10, 2947-54	1	14
1440	Organic/Organic' heterojunctions: organic light emitting diodes and organic photovoltaic devices. 2009 , 30, 717-31		170
1439	Adsorption structure of phenylphosphonic acid on an alumina surface. 2009 , 256, 1140-1143		9
1438	Surface characteristics of indium tin oxide deposited by facing target sputtering and its effect on the performance of organic light emitting diode. 2009 , 9, S237-S240		1
1437	Low-temperature scanning tunneling microscopy and near-edge X-ray absorption fine structure investigation of epitaxial growth of F16CuPc thin films on graphite. 2009 , 95, 107-111		23
1436	Energy level alignment at interfaces between organic semiconductors and clean ferromagnetic La0.7Sr0.3MnO3 thin film contacts for spin injection. 2009 , 95, 95-99		7
1435	Charge transfer and polarization screening in organic thin films: phthalocyanines on Au(100). 2009 , 95, 173-178		18
1434	Dipoles and band alignment for benzene/Au(111) and C60/Au(111) interfaces. 2009 , 95, 119-124		28
1433	Electronic structure at rubrene metal interfaces. 2009 , 95, 89-94		23

1432	Organic heterojunctions of layered perylene and phthalocyanine dyes: characterization with UV-photoelectron spectroscopy and luminescence quenching. 2009 , 95, 209-218	20
1431	Structural and electronic implications for carrier injection into organic semiconductors. 2009 , 97, 1-9	12
1430	Tuning the electrical properties of Si nanowire field-effect transistors by molecular engineering. 2009 , 5, 2761-9	72
1429	Synthesis, characterization, and electroluminescent performance of a novel copolyfluorene containing pendant crown ether groups. 2009 , 47, 2985-2995	7
1428	Tuning intermolecular interaction in long-range-ordered submonolayer organic films. 2009 , 5, 153-158	221
1427	Energetics of metalorganic interfaces: New experiments and assessment of the field. 2009, 64, 1-31	526
1426	Low-voltage, high-performance n-channel organic thin-film transistors based on tantalum pentoxide insulator modified by polar polymers. 2009 , 10, 346-351	31
1425	Investigation of the interfaces formed between ITO and metal phthalocyanines (NiPc and CoPc) by photoelectron spectroscopy. 2009 , 10, 1382-1387	17
1424	Optical absorption spectra of ultrathin PTCDA films on gold single crystals: Charge transfer beyond the first monolayer. 2009 , 10, 1448-1453	21
1423	Photoisomerization of azobenzene containing self-assembled monolayers investigated by Kelvin probe work function measurements. 2009 , 172, 128-133	23
1422	Impact of interface geometric structure on organichetal interface energetics and subsequent films electronic structure. 2009 , 174, 28-34	27
1421	Classical ultraviolet photoelectron spectroscopy of polymers. 2009 , 174, 3-9	17
1420	First-principles study of the pentacene/Cu(111) interface: Adsorption states and vacuum level shifts. 2009 , 174, 78-84	43
1419	Electronic non-equilibrium conditions at C60pentacene heterostructures. 2009, 174, 40-44	10
1418	Modification of Shockley surface state by long-chain n-alkane: Photoemission study on tetratetracontane/Au(111) interface. 2009 , 517, 3276-3280	11
1417	Surface potentials of magnetron sputtered transparent conducting oxides. 2009 , 518, 1197-1203	125
1416	Theoretical study on possible usage of difluoromethylene fullerenes as electron-transport materials. 2009 , 518, 477-480	15
1415	Improvement of stability for organic solar cells by using molybdenum trioxide buffer layer. 2009 , 518, 537-540	33

1414 Structural analysis and transistor properties of hetero-molecular bilayers. 2009 , 518, 441-443	8
Internal photoemission spectroscopy measurement of Alq3/cathode interface by three layered electron only device. 2009 , 518, 791-794	6
1412 Work function changes in gas sensitive materials: Fundamentals and applications. 2009 , 142, 470-493	119
Enhanced electron injection in organic light-emitting devices by using a composite electron injection layer composed of 8-hydroquinolatolithium and cesium oxide. 2009 , 149, 652-656	15
1410 Fresh perspectives for surface coordination chemistry. 2009 , 603, 1533-1541	227
Understanding the electronic properties of molecule/metal junctions: The case study of thiols on gold. 2009 , 603, 1518-1525	21
First-principles study of benzene on noble metal surfaces: Adsorption states and vacuum level shifts. 2009 , 603, 2912-2922	79
1407 Isomeric effects with di-iodobenzene (C6H4I2) on adsorption on graphite. 2009 , 603, 2964-2971	5
1406 Efficient organic solar cells with polyfluorene derivatives as a cathode interfacial layer. 2009 , 10, 496-500	109
1405 Role of interfacial dipole layer for energy-level alignment at organic/metal interfaces. 2009 , 10, 990-993	19
Using metal/organic junction engineering to prepare an efficient organic base-modulation triode and its inverter. 2009 , 10, 1636-1640	7
Electron injection property at the organic interface in organic light-emitting devices revealed by current voltage characteristics. 2009 , 404, 1247-1250	6
Size-reduction induced ferromagnetism and photo-magnetic effects in azobenzene-thiol-passivated gold nanoparticles. 2009 , 28, 1868-1874	20
1401 Surface transfer doping of semiconductors. 2009 , 84, 279-321	240
1400 Layer growth and desorption kinetics of a discoid molecular acceptor on Au(1 1 1). 2009 , 473, 321-325	28
On the difference in electronic properties between fullerene C60 and C60X2. 2009 , 476, 253-257	14
Synchrotron PES and NEXAFS studies of self-assembled aromatic thiol monolayers on Au(1 1 1). 2009 , 172, 54-63	12
Electronic structure of self-assembled (fluoro)methylthiol monolayers on the Au(111) surface: Impact of fluorination and coverage density. 2009 , 174, 70-77	12

1396	diodes. 2009 , 45, 1545-1553	11
1395	An inverted polymer photovoltaic cell with increased air stability obtained by employing novel hole/electron collecting layers. 2009 , 19, 1643	126
1394	Formation of electronic junctions on molecularly modified surfaces by lift-and-float electrical contacts. 2009 , 25, 3305-9	14
1393	Molecular understanding of organic solar cells: the challenges. 2009 , 42, 1691-9	1176
1392	Orientation-controlled charge transfer at CuPc/F16CuPc interfaces. 2009 , 106, 064910	48
1391	Fullerene/thiol-terminated molecules. 2009 , 74, 7885-97	32
1390	Formation and electron properties of the interface between organic (TPD) and inorganic (ZnO) materials. 2009 , 35, 359-361	1
1389	Spatial Tuning of the Metal Work Function by Means of Alkanethiol and Fluorinated Alkanethiol Gradients. 2009 , 113, 5620-5628	47
1388	Charge conduction and breakdown mechanisms in self-assembled nanodielectrics. 2009, 131, 7158-68	58
1387	Surface-segregated monolayers: a new type of ordered monolayer for surface modification of organic semiconductors. 2009 , 131, 17597-604	75
1386	Direct detection of molecular biorecognition by dipole sensing mechanism. 2009 , 131, 4788-94	28
1385	Modification of Charge Transfer and Energy Level Alignment at Organic/TiO2 Interfaces. 2009 , 113, 13765-13	771
1384	A Photoemission Study of the Morphology and Barrier Heights of the Interface between Chyrsene and Inert Substrates. 2009 , 113, 1837-1849	11
1383	Ultrathin Films of Diindenoperylene on Graphite and SiO2. 2009 , 113, 9251-9255	25
1382	Preparation and characterization of 4'-donor substituted stilbene-4-thiolate monolayers and their influence on the work function of gold. 2009 , 25, 7967-75	24
1381	Reversible phototuning of the large anisotropic magnetization at the interface between a self-assembled photochromic monolayer and gold. 2009 , 131, 865-70	59
1380	Site-Specific Charge-Transfer Screening at Organic/Metal Interfaces. 2009 , 113, 19244-19250	45
1379	Controlling Surface Energetics of Silicon by Intermolecular Interactions between Parallel Self-Assembled Molecular Dipoles. 2009 , 113, 1993-1997	19

1378	Continuous modulation of electrode work function with mixed self-assembled monolayers and its effect in charge injection. 2009 , 25, 6232-8	81
1377	Cationic Conjugated Polyelectrolyte Electron Injection Layers: Effect of Halide Counterions. 2009 , 113, 2950-2954	38
1376	Understanding the electronic structure of metal/SAM/organic-semiconductor heterojunctions. 2009 , 3, 3513-20	45
1375	Molecular design, device function and surface potential of zwitterionic electron injection layers. 2009 , 131, 8903-12	39
1374	Anomalous tunneling in carbon/alkane/TiO(2)/gold molecular electronic junctions: energy level alignment at the metal/semiconductor interface. 2009 , 1, 443-51	17
1373	Comprehensive Evaluation of Electron Mobility for a Trifluoroacetyl-Terminated Electronegative Conjugated Oligomer. 2009 , 113, 17189-17193	25
1372	Energy level alignment at the anode of poly(3-hexylthiophene)/fullerene-based solar cells. 2009, 1, 741-5	8
1371	Improved injection in n-type organic transistors with conjugated polyelectrolytes. 2009, 131, 18220-1	106
1370	Red-emission oligofluorene electrophosphorescent diodes based on bis[2-(9,9-dihexyl-9H-fluoren-2-yl)quinolineC3,N]acetylacetonatoiridium(III) and solvent treatment for interface modification. 2009 , 1, 76-82	2
1369	Tuning Work Function of Noble Metals As Promising Cathodes in Organic Electronic Devices. 2009 , 21, 2798-2802	20
1368	Resistive molecular memories: influence of molecular parameters on the electrical bistability. 2009 , 131, 6591-8	79
1367	Engineering of the Energy Level Alignment at Organic Semiconductor Interfaces by Intramolecular Degrees of Freedom: Transition Metal Phthalocyanines. 2009 , 113, 13219-13222	44
1366	Thiophene-based hydrazones as hole-transporting materials. 2009 , 159, 223-227	10
1365	The origin of hole injection improvements with MoO3/Al bilayer electrodes in pentacene thin-film transistors. 2009 , 159, 2502-2505	24
1364	The role of the interface in the electronic structure of adsorbed metal(II) (Co, Ni, Cu) phthalocyanines. 2009 , 19, 2172	33
1363	The fabrication and analysis of a PbS nanocrystal:C(60) bilayer hybrid photovoltaic system. 2009 , 20, 245202	22
1362	Organic field-effect transistors using single crystals. 2009 , 10, 024314	305
1361	ELECTROLUMINESCENT PROPERTIES OF CERTAIN POLYAROMATIC COMPOUNDS: PART 1THARACTERISTICS OF OLED DEVICES BASED ON FLUORESCENT POLYAROMATIC DOPANTS. 2009, 29, 123-138	4

1360	Contact resistance and threshold voltage extraction in n-channel organic thin film transistors on plastic substrates. 2009 , 105, 084510	45
1359	Tuning the graphene work function by electric field effect. 2009 , 9, 3430-4	1073
1358	Self-assembly of carboranethiol isomers on Au111: intermolecular interactions determined by molecular dipole orientations. 2009 , 3, 527-36	77
1357	The formation of a charge layer at the interface of GaMnAs and an organic material. 2009 , 88, 46002	1
1356	Theoretical investigation of the electronic structure of the Alq(3)/Mg interface. 2009, 21, 064247	12
1355	Energy level alignment at the interfaces in a multilayer organic light-emitting diode structure. 2009 , 79,	62
1354	Energy-level alignment and charge injection at metal/C60/organic interfaces. 2009, 95, 043302	22
1353	Photoinduced hole-transfer in semiconducting polymer/low-bandgap cyanine dye blends: evidence for unit charge separation quantum yield. 2009 , 11, 8886-94	23
1352	Optical differential reflectance spectroscopy of ultrathin epitaxial organic films. 2009, 11, 2142-55	81
1351	Molybdenum-Doped Zinc Oxide Electrodes for Organic Light-Emitting Devices. 2009 , 12, J47	3
1350	Modelling energy level alignment at organic interfaces and density functional theory. 2009 , 11, 8658-75	129
1349	Carrier Transport in Zinc Phthalocyanine Doped with a Fluorinated Perylene Derivative: Bulk Conductivity versus Interfacial Injection. 2009 , 113, 17160-17169	6
1348	Inkjet-printed zinc tin oxide thin-film transistor. 2009 , 25, 11149-54	97
1347	Chemical and electronic properties of the ITO/Al(2)O(3) interface. 2009 , 11, 3049-54	37
1346	Studying Transient Carrier Behaviors in Pentacene Field Effect Transistors Using Visualized Electric Field Migration. 2009 , 113, 10279-10284	35
1345	Molecular Orientation Dependent Energy Level Alignment at Organic Drganic Heterojunction Interfaces. 2009 , 113, 12832-12839	74
1344	Surface Structure and Electronic Properties of In2O3(111) Single-Crystal Thin Films Grown on Y-Stabilized ZrO2(111). 2009 , 21, 4353-4355	51
1343	Nanoscale contacts between carbon nanotubes and metallic pads. 2009 , 3, 4117-21	13

1342	Low Threshold Voltage and Carrier Injection Properties of Inverted Organic Light-Emitting Diodes with [Ca24Al28O64]4+(4e]ICathode and Cu2ISe Anode. 2009 , 113, 18379-18384	42
1341	Fluorine Substitution of Hexa-peri-hexabenzocoronene: Change in Growth Mode and Electronic Structure. 2009 , 113, 6202-6207	11
1340	Photocurrent hysteresis by ion motion within conjugated polyelectrolyte electron transporting layers. 2009 , 19, 211-214	20
1339	CapacitanceNoltage and currentNoltage characteristics of Au Schottky contact on n-type Si with a conducting polymer. 2009 , 42, 165104	35
1338	Selective metal deposition for a structure with a thin intermediate layer on a photochromic diarylethene film. 2009 , 19, 3176	12
1337	Fabrication of titanium oxide/phthalocyanine hybrid multilayers and their application to interface control for an organic diode. 2009 , 19, 8403	8
1336	Enhanced hole injection in organic light-emitting devices by using Fe3O4 as an anodic buffer layer. 2009 , 94, 223306	40
1335	Fermi level depinning at metal-organic semiconductor interface for low-resistance Ohmic contacts. 2009 ,	4
1334	Temperature dependence of the electrical and interface states of the Sn/Rhodamine-101/p-Si Schottky structures. 2009 , 159, 347-351	22
1333	Electronic structure at the perylene-tetracarboxylic acid dianhydride/Ag(111) interface studied with two-photon photoelectron spectroscopy. 2009 , 131, 144701	35
1332	Interfacial energy levels and related properties of atomic-layer-deposited Al2O3 films on nanoporous TiO2 electrodes of dye-sensitized solar cells. 2009 , 20, 305201	42
1331	Tuning the Effective Work Function of Gold and Silver Using Functionalized Alkanethiols: Varying Surface Composition through Dilution and Choice of Terminal Groups. 2009 , 113, 20328-20334	107
1330	Interfaces in Organic Field-Effect Transistors. 2009 , 113-153	17
1329	Changes in the adsorbate dipole layer with changing d-filling of the metal (II) (Co, Ni, Cu) phthalocyanines on Au(111). 2009 , 21, 052001	15
1328	Interface dipole formation between GaMnAs and organic material. 2009, 193, 012105	
1327	Influence of side chain of [6,6]-phenyl-C61-butyric acid methyl ester on interfacial electronic structure of [6,6]-phenyl-C61-butyric acid methyl ester /Ag substrate. 2009 , 94, 043309	10
1326	Carrier injection property of C60thin film transistor via displacement current measurement. 2009 , 159, 012014	
1325	Stability of Chemically Modified IndiumIIinDxide Surfaces against Water. 2009 , 38, 266-267	3

1324	Electric Conduction Properties of Self-assembled Monolayer Films of Ru Complexes with Disulfide/Phosphonate Anchors in a Au[Molecular Ensemble][Au Nanoparticle] Junction. 2009 , 38, 416-417	31
1323	Energy-level alignment of aryl thiols chemisorbed on metal surfaces: implications for charge transport. 2009 ,	1
1322	Vertical alignment of liquid crystals by ordering effect of selfassembled monolayers on the Ion-beam-irradiated anisotropic surface. 2010 , 11, 144-148	2
1321	Electronic Processes at Organic/Metal Interfaces: Recent Progress and Pitfalls. 2010 , 14, 198-211	8
1320	P-158: Connecting Architecture for Organic Light-emitting Diodes Integrated with Organic Photovoltaic Device. 2010 , 41, 1841	
1319	Origin of Surface-Band Dispersion at the Pentacene/Cu Interface. 2010 , 3, 025701	9
1318	The Synthesis of EDOT Monomer, and Its Physical and Chemical Properties. 2010, 69-88	2
1317	Time-resolved measurements of electron transfer processes at the PTCDA/Ag(111) interface. 2010 , 75, 23-30	18
1316	Prospects of colloidal nanocrystals for electronic and optoelectronic applications. 2010 , 110, 389-458	3354
1315	Molecular semiconductors in organic photovoltaic cells. 2010 , 110, 6689-735	773
1314	Interface investigation and engineering lachieving high performance polymer photovoltaic devices. 2010 , 20, 2575	521
1313	ToF-SIMS study of gold/phthalocyanine interface. 2010 , 256, 1946-1950	8
1312	Experimental measurement of work function in doped silicon surfaces. 2010 , 54, 8-13	60
1311	Structural Analysis on Organic Thin-Film Transistor With Device Simulation. 2010 , 57, 195-200	89
1310	Energy-Level Alignment at Metal Organic and Organic Organic Interfaces in Bulk-Heterojunction Solar Cells. 2010 , 16, 1718-1724	25
1309	Electronic structure and interface properties of a model molecule for organic solar cells. 2010 , 11, 269-75	18
1308	Controlled reorientation of CuPc molecules in ordered structures assembled on the TiO(2)(011)-(2x1) surface. 2010 , 11, 1863-6	13
1307	Polarizability, Susceptibility, and Dielectric Constant of Nanometer-Scale Molecular Films: A Microscopic View. 2010 , 20, 2077-2084	47

1306	Interface Engineering for Organic Electronics. 2010 , 20, 1371-1388		806
1305	Water-Soluble Polyfluorenes as an Interfacial Layer Leading to Cathode-Independent High Performance of Organic Solar Cells. 2010 , 20, 1977-1983		191
1304	Recent progress in n-channel organic thin-film transistors. Advanced Materials, 2010, 22, 1331-45	24	268
1303	Molecules on si: electronics with chemistry. <i>Advanced Materials</i> , 2010 , 22, 140-59	24	197
1302	Chemical and physical sensing by organic field-effect transistors and related devices. <i>Advanced Materials</i> , 2010 , 22, 3799-811	24	250
1301	Modeling the electronic properties of pi-conjugated self-assembled monolayers. <i>Advanced Materials</i> , 2010 , 22, 2494-513	24	107
1300	Dipolar compounds containing fluorene and a heteroaromatic ring as the conjugating bridge for high-performance dye-sensitized solar cells. 2010 , 16, 3184-93		123
1299	Reversible Optical Manipulation of Superconductivity. 2010 , 122, 382-384		5
1298	Reversible optical manipulation of superconductivity. 2010 , 49, 372-4		25
1297	Gap states at organicfhetal interfaces: A combined spectroscopic and theoretical study. 2010 , 256, 4054	1-4064	11
<i>,</i>	Gap states at organichetal interfaces: A combined spectroscopic and theoretical study. 2010 , 256, 4054 Electrochemical promotion of catalytic reactions. 2010 , 85, 241-278	1-4064	32
<i>,</i>		1-4064	
1296	Electrochemical promotion of catalytic reactions. 2010 , 85, 241-278 Efficient hole injection in organic light-emitting diodes using polyvinylidenefluoride as an	1-4064	
1296 1295	Electrochemical promotion of catalytic reactions. 2010 , 85, 241-278 Efficient hole injection in organic light-emitting diodes using polyvinylidenefluoride as an interlayer. 2010 , 130, 1708-1710 Role of air exposure in the improvement of injection efficiency of transition metal oxide/organic	1-4064	32
1296 1295 1294	Electrochemical promotion of catalytic reactions. 2010 , 85, 241-278 Efficient hole injection in organic light-emitting diodes using polyvinylidenefluoride as an interlayer. 2010 , 130, 1708-1710 Role of air exposure in the improvement of injection efficiency of transition metal oxide/organic contact. 2010 , 11, 89-94	1-4064	32
1296 1295 1294 1293	Electrochemical promotion of catalytic reactions. 2010, 85, 241-278 Efficient hole injection in organic light-emitting diodes using polyvinylidenefluoride as an interlayer. 2010, 130, 1708-1710 Role of air exposure in the improvement of injection efficiency of transition metal oxide/organic contact. 2010, 11, 89-94 Electronic structure of anode interface with molybdenum oxide buffer layer. 2010, 11, 188-194 Modification of gold source and drain electrodes by self-assembled monolayer in staggered n- and	1-4064	32 37 156
1296 1295 1294 1293	Electrochemical promotion of catalytic reactions. 2010, 85, 241-278 Efficient hole injection in organic light-emitting diodes using polyvinylidenefluoride as an interlayer. 2010, 130, 1708-1710 Role of air exposure in the improvement of injection efficiency of transition metal oxide/organic contact. 2010, 11, 89-94 Electronic structure of anode interface with molybdenum oxide buffer layer. 2010, 11, 188-194 Modification of gold source and drain electrodes by self-assembled monolayer in staggered n- and p-channel organic thin film transistors. 2010, 11, 227-237 Charging energy, self-interaction correction and transport energy gap for a nanogap organic	1-4064	32 37 156 96

1288	Surface analytical studies of interfaces in organic semiconductor devices. 2010 , 68, 39-87	180
1287	The initial interface formation between Al and tris-(8-hydroquinoline) aluminum (Alq3) with LiF interlayer. 2010 , 11, 164-168	7
1286	Fermi level equilibrium at donor acceptor interfaces in multi-layered thin film stack of TTF and TCNQ. 2010 , 11, 212-217	49
1285	Anomalous hysteresis in organic field-effect transistors with SAM-modified electrodes: Structural switching of SAMs by electric field. 2010 , 11, 1025-1030	15
1284	Synthesis of dihydroindolizines for potential photoinduced work function alteration. 2010 , 51, 6839-6842	12
1283	Light-emitting characteristics of organic light-emitting diodes with the MoOx-doped NPB and C60/LiF layer. 2010 , 518, 6339-6342	8
1282	Interface controlled current injection in hydrazone doped polyesters. 2010 , 519, 1391-1396	2
1281	Extraction of electronic parameters of Schottky diode based on an organic Indigotindisulfonate Sodium (IS). 2010 , 150, 1592-1596	21
1280	Modifying electronic properties at the siliconholecule interface using atomic tethers. 2010 , 54, 1657-1664	29
1279	Electronic energy alignment at the PbSe quantum dots/ZnO(101 0) interface. 2010 , 604, 1335-1341	39
1278	Interfacial electronic structure of vanadyl naphthalocyanine on highly ordered pyrolytic graphite. 2010 , 604, 1649-1657	17
1277	Two-dimensional ordering of pentafluorobenzenethiol self-assembled monolayers on Au(111) prepared by ambient-pressure vapor deposition. 2010 , 110, 666-9	3
1276	Interaction of bathocuproine with metals (Ca, Mg, Al, Ag, and Au) studied by density functional theory. 2010 , 256, 2661-2667	13
1275	CurrentWoltage characterization of Au contact on solgel ZnO films with and without conducting polymer. 2010 , 256, 4493-4496	14
1274	Thickness-dependent electronic properties and molecular orientation of diradical metal complex thin films grown on SiO2. 2010 , 487, 67-70	5
1273	The interfacial electronic structure of fullerene/ultra thin dielectrics of SiO2 and SiON. 2010 , 499, 136-140	3
1272	Control of charge separation by electric field manipulation in polymer-oxide hybrid organic photovoltaic bilayer devices. 2010 , 207, 1257-1265	12
1271	The role of exact-exchange in the theoretical description of organic-metal interfaces. 2010 , 110, 2162-2171	16

1270	Charge-transfer-induced structural rearrangements at both sides of organic/metal interfaces. 2010 , 2, 374-9	244
1269	Portrait of the potential barrier at metal-organic nanocontacts. 2010 , 9, 320-3	73
1268	Azine- and Azole-Functionalized Oligo: and Polythiophene Semiconductors for Organic Thin-Film Transistors. 2010 , 3, 1533-1558	32
1267	Issue of Interfaces in Organic Light-Emitting Diodes. 2010 , 53, 8-12	
1266	Interfacial energy level alignment at acid oxidised carbon nanotube -triphenyldiamine contacts. 2010 , 1258, 1	
1265	Built-in Potential of a Pentacene Pin Homojunction Studied by Ultraviolet Photoemission Spectroscopy. 2010 , 1270, 1	1
1264	Revised hole injection mechanism of a thin LiF layer introduced between pentacene and an indium tin oxide anode. 2010 , 108, 053701	18
1263	Fullerene and Pentacene as a Pure Organic Connecting Layer in Tandem Organic Light Emitting Devices. 2010 , 157, H69	14
1262	Barrier formation and charging energy for a variable nanogap organic molecular junction: a tip/C60/Au(111) configuration. 2010 , 22, 304007	13
1261	Enhanced performance of inverted polymer solar cells with cathode interfacial tuning via water-soluble polyfluorenes. 2010 , 97, 223305	117
1260	Distinct C60 growth modes on anthracene carboxylic acid templates. 2010 , 96, 143115	10
1259	Submolecular-scale Investigations on metal-phthalocyanine monolayers by frequency modulation atomic force microscopy. 2010 , 107, 024315	8
1258	Effect of electrostatic screening on apparent shifts in photoemission spectra near metal/organic interfaces. 2010 , 81,	32
1257	Influence of intramolecular polar bonds on interface energetics in perfluoro-pentacene on Ag(111). 2010 , 81,	63
1256	Contact engineering for organic semiconductor devices via Fermi level depinning at the metal-organic interface. 2010 , 82,	62
1255	Electronic mapping of molecular orbitals at the molecule-metal interface. 2010 , 105, 066801	22
1254	Tuning the electron injection barrier between Co and C60 using Alq3 buffer layer. 2010 , 108, 103719	6
1253	Site-specific geometric and electronic relaxations at organic-metal interfaces. 2010 , 105, 046103	43

(2010-2010)

1252	energy structure. 2010 , 97, 073303	24
1251	Transistor gating by polar molecular monolayers. 2010 , 97, 053501	8
1250	Influence of gap states on electrical properties at interface between bathocuproine and various types of metals. 2010 , 107, 043707	50
1249	Hybridization and charge transfer at the anthracene/Cu(110) interface: Comparison to pentacene. 2010 , 81,	6
1248	Work function control of hole-selective polymer/ITO anode contacts: an electrochemical doping study. 2010 , 20, 2672	49
1247	Single cysteine adsorption on Au(110): A first-principles study. 2010 , 81,	41
1246	Electronic structure of ultrathin heteromolecular organic-metal interfaces: SnPc/PTCDA/Ag(111) and SnPc/Ag(111). 2010 , 82,	35
1245	Infrared spectroscopy of the organic monolayer sandwiched between a Hg electrode and a Si substrate. 2010 , 81, 053103	3
1244	Resonant effects on two-photon photoemission spectroscopy: Linewidths and intensities of occupied and unoccupied features for lead phthalocyanine films on graphite. 2010 , 81,	28
1243	Charge carrier injection into insulating media: Single-particle versus mean-field approach. 2010 , 81,	14
1242	Current-voltage characteristics of organic photovoltaic cells following deposition of cathode electrode. 2010 , 97, 193307	3
1241	Hybrid interfaces of biological molecules and metals: The prototypical case of adenine on Cu(110). 2010 , 132, 184705	9
1240	In situ study of pentacene interaction with archetypal hybrid contacts: Fluorinated versus alkane thiols on gold. 2010 , 82,	40
1239	On the origin of efficient electron injection at phosphonate-functionalized polyfluorene/aluminum interface in efficient polymer light-emitting diodes. 2010 , 97, 043506	20
1238	Electronic Structure and Dynamics at Organic Donor/Acceptor Interfaces. 2010, 35, 443-448	36
1237	Effect of Self-Assembled Monolayer Modification on Indium I in Oxide Surface for Surface-Initiated Vapor Deposition Polymerization of Carbazole Thin Films. 2010 , 49, 04DK21	12
1236	Interfacial properties and formation of a Schottky barrier at the CdS/PEDOT : PSS hybrid junction. 2010 , 43, 185301	12
1235	Field-effect-tuned lateral organic diodes. 2010 , 107, 3972-6	36

1234	Transparent Conducting Oxides for Photovoltaics: Manipulation of Fermi Level, Work Function and Energy Band Alignment. 2010 , 3, 4892-4914	300
1233	Tuning of C60 energy levels using orientation-controlled phthalocyanine films. 2010 , 108, 053706	20
1232	High-efficiency inverted bulk heterojunction polymer solar cells with UV ozone-treated ultrathin aluminum interlayer. 2010 , 97, 063509	41
1231	Charge injection barrier and interface dipole formation in pentacene/semimetal heterostructures. 2010 , 97, 093303	3
1230	Comparison of Surface Modifications by Wet and Dry Methods on Indium Tin Oxide Using Self-Assembled Monolayers. 2010 , 49, 025701	3
1229	Surface Potential Switching of Au-Depositedp-Sexiphenyl Film Controlled by Visible Light Irradiation. 2010 , 49, 01AE11	
1228	Ambipolar Transport in Bilayer Organic Field-Effect Transistor Based on Poly(3-hexylthiophene) and Fullerene Derivatives. 2010 , 49, 041601	25
1227	Image states at the interface with a dipolar organic semiconductor. 2010 , 133, 124701	17
1226	Potassium-benzene interactions on Pt(111) studied by metastable atom electron spectroscopy. 2010 , 133, 134704	3
1225	Electronic Properties of Organic-Based Interfaces. 2010 , 35, 417-421	42
1224	The interface bonding and orientation of a quinonoid zwitterion. 2010 , 12, 10329-40	29
1223	Density-dependent reorientation and rehybridization of chemisorbed conjugated molecules for controlling interface electronic structure. 2010 , 104, 246805	51
1222	Improvement of power conversion efficiency of phthalocyanine/C60 heterojunction solar cells by inserting a lithium phthalocyanine layer at the indium-tin oxide/phthalocyanine interface. 2010 , 97, 253306	8
1221	Band-offset engineering in organic/inorganic semiconductor hybrid structures. 2010 , 12, 11642-6	50
1220	Electronic Structure of Co-Phthalocyanine on Gold Investigated by Photoexcited Electron Spectroscopies: Indication of Co IonMetal Interaction. 2010 , 114, 17638-17643	76
1219	Resistive memories based on Rose Bengal and related xanthene derivatives: insights from modeling charge transport properties. 2010 , 12, 1600-9	14
1218	Intermolecular Effects on the Hole States of Triisopropylsilylethynyl-Substituted Oligoacenes. 2010 , 114, 13838-13845	22
1217	Surface engineering for high performance organic electronic devices: the chemical approach. 2010 ,	

1216	Interface materials for organic solar cells. 2010 , 20, 2499	634
1215	Electronic Structure of C60/Phthalocyanine/ITO Interfaces Studied using Soft X-ray Spectroscopies. 2010 , 114, 1928-1933	91
1214	Site-specific electronic and geometric interface structure of Co-tetraphenyl-porphyrin layers on Ag(111). 2010 , 81,	119
1213	On the Interface Dipole at the Pentacene Hullerene Heterojunction: A Theoretical Study. 2010 , 114, 3215-3224	121
1212	Fully solution-processed inverted polymer solar cells with laminated nanowire electrodes. 2010, 4, 30-4	253
1211	Hole transport in the organic small molecule material ENPD: evidence for the presence of correlated disorder. 2010 , 107, 113710	69
121 0	Organic photovoltaics: principles and techniques for nanometre scale characterization. 2010 , 21, 492001	68
1209	Electronic structure of large disc-type donors and acceptors. 2010 , 12, 7184-93	17
1208	Photoemission spectroscopy of tethered CdSe nanocrystals: shifts in ionization potential and local vacuum level as a function of nanocrystal capping ligand. 2010 , 2, 863-9	73
1207	Work-function modification beyond pinning: when do molecular dipoles count?. 2010 , 10, 4369-74	63
1206	Template-directed molecular assembly on silicon carbide nanomesh: comparison between CuPc and pentacene. 2010 , 4, 849-54	13
1205	Novel Growth of Naphthalene Overlayer on Cu(111) Studied by STM, LEED, and 2PPE. 2010 , 114, 13334-13339	30
1204	Electrical Properties of Organic Light-Emitting Diodes with an Insertion of CMTS Self-Assembled Monolayers. 2010 , 520, 49/[325]-54/[330]	
1203	The electronic structure of mixed self-assembled monolayers. 2010 , 4, 6735-46	34
1202	MetalMolecule Interfaces Formed by Noble-MetalChalcogen Bonds for Nanoscale Molecular Devices. 2010 , 114, 4044-4050	12
1201	Effect of Fluorination on the Molecular Packing of Perfluoropentacene and Pentacene Ultrathin Films on Ag (111). 2010 , 114, 9356-9361	35
1200	The effect of nonideal polar monolayers on molecular gated transistors. 2010 , 2, 2289-92	2
1199	Simultaneously Understanding the Geometric and Electronic Structure of Anthraceneselenolate on Au(111): A Combined Theoretical and Experimental Study. 2010 , 114, 2677-2684	32

1198	Organic heterostructures in organic field-effect transistors. 2010 , 2, 69-78	124
1197	Analysis of Bonding between Conjugated Organic Molecules and Noble Metal Surfaces Using Orbital Overlap Populations. 2010 , 6, 3481-3489	9
1196	Charge Transfer and Molecular Orientation of Tetrafluoro-tetracyanoquinodimethane on a Hydrogen-Terminated Si(111) Surface Prepared by a Wet Chemical Method. 2010 , 1, 1655-1659	18
1195	Control of Two-Dimensional Ordering of F16CuPc on Bi/Ag(111): Effect of Interfacial Interactions. 2010 , 114, 11234-11241	15
1194	Copper phthalocyanine on hydrogenated and bare diamond (001)-2 \times 1: influence of interfacial interactions on molecular orientations. 2010 , 26, 165-72	21
1193	Soft X-ray Spectroscopy of C60/Copper Phthalocyanine/MoO3 Interfaces: Role of Reduced MoO3 on Energetic Band Alignment and Improved Performance. 2010 , 114, 18252-18257	33
1192	Fluorinated Phenoxy Boron Subphthalocyanines in Organic Light-Emitting Diodes. 2010 , 2, 1934-1944	97
1191	Nanoscale quantitative measurement of the potential of charged nanostructures by electrostatic and Kelvin probe force microscopy: unraveling electronic processes in complex materials. 2010 , 43, 541-50	147
1190	Linear tuning of charge carriers in graphene by organic molecules and charge-transfer complexes. 2010 , 81,	79
1189	Adsorption kinetics and charge inversion in layer-by-layer films from nickel tetrasulfonated phthalocyanine and poly(allylamine hydrochloride). 2010 , 356, 937-940	8
1188	A photoemission study of interfaces between organic semiconductors and Co as well as Al2O3/Co contacts. 2010 , 160, 238-243	18
1187	N-channel operation of pentacene thin-film transistors with ultrathin polymer gate buffer layer. 2010 , 160, 83-87	8
1186	The effect of copper hexadecafluorophthalocyanine (F16CuPc) inter-layer on pentacene thin-film transistors. 2010 , 160, 108-112	10
1185	A particularly strong organic acceptor for tuning the hole-injection barriers in modern organic devices. 2010 , 160, 1456-1462	6
1184	Ultrafast interfacial proton-coupled electron transfer. 2010 , 110, 7082-99	65
1183	Nanoparticles functionalised with reversible molecular and supramolecular switches. 2010 , 39, 2203-37	447
1182	Water/alcohol soluble conjugated polymers as highly efficient electron transporting/injection layer in optoelectronic devices. 2010 , 39, 2500-21	383
1181	Elucidating the factors that determine the open circuit voltage in discrete heterojunction organic photovoltaic cells. 2010 , 20, 1173-1178	25

(2011-2010)

1180	semiconductorfhetal contact measured with in situ ultraviolet photoemission spectroscopy. 2010 , 20, 9754	13
1179	Control of electronic structure of graphene by various dopants and their effects on a nanogenerator. 2010 , 132, 15603-9	223
1178	Controlling charge balance and exciton recombination by bipolar host in single-layer organic light-emitting diodes. 2010 , 108, 034508	63
1177	Density functional theoretical study of pentacene/noble metal interfaces with van der Waals corrections: vacuum level shifts and electronic structures. 2010 , 132, 134703	114
1176	Controlling carrier accumulation and exciton formation in organic light emitting diodes. 2010 , 96, 043303	41
1175	Van der Waals Interactions Between Organic Adsorbates and at Organic/Inorganic Interfaces. 2010 , 35, 435-442	244
1174	Electronic properties of pentacene versus triisopropylsilylethynyl-substituted pentacene: environment-dependent effects of the silyl substituent. 2010 , 132, 580-6	97
1173	First-principles study of the dipole layer formation at metal-organic interfaces. 2010 , 81,	45
1172	Band gap states of copper phthalocyanine thin films induced by nitrogen exposure. 2010 , 96, 093303	78
1171	Ambipolar all-polymer bulk heterojunction field-effect transistors. 2010 , 20, 1317-1321	73
1170	Chemisorption-induced gap state at organic-metal interface: Benzenethiol on Pt(111). 2010 , 12, 10914-8	7
1169	Influence of electrostatic fields on molecular electronic structure: insights for interfacial charge transfer. 2010 , 12, 12390-400	29
1168	Increased efficiency of small molecule photovoltaic cells by insertion of a MoO3 hole-extracting layer. 2010 , 3, 107-110	62
1167	Two-color sum frequency generation study of poly(9,9-dioctylfluorene)/electrode interfaces. 2010 , 12, 14666-9	7
1166	Electron injection barrier reduction for organic light-emitting devices by quinacridone derivatives. 2010 , 46, 8210-2	31
1165	Near- and Far-Field Effects on Molecular Energy Level Alignment at an Organic/Electrode Interface. 2010 , 1, 145-148	38
1164	Gap state formation by interfacial interaction between Al and 8-hydroxyquinolatolithium. 2010, 12, 9441-4	4
1163	Potassium-Induced Charge Transfer Effects in Oligo(-phenylene ethynylene)-Based Molecular Layers. 2011 , 115, 15425-15431	

1162	Poly(ethylene oxide)-functionalized Al cathodes of tunable electron-injection capabilities for efficient polymer light-emitting diodes. 2011 , 21, 18840	13
1161	Layer inversion in organic heterostructures. 2011 , 13, 13382-6	13
1160	Tunable symmetry and periodicity in binary supramolecular nanostructures. 2011 , 13, 4220-3	17
1159	Assembly of 2D ionic layers by reaction of alkali halides with the organic electrophile 7,7,8,8-tetracyano-p-quinodimethane (TCNQ). 2011 , 47, 9146-8	66
1158	Electronic Structure of Self-Assembled Peptide Nucleic Acid Thin Films. 2011 , 115, 17123-17135	15
1157	Structure and Energy Level Alignment of Tetramethyl Benzenediamine on Au(111). 2011 , 115, 12625-12630	9
1156	Role of Backbone Charge Rearrangement in the Bond-Dipole and Work Function of Molecular Monolayers. 2011 , 115, 24888-24892	28
1155	Structure and Electron States of Co-phthalocyanine Interacting With the Cu(111) Surface. 2011 , 115, 17409-17416	26
1154	First-principles study of electronic structure and charge transport at PTCDA molecular layers on Ag(111) and Al(111) electrodes. 2011 , 84,	7
1153	Mobility Improvement in C\$_{60}\$-Based Field-Effect Transistors Using LiF/Ag Source/Drain Electrodes. 2011 , 50, 124203	2
1152	Density Functional Theoretical Study of Perfluoropentacene/Noble Metal Interfaces with van der Waals Corrections: Adsorption States and Vacuum Level Shifts. 2011 , 115, 5767-5772	22
1151	Impact of Nitrogen Substitution and Molecular Orientation on the Energy-Level Alignment of Heteroacene Films. 2011 , 115, 15502-15508	9
1150	Metal-to-Acceptor Charge Transfer through a Molecular Spacer Layer. 2011 , 115, 17503-17507	20
1149	Direct comparison of solution- and vacuum-processed small molecular organic light-emitting devices with a mixed single layer. 2011 , 3, 2496-503	40
1148	Metal-molecule Schottky junction effects in surface enhanced Raman scattering. 2011 , 115, 318-28	14
1147	Dipole Layer Formation by Surface Segregation of Regioregular Poly(3-alkylthiophene) with Alternating Alkyl/Semifluoroalkyl Side Chains. 2011 , 23, 4257-4263	34
1146	Decay Mechanism of Spontaneously Built-up Surface Potential in a Thin Film of a Zwitterionic Molecule Having Noncentrosymmetric Crystal Structure. 2011 , 115, 2356-2359	
1145	Organic Semiconductors. 2011 , 448-507	7

1144	Hole transparent and hole blocking transport in single-crystal-like organic heterojunction: when rods hold up disks. 2011 , 3, 2195-9	10
1143	Effect of Gap States on the Orientation-Dependent Energy Level Alignment at the DIP/F16CuPc DonorAcceptor Heterojunction Interfaces. 2011 , 115, 23922-23928	38
1142	Interface engineering of semiconductor/dielectric heterojunctions toward functional organic thin-film transistors. 2011 , 11, 4939-46	128
1141	Photoemission and STM Study of the Morphology and Electronic Structure of Benz[a]anthracene on Cu(111) on Mica and on HOPG. 2011 , 115, 5910-5918	3
1140	Highly Efficient Electron Injection from Indium Tin Oxide/Cross-Linkable Amino-Functionalized Polyfluorene Interface in Inverted Organic Light Emitting Devices. 2011 , 23, 4870-4876	106
1139	Coverage-Driven Electronic Decoupling of Fe-Phthalocyanine from a Ag(111) Substrate. 2011 , 115, 12173-121	7 9 1
1138	Tailoring the Cu(100) work function by substituted benzenethiolate self-assembled monolayers. 2011 , 115, 7234-41	43
1137	Lock and Key Adsorption Chemistry: Preferential Absorption of an Isomer of Di-iodobenzene on Molecular Films of Quinonoid Zwitterions. 2011 , 115, 2812-2818	13
1136	Solution-processed flexible polymer solar cells with silver nanowire electrodes. 2011 , 3, 4075-84	318
1135	Polarization Mediated Chemistry on Ferroelectric Polymer Surfaces. 2011 , 115, 13041-13046	16
1134	Characterization of the Interactions between Alq3 Thin Films and Al Probed by Two-Color Sum-Frequency Generation Spectroscopy. 2011 , 115, 9551-9560	18
1133	Observation and Analysis of Small Inclination of Thymine Molecules on Graphite. 2011 , 115, 511-515	4
1132	Electronic Structure, Chemical Interactions and Molecular Orientations of 3,4,9,10-Perylene-tetracarboxylic-dianhydride on TiO2(110). 2011 , 115, 24880-24887	48
1131	DNA electron injection interlayers for polymer light-emitting diodes. 2011 , 133, 11010-3	70
1130	Atomic Structures and Electronic Properties of Semiconductor Interfaces. 2011 , 113-174	12
1129	Highly Photoactive Titanyl Phthalocyanine Polymorphs as Textured Donor Layers in Organic Solar Cells. 2011 , 115, 18873-18884	47
1128	Molecular and supramolecular control of the work function of an inorganic electrode with self-assembled monolayer of umbrella-shaped fullerene derivatives. 2011 , 133, 16997-7004	56
1127	Tuning hole-injection barriers at organic/metal interfaces exploiting the orientation of a molecular acceptor interlayer. 2011 , 84,	38

1126	Electronic Structure of Aromatic Monomolecular Films: The Effect of Molecular Spacers and Interfacial Dipoles. 2011 , 115, 22422-22428	18
1125	Angle- and Time-Resolved Two-Photon Photoemission Spectroscopy for Unoccupied Levels of Lead Phthalocyanine Film. 2011 , 115, 19269-19273	14
1124	Current challenges in organic photovoltaic solar energy conversion. 2012 , 312, 175-212	25
1123	Electronic level alignment at a metal-molecule interface from a short-range hybrid functional. 2011 , 135, 164706	65
1122	Electronic Modification of C\$_{60}\$ Monolayers via Metal Substrates. 2011 , 50, 08LB06	5
1121	Independent Tuning of the Band Gap and Redox Potential of Graphene Quantum Dots. 2011 , 2, 1119-24	164
112 0	The molecular nature of photovoltage losses in organic solar cells. 2011 , 47, 3702-16	117
1119	Enhanced performance of C60 organic field effect transistors using a tris(8-hydroxyquinoline) aluminum buffer layer. 2011 , 32, 094005	2
1118	Preparation of Polymer Thin Films by Physical Vapor Deposition. 2011 , 287-318	8
1117	An Overview of Organic Light-Emitting Diodes and their Applications. 2011 , 73-107	7
1116	Electronic Processes at Organic Interfaces: Insight from Modeling and Implications for Opto-electronic Devices 2011 , 23, 591-609	170
1115	Energy-Level Alignment in 4?-Substituted Stilbene-4-thiolate Self-Assembled Monolayers on Gold. 2011 , 115, 7487-7495	1
1114	Collectively induced quantum-confined Stark effect in monolayers of molecules consisting of polar repeating units. 2011 , 133, 18634-45	31
1113	STM studies of PTCDA supramolecular self-assembling on anisotropic surfaces of reconstructed InSb. 2011 , 258, 1300-1305	4
1112	Recent Advances in Conjugated Polyelectrolytes for Emerging Optoelectronic Applications 2011, 23, 501-515	316
1111	Work-Function Engineering of Graphene Electrodes by Self-Assembled Monolayers for High-Performance Organic Field-Effect Transistors. 2011 , 2, 841-5	224
1110	Studies of photovoltaic properties of nanocrystalline thin films of CdSIIdTe. 2011 , 509, 10003-10006	12
1109	Molecular Insight Into the Energy Levels at the Organic Donor/Acceptor Interface: A Quantum Mechanics/Molecular Mechanics Study. 2011 , 115, 14431-14436	82

1108	Electrical and optical properties of p-type silicon based on polypyrrole-derivative polymer. 2011 , 161, 692-697	5
1107	The interfacial electronic structure between pentacene and multilayer graphene. 2011 , 161, 2488-2491	4
1106	Design of Organic Semiconductors from Molecular Electrostatics 2011, 23, 359-377	177
1105	Optical, Magnetic, Electrochemical, and Electrical Properties of 8-Hydroxyquinoline-Based Complexes with Al3+, Cr3+, Mn2+, Co2+, Ni2+, Cu2+, and Zn2+. 2011 , 115, 9182-9192	65
1104	Band alignment at organic-inorganic heterojunctions between P3HT and n-type 6H-SiC. 2011 , 3, 4286-91	15
1103	Characterizing TiO2(110) surface states by their work function. 2011 , 13, 15442-7	87
1102	Molecular controlled nano-devices. 2011 , 13, 13153-61	19
1101	Unlocking the full potential of organic light-emitting diodes on flexible plastic. 2011 , 5, 753-757	325
1100	On Voltage, Photovoltage, and Photocurrent in Bulk Heterojunction Organic Solar Cells. 2011 , 2, 1950-1964	139
1099	Evidence for near-Surface NiOOH Species in Solution-Processed NiOx Selective Interlayer Materials: Impact on Energetics and the Performance of Polymer Bulk Heterojunction Photovoltaics. 2011 , 23, 4988-500	0 ²⁸³
1098	Spin polarized electron tunneling and magnetoresistance in molecular junctions. 2012 , 312, 275-302	1
1097	Transparent Conductive Oxide (TCO) Films for Organic Light Emissive Devices (OLEDs). 2011,	9
1096	Highly simplified small molecular phosphorescent organic light emitting devices with a solution-processed single layer. 2011 , 1, 032130	7
1095	Determination of Carrier Type Doped from Metal Contacts to Graphene by Channel-Length-Dependent Shift of Charge Neutrality Points. 2011 , 4, 035101	25
1094	Organic Charge-transfer Salts and the Component Molecules in Organic Transistors. 2011 , 40, 428-434	32
1093	Electrical Conduction Behavior of Organic Light-Emitting Diodes Using Inhomogeneous Fluorinated Self-Assembled Monolayer as a Hole-Injection Layer. 2011 , 4, 071601	16
1092	Functionalization of Silica Surface by Tetrahydroxyporphyrin via SiD Linkages. 2011 , 84, 794-801	6
1091	Influence of the Performance of Organic Light Emitting Devices by Chemical Reaction at the Interface between Electron Transport Material and Ba Cathode. 2011 , 52, 1316-1319	

Molecular semiconductor-doped insulator (MSDI) heterojunctions as new transducers for chemical sensors. 2011 , 56, 34103	10
1089 Tailoring organic heterojunction interfaces in bilayer polymer photovoltaic devices. 2011 , 10, 450-5	246
Effect of indium and tin contamination on the efficiency and electronic properties of organic bulk hetero-junction solar cells. 2011 , 95, 3251-3255	34
Influence of thermal radiation during aluminum thermal evaporation on organic solar cells. 2011 , 95, 3311-3317	8
Performance improvement mechanisms of organic thin-film transistors using MoOx-doped pentacene as channel layer. 2011 , 12, 1852-1857	28
Modifying organic/metal interface via solvent treatment to improve electron injection in organic light emitting diodes. 2011 , 12, 1858-1863	68
Nanoparticles with logic and numeracy: towards Bomputer-on-a-particleDoptoelectronic devices. 2011, 5, 103	6
1083 Energy level alignment in TiO2/dipole-molecule/P3HT interfaces. 2011 , 515, 146-150	25
Bistability in the surface dipole of silicon grafted with copper nanoparticles: An in-situ electrochemical MIR-FTIR study. 2011 , 13, 1447-1450	
Nanoscale Digital Devices Based on the Photoelectrochemical Photocurrent Switching Effect: Preparation, Properties and Applications. 2011 , 51, 36-55	29
1080 Organic host materials for phosphorescent organic light-emitting diodes. 2011 , 40, 2943-70	983
Experimental techniques for the fabrication and characterization of organic thin films for field-effect transistors. 2011 , 111, 3358-406	215
1078 The organic transistor: state-of-the-art and outlook. 2011 , 53, 33602	12
Bis-cinnolines as n-type semiconducting material with high electron mobility and thermal stability and their application in organic photovoltaic cells. 2011 , 6, 2005-8	30
1076 Energy level alignment of single-wall carbon nanotubes on metal surfaces. 2011 , 83,	11
1075 Charge transport in organic semiconductors. 2012 , 312, 1-65	147
1074 Molecular orientation in small-molecule organic light-emitting diodes. 2011 , 21, 19187	428
Enhanced performance and stability of inverted organic solar cells by using novel zinc-benzothiazole complexes as anode buffer layers. 2011 , 21, 15587	20

1072	Effect of electrode material on contact high-voltage polarization in a vinylidene fluoride-hexafluoropropylene copolymer. 2011 , 53, 912-928		9
1071	Study of the electronic structure of Al(III) and Zn(II) complexes with organic ligands by quantum chemistry and photoelectron spectroscopy methods. 2011 , 5, 11-16		
1070	Integer charge transfer states in organic light-emitting diodes: Optical detection of hole carriers at the anode organic interface. 2011 , 109, 013709		14
1069	Photoionization cross-section weighted DFT simulations as promising tool for the investigation of the electronic structure of open shell metal-phthalocyanines. 2011 , 400, 673-8		17
1068	Effect of doping on metal doped semiconductor. 2011 , 11, 188-190		3
1067	Facile fabrication of all-SWNT field-effect transistors. 2011 , 4, 580-588		10
1066	Role of Room Temperature Sputtered High Conductive and High Transparent Indium Zinc Oxide Film Contacts on the Performance of Orange, Green, and Blue Organic Light Emitting Diodes. 2011 , 8, 340-345		24
1065	Local surface potential of Econjugated nanostructures by Kelvin probe force microscopy: effect of the sampling depth. 2011 , 7, 634-9		20
1064	Organic Drganic Heterojunction Interfaces: Effect of Molecular Orientation. 2011, 21, 410-424		193
1063	Molecular Stacking Induced by Intermolecular CHIIIN Hydrogen Bonds Leading to High Carrier Mobility in Vacuum-Deposited Organic Films. 2011 , 21, 1375-1382		130
1062	Simultaneous Modification of Bottom-Contact Electrode and Dielectric Surfaces for Organic Thin-Film Transistors Through Single-Component Spin-Cast Monolayers. 2011 , 21, 1476-1488		67
1061	Poly(diketopyrrolopyrrole-benzothiadiazole) with Ambipolarity Approaching 100% Equivalency. 2011 , 21, 1910-1916		138
1060	Profiles of Work Function Shifts and Collective Charge Transfer in Submonolayer Metal © rganic Films. 2011 , 21, 1931-1940		24
1059	Quantifying Interfacial Electric Fields and Local Crystallinity in Polymer E ullerene Bulk-Heterojunction Solar Cells. 2011 , 21, 2666-2673		25
1058	Manipulation of the Open-Circuit Voltage of Organic Solar Cells by Desymmetrization of the Structure of Acceptor Donor Acceptor Molecules. 2011 , 21, 4379-4387		93
1057	Enhanced charge injection in pentacene field-effect transistors with graphene electrodes. <i>Advanced Materials</i> , 2011 , 23, 100-5	24	112
1056	Enhanced performance and air stability of polymer solar cells by formation of a self-assembled buffer layer from fullerene-end-capped poly(ethylene glycol). <i>Advanced Materials</i> , 2011 , 23, 1782-7	24	102
1055	Molecular self-assembly at solid surfaces. <i>Advanced Materials</i> , 2011 , 23, 5148-76	24	167

1054	Simultaneous enhancement of open-circuit voltage, short-circuit current density, and fill factor in polymer solar cells. <i>Advanced Materials</i> , 2011 , 23, 4636-43	1860
1053	An Electrode Design Rule for Organic Photovoltaics Elucidated Using Molecular Nanolayers. 2011 , 1, 440-447	17
1052	High Performance Organic Photovoltaic Cells Using Polymer-Hybridized ZnO Nanocrystals as a Cathode Interlayer. 2011 , 1, 690-698	112
1051	Electrodeposited Porous ZnO Sensitized by Organic Dyes Promising Materials for Dye-Sensitized Solar Cells with Potential Application in Large-Scale Photovoltaics. 2011 , 221-275	
1050	Electronic properties of interfaces between PCPDTBT and prototypical electrodes studied by photoemission spectroscopy. 2011 , 12, 2345-51	15
1049	Synthesis of oxadiazole-based polymers containing a carbazolelinylene or fluorenelinylene group and their hole-injection/transport behavior in light-emitting diodes. 2011 , 119, 377-386	5
1048	Surface Energy-Level Tuning of Silver Nanoparticles for Facilitated Olefin Transport. 2011 , 123, 3038-3041	20
1047	Enhancement of DonorAcceptor Polymer Bulk Heterojunction Solar Cell Power Conversion Efficiencies by Addition of Au Nanoparticles. 2011 , 123, 5633-5637	83
1046	Surface energy-level tuning of silver nanoparticles for facilitated olefin transport. 2011 , 50, 2982-5	44
1045	Enhancement of donor-acceptor polymer bulk heterojunction solar cell power conversion efficiencies by addition of Au nanoparticles. 2011 , 50, 5519-23	310
1045	efficiencies by addition of Au nanoparticles. 2011 , 50, 5519-23 Bis(azobenzene)-based photoswitchable, prochiral, Cftetrasubstituted famino acids for	310 9
	efficiencies by addition of Au nanoparticles. 2011 , 50, 5519-23 Bis(azobenzene)-based photoswitchable, prochiral, C\text{\text{\text{Petrasubstituted \text{\text{\text{Bmino}}} acids for	Ĭ
1044	efficiencies by addition of Au nanoparticles. 2011, 50, 5519-23 Bis(azobenzene)-based photoswitchable, prochiral, Ctetrasubstituted tamino acids for nanomaterials applications. 2011, 17, 12606-11 Electronic states at 4,4?-N,N?-dicarbazol-biphenyl (CBP)Thetal (Mg, Ag, and Au) interfaces: A joint experimental and theoretical study. 2011, 11, 346-352	9
1044 1043 1042	efficiencies by addition of Au nanoparticles. 2011, 50, 5519-23 Bis(azobenzene)-based photoswitchable, prochiral, Ctetrasubstituted tamino acids for nanomaterials applications. 2011, 17, 12606-11 Electronic states at 4,4?-N,N?-dicarbazol-biphenyl (CBP)thetal (Mg, Ag, and Au) interfaces: A joint experimental and theoretical study. 2011, 11, 346-352	9
1044 1043 1042	Bis(azobenzene)-based photoswitchable, prochiral, Cletrasubstituted lamino acids for nanomaterials applications. 2011, 17, 12606-11 Electronic states at 4,4?-N,N?-dicarbazol-biphenyl (CBP) Thetal (Mg, Ag, and Au) interfaces: A joint experimental and theoretical study. 2011, 11, 346-352 Barrier formation at organic-metal interfaces studied by density functional theory. 2011, 11, 447-450	9 6 3
1044 1043 1042	Bis(azobenzene)-based photoswitchable, prochiral, Ctetrasubstituted themino acids for nanomaterials applications. 2011, 17, 12606-11 Electronic states at 4,4?-N,N?-dicarbazol-biphenyl (CBP)thetal (Mg, Ag, and Au) interfaces: A joint experimental and theoretical study. 2011, 11, 346-352 Barrier formation at organic-metal interfaces studied by density functional theory. 2011, 11, 447-450 Study on the interface between the organic and inorganic semiconductors. 2011, 257, 4994-4999 Energy level alignments at poly[N-9??-hepta-decanyl-2,7-carbazole-alt-5,5-(4?,7?-di-2-thienyl-2?,1?,3?-benzothiadiazole)] on	9 6 3
1044 1043 1042 1041 1040	Bis(azobenzene)-based photoswitchable, prochiral, CEtetrasubstituted Emino acids for nanomaterials applications. 2011, 17, 12606-11 Electronic states at 4,4?-N,N?-dicarbazol-biphenyl (CBP)Enetal (Mg, Ag, and Au) interfaces: A joint experimental and theoretical study. 2011, 11, 346-352 Barrier formation at organic-metal interfaces studied by density functional theory. 2011, 11, 447-450 Study on the interface between the organic and inorganic semiconductors. 2011, 257, 4994-4999 Energy level alignments at poly[N-9??-hepta-decanyl-2,7-carbazole-alt-5,5-(4?,7?-di-2-thienyl-2?,1?,3?-benzothiadiazole)] on metal and polymer interfaces. 2011, 503, 101-104 The depth profile of core energy levels: Electronic structure of buried organic/metal interfaces	9 6 3 3 20

1036	Planar and textured heterojunction organic photovoltaics based on chloroindium phthalocyanine (ClInPc) versus titanyl phthalocyanine (TiOPc) donor layers. 2011 , 12, 383-393	41
1035	Ambipolar thin-film transistors and an inverter based on pentacene/self-assembled monolayer modified ZnO hybrid structures for balanced hole and electron mobilities. 2011 , 12, 411-418	23
1034	Interfacial charge transfer and charge generation in organic electronic devices. 2011 , 12, 520-528	63
1033	Mechanism of the Fermi level pinning at organic donor acceptor heterojunction interfaces. 2011 , 12, 534-540	81
1032	OddBven modulation of electrode work function with self-assembled layer: Interplay of energy barrier and tunneling distance on charge injection in organic light-emitting diodes. 2011 , 12, 602-608	13
1031	Time dependence and freezing-in of the electrode oxygen plasma-induced work function enhancement in polymer semiconductor heterostructures. 2011 , 12, 623-633	45
1030	Ultrathin polythiophene films on an intrinsically conducting polymer electrode: Charge transfer induced valence states and interface dipoles. 2011 , 12, 916-922	33
1029	Benzimidazole derivatives in the electrolyte of new-generation organic dye-sensitized solar cells with an iodine-free redox mediator. 2011 , 219, 148-153	23
1028	Controlling of electronic parameters of GaAs Schottky diode by poly(3,4-ethylenedioxithiophene)-block-poly(ethylene glycol) organic interlayer. 2011 , 88, 867-871	15
1027	Organic light-emitting diode with indium-free metallic bilayer as transparent anode. 2011 , 12, 818-822	15
1026	Impact of alkyl side chains at self-assembly, electronic structure and charge arrangement in sexithiophene thin films. 2011 , 12, 903-910	17
1025	Self-assembly of gold nanoparticles on functional organic molecular crystals. 2011 , 360, 422-9	4
1024	Effect of cathodes on high efficiency inorganic@rganic hybrid LEDs based on CdSe/ZnS quantum dots. 2011 , 326, 109-112	11
1023	The effect of a concentration graded cathode for organic solar cells. 2011 , 95, 2443-2447	8
1022	Lateral inhomogeneity of unoccupied states for PbPc films. 2011 , 605, 982-986	18
1021	Orientation dependent ionization potential of In2O3: a natural source for inhomogeneous barrier formation at electrode interfaces in organic electronics. 2011 , 23, 334203	27
1020	Surface Potential Measurement of Tris(8-hydroxyquinolinato)aluminum and Bis[N-(1-naphthyl)-N-phenyl]benzidine Thin Films Fabricated on IndiumII in Oxide by Kelvin Probe Force Microscopy. 2011 , 50, 071601	2
1019	Control of molecule-based transport for future molecular devices. 2011 , 23, 013001	57

Influence of gate dielectric on the ambipolar characteristics of solution-processed organic field-effect transistors. 2011 , 44, 205102	10
Fine tuning of the electronic structure of Econjugated molecules for molecular electronics. 2011 , 22, 145701	10
1016 Adsorption of Phenylphosphonic Acid on Gold and Platinum Surfaces. 2011 , 50, 081606	3
1015 Molecular-scale investigation of C60/p-sexiphenyl organic heterojunction interface. 2011 , 134, 1	54706 26
Charging energy and barrier height of pentacene on Au(111): a local-orbital hybrid-functional density functional theory approach. 2011 , 135, 084702	13
1013 Quantum confinement and anisotropy in thin-film molecular semiconductors. 2011 , 83,	13
1012 Architecture of PTCDA molecular structures on a reconstructed InSb(001) surface. 2011 , 83,	7
Systematic measurement of pentacene assembled on Cu(111) by bimodal dynamic force microscopy at room temperature. 2011 , 84,	22
Adsorption of Alq3 on Mg(001) surface: Role of chemical bonding, molecular distortion, and van Waals interaction. 2011 , 83,	der 6
1009 Suppression of multiphoton intrashell resonances in Li Rydberg atoms. 2011 , 83,	2
Direct determination of energy level alignment and charge transport at metal-Alq3 interfaces viballistic-electron-emission spectroscopy. 2011 , 106, 156807	21
1007 Incorporation of potassium at CuPc/C60 interface for photovoltaic application. 2011 , 98, 113307	9
1006 Impact of structural imperfections on the energy-level alignment in organic films. 2011 , 83,	30
Fermi level pinning by integer charge transfer at electrode-organic semiconductor interfaces. 20^{1005} 98, 113303	11 , 41
1004 Monolayer and bilayer pentacene on Cu(111). 2011 , 84,	34
Orientational ordering of nonplanar phthalocyanines on Cu(111): strength and orientation of the electric dipole moment. 2011 , 106, 156102	41
Significant Improvement of Organic Thin-Film Transistor Mobility Utilizing an Organic Heterojunction Buffer Layer. 2011 , 28, 078504	7
Enhanced Driving Performance of Organic Light-Emitting Diodes with All Carrier Ohmic-Contact: 2011, 158, J10	5. 5

1000	Effects of an oxygen environment on the electrical properties of a single CdS nanobelt device. 2011 , 22, 135702	11
999	Effect of dielectric barrier on rectification, injection and transport properties of printed organic diodes. 2011 , 44, 295301	9
998	LT-STM studies on substrate-dependent self-assembly of small organic molecules. 2011 , 44, 464005	30
997	The direct measurement of energy barrier height at metal/ polyfluorene derivatives interface by internal photoemission spectroscopy. 2011 , 1286, 8	
996	Orientation dependence of charge transfer for C60 on Cu(100). 2011 , 98, 133303	8
995	Interface Phenomena of Self-Assembled Monolayer with Various Alkyl Chain as a Hole-Injection Layer for Organic Light-Emitting Diodes. 2012 , 567, 163-170	4
994	Metal-diffusion-induced ITO nanoparticles at the organic/ITO interface. 2012 , 45, 165104	3
993	Interfacial energetics of NaClBrganic composite layer at an OLED anode. 2012 , 45, 455304	2
992	Doping Effect on Chloroindium Phthalocyanine (ClInPc)/C60 Solar Cells. 2012, 1390, 53	1
991	Charge Injection Enhanced by Guest Material in Molecularly Doped Liquid Crystalline Thin Films. 2012 , 51, 011701	1
990	Properties of Interface between Organic Hole-Transporting Layer and Indium Tin Oxide Anode Modified by Fluorinated Self-Assembled Monolayer. 2012 , 51, 035701	8
989	Device Simulation of Ditch and Elevated Electrode Structures in Organic Thin-Film Transistors. 2012 , 51, 024303	2
988	Electrostatic Properties of Organic Monolayers on Silicon Oxides Studied by Kelvin Probe Force Microscopy. 2012 , 51, 045702	1
987	Correlation between interface energetics and open circuit voltage in organic photovoltaic cells. 2012 , 101, 233301	81
986	Methodological aspects of the quantum-chemical description of interface dipoles at tetrathiafulvalenelletracyanoquinodimethane interfaces. 2012 , 137, 174708	7
985	Tuning the surface plasmon on Ag(111) by organic molecules. 2012 , 112, 023302	4
984	Manipulating spin injection into organic materials through interface engineering. 2012, 101, 022416	17
983	Tandem photovoltaic cells formed in single fullerene films by impurity doping. 2012 , 101, 233303	17

982	Inverted Organic Solar Cells with Improved Performance using Varied Cathode Buffer Layers. 2012 , 25, 625-630	2
981	Realization of ohmic-like contact between ferromagnet and rubrene single crystal. 2012, 101, 073501	5
980	Charge depletion in organic heterojunction. 2012 , 100, 113301	17
979	Post-growth surface smoothing of thin films of diindenoperylene. 2012 , 101, 033307	21
978	Polarization effects on energy-level alignment at the interfaces of polymer organic semiconductor films. 2012 , 101, 053304	16
977	Nonvolatile organic write-once-read-many-times memory devices based on hexadecafluoro-copper-phthalocyanine. 2012 , 100, 213303	14
976	Energy level pinning of an n-type semiconducting polymer on conductive polymer electrodes: Effects of work function and annealing. 2012 , 112, 033712	8
975	Probing buried organic-organic and metal-organic heterointerfaces by hard x-ray photoelectron spectroscopy. 2012 , 101, 221603	4
974	Ambipolar transport and charge transfer at the interface between sexithiophene and N,N-bis(n-octyl)-dicyanoperylenediimide films. 2012 , 85,	10
973	Probing buried organic layers in organic light-emitting diodes under operation by electric-field-induced doubly resonant sum-frequency generation spectroscopy. 2012 , 101, 073304	28
972	The role of micro-shorts and electrode-film interface in the electrical transport of ultra-thin metallophthalocyanine capacitive devices. 2012 , 101, 133304	8
971	Direct evidence of n-type doping in organic light-emitting devices: N free Cs doping from CsN3. 2012 , 100, 203301	18
970	Different contact formations at the interfaces of C60/LiF/Al and C60/LiF/Ag. 2012, 111, 073711	7
969	Reversible change of the spin state in a manganese phthalocyanine by coordination of CO molecule. 2012 , 109, 147202	104
968	Doping of C60 (sub)monolayers by Fermi-level pinning induced electron transfer. 2012 , 86,	42
967	Interfacial properties at the organic-metal interface probed using quantum well states. 2012, 86,	7
966	Organic semiconductor heterojunctions as charge generation layers and their application in tandem organic light-emitting diodes for high power efficiency. 2012 , 22, 18718	73
965	Charge transport in molecular electronic junctions: compression of the molecular tunnel barrier in the strong coupling regime. 2012 , 109, 11498-503	115

(2012-2012)

964	Performance Improvement of Ambipolar Organic Field Effect Transistors by Inserting a MoO 3 Ultrathin Layer. 2012 , 29, 098503	1
963	Electrical Conduction of Organic Light-Emitting Diodes Using Self-Assembled Monolayer-Modified Indium Tin Oxide Electrode. 2012 , 25, 327-332	4
962	Study of Ultrathin Films of P3HT/PCBM by Means of Highly Sensitive Absorption Spectroscopy. 2012 , 41, 184-186	2
961	Optical differential reflectance spectroscopy on thin molecular films. 2012 , 108, 34	73
960	Non-conventional metallic electrodes for organic field-effect transistors. 2012 , 13, 2301-2306	9
959	Origin of Hole Selectivity and the Role of Defects in Low-Temperature Solution-Processed Molybdenum Oxide Interfacial Layer for Organic Solar Cells. 2012 , 116, 16346-16351	70
958	Structural and Electronic Properties of the TTF/ZnO(10៧0) Interface: Insights From Modeling. 2012 , 3, 58-63	10
957	Highly efficient tandem white organic light-emitting diodes based upon C60/NaT4 organic heterojunction as charge generation layer. 2012 , 22, 8492	27
956	Fabrication of unipolar graphene field-effect transistors by modifying source and drain electrode interfaces with zinc porphyrin. 2012 , 4, 1434-9	10
955	High contrast tandem organic light emitting devices. 2012 , 101, 133305	7
954	Electron-Transfer Processes in Zinc Phthalocyanine-Phosphonic Acid Monolayers on ITO: Characterization of Orientation and Charge-Transfer Kinetics by Waveguide Spectroelectrochemistry. 2012 , 3, 1154-8	28
953	Adsorption studies of C6H6 on Cu (111), Ag (111), and Au (111) within dispersion corrected density functional theory. 2012 , 137, 134703	36
952	Effects of Gaussian disorder on charge carrier transport and recombination in organic semiconductors. 2012 , 209, 2354-2377	80
951	Growth and adsorption geometry of naphthalene overlayers on HOPG studied by low-temperature scanning tunneling microscopy. 2012 , 546, 136-140	11
950	Altering the static dipole on surfaces through chemistry: molecular films of zwitterionic quinonoids. 2012 , 134, 8494-506	35
949	Alkyl Surface Treatments of Planar Zinc Oxide in Hybrid Organic/Inorganic Solar Cells. 2012 , 116, 8872-8880	27
948	Interfacial dipole formation and surface-electron confinement in low-coverage self-assembled thiol layers: thiophenol and p-fluorothiophenol on Cu(111). 2012 , 6, 10622-31	17
947	First-principles theoretical study of organic/metal interfaces: Vacuum level shifts and interface dipoles. 2012 , 12, S2-S9	14

946	The effects of organic material-treated SiO2 dielectric surfaces on the electrical characteristics of inorganic amorphous In-Ga-Zn-O thin film transistors. 2012 , 100, 102110	16
945	Crystallisation kinetics in thin films of dihexyl-terthiophene: the appearance of polymorphic phases. 2012 , 2, 4404	59
944	Surface charge transfer doping of germanium nanowires by MoO3 deposition. 2012 , 2, 3361	7
943	Chemisorption-induced gap states at organic-metal interfaces: benzenethiol and benzeneselenol on metal surfaces. 2012 , 14, 4101-8	8
942	Reaction Chemistry of Solid-State Pyridine Thin Films with Vapor Deposited Ag, Mg, and Al. 2012 , 116, 11548-11555	8
941	Surface state engineering of molecule-molecule interactions. 2012 , 14, 4971-6	52
940	Widely applicable coinage metal window electrodes on flexible polyester substrates applied to organic photovoltaics. 2012 , 4, 6013-20	27
939	Observation of n-Type Conduction in Carbon Nanotube Field-Effect Transistors with Au Contacts in Vacuum. 2012 , 51, 02BN06	3
938	Structure Matters: Correlating temperature dependent electrical transport through alkyl monolayers with vibrational and photoelectron spectroscopies. 2012 , 3, 851-862	42
937	Dipole driven bonding schemes of quinonoid zwitterions on surfaces. 2012 , 48, 7143-5	28
936	Electron injection enhancement by a Cs-salt interlayer in ambipolar organic field-effect transistors and complementary circuits. 2012 , 22, 16979	30
935	Amino-carboxylic recognition on surfaces: from 2D to 2D + 1 nano-architectures. 2012 , 14, 13154-62	11
934	High-Contrast Tandem Organic Light-Emitting Devices Employing Semitransparent Intermediate Layers of LiF/Al/C60. 2012 , 116, 24690-24694	11
933	Self-metalation of 2H-tetraphenylporphyrin on Cu(111): an x-ray spectroscopy study. 2012 , 136, 014705	138
932	Approaching charge balance in organic light-emitting diodes by tuning charge injection barriers with mixed monolayers. 2012 , 28, 424-30	30
931	Magic Electret Clusters of 4-Fluorostyrene on Metal Surfaces. 2012 , 3, 2069-2075	20
930	Investigation of Interface Properties for ClAlPc/C60 Heterojunction-Based Inverted Organic Solar Cell. 2012 , 116, 2521-2526	24
929	Preparation of Poly(9-Vinylcarbazole) Thin Films Chemically Tethered to ITO Surface via Self-Assembled Monolayer Having Benzophenone Terminal Group. 2012 , 568, 125-133	6

928	Charge Generation Mechanism of Metal Oxide Interconnection in Tandem Organic Light Emitting Diodes. 2012 , 116, 6427-6433	30
927	Binding Modes of Fluorinated Benzylphosphonic Acids on the Polar ZnO Surface and Impact on Work Function. 2012 , 116, 19125-19133	54
926	How the charge-neutrality level of interface states controls energy level alignment in cathode contacts of organic bulk-heterojunction solar cells. 2012 , 6, 3453-60	104
925	Potential steps at CETiOPc-Ag(111) interfaces: ultrahigh-vacuum-noncontact scanning probe metrology. 2012 , 12, 2859-64	5
924	Reaction of thin films of solid-state benzene and pyridine with calcium. 2012, 134, 12989-97	7
923	Modeling the transition from ohmic to space charge limited current in organic semiconductors. 2012 , 13, 1700-1709	20
922	Exciplex emission and its relationship with depletion organic heterojunction. 2012 , 13, 1641-1645	19
921	Hole-enhanced electron injection from ZnO in inverted polymer light-emitting diodes. 2012 , 13, 1693-1699	27
920	Charge equilibration and potential steps in organic semiconductor multilayers. 2012 , 13, 1793-1801	19
919	Analysis of contact effects in fully printed p-channel organic thin film transistors. 2012 , 13, 2017-2027	28
918	Evaluating effect of surface state density at the interfaces in degraded bulk heterojunction organic solar cell. 2012 , 407, 3044-3046	7
917	A systematic spectroscopic study of the FePcBi interfaces. 2012 , 44, 1572-1579	3
916	Surface interactions of Au(I) cyclo-trimer with Au(111) and Al(111) surfaces: A computational study. 2012 , 606, 1100-1107	7
915	Surface stoichiometry of La0.7Sr0.3MnO3 during in vacuo preparation; A synchrotron photoemission study. 2012 , 606, 1360-1366	23
914	The Li3PO4/Al electrode: An alternative, efficient cathode for organic light-emitting diodes. 2012 , 161, 2575-2579	2
913	Organic field-effect transistors with nearly non-injection barrier from source/drain electrodes to pentacene. 2012 , 162, 936-940	8
912	Effects of channel widths, thicknesses of active layer on the electrical and photosensing properties of the 6,13-bis(triisopropylsilylethynyl) pentacene transistors by thermal evaporation method: Comparison study. 2012 , 162, 1210-1239	28
911	Electron injection barriers between air-stable electride with low work function, C12A7:epand pentacene, C60 and copper phthalocyanine. 2012 , 22, 4278	21

910	Open-circuit voltage in organic solar cells. 2012 , 22, 24315	217
909	Enhanced power-conversion efficiency in polymer solar cells using an inverted device structure. 2012 , 6, 591-595	3384
908	Effect of HNO3 functionalization on large scale graphene for enhanced tri-iodide reduction in dye-sensitized solar cells. 2012 , 22, 20490	92
907	A periodic charge-dipole electrostatic model: parametrization for silver slabs. 2012 , 137, 134702	2
906	Nanoscale geometric electric field enhancement in organic photovoltaics. 2012 , 6, 4722-30	28
905	Sputter deposition of indium tin oxide onto zinc pthalocyanine: Chemical and electronic properties of the interface studied by photoelectron spectroscopy. 2012 , 258, 3913-3919	6
904	Molecular gating of transistors by amine-terminated layers. 2012 , 258, 4069-4072	1
903	Excitation Energy Dependent Charge Separation at Hole-Transporting Dye/TiO2 Hetero Interface. 2012 , 116, 21148-21156	4
902	Tripyridyltruxenes: Thermally Stable Cathode Buffer Materials for Organic Thin-Film Solar Cells. 2012 , 1, 34-37	13
901	Modification of metalBrganic interface using F4-TCNQ for enhanced hole injection properties in optoelectronic devices. 2012 , 209, 2539-2545	20
900	Different interface orientations of pentacene and PTCDA induce different degrees of disorder. 2012 , 7, 248	9
899	Interface engineering for high-performance organic field-effect transistors. 2012 , 14, 14165-80	79
898	Small molecule solar cells based on a series of water-soluble zinc phthalocyanine donors. 2012, 48, 6094-6	18
897	Semiconductor Heterojunctions. 2012 , 383-445	
896	The role of gap states in the energy level alignment at the organic-organic heterojunction interfaces. 2012 , 14, 14127-41	47
895	Energy Level Shifts in Spiro-OMeTAD Molecular Thin Films When Adding Li-TFSI. 2012 , 116, 26300-26305	108
894	Thermionic emission and tunneling at carbon nanotube-organic semiconductor interface. 2012, 6, 4993-9	86
893	Determination of the interface energy level alignment of a doped organic hetero-junction using capacitance loltage measurements. 2012 , 13, 2346-2351	34

(2012-2012)

892	Solution processed small molecule organic interfacial layers for low dark current polymer photodiodes. 2012 , 13, 2727-2732	45
891	Electronic structures at organic heterojunctions of N,N?-bis(1-naphthyl)-N,N?-diphenyl-1,1?-biphenyl-4,4?-diamin (NPB)-based organic light emitting diodes. 2012 , 13, 2850-2855	23
890	Dimensionality effects in the electronic structure of organic semiconductors consisting of polar repeat units. 2012 , 13, 3165-3176	19
889	Determination of the structure, morphology and complex refractive index in ZnO-nanopencils/P3HT hybrid structures. 2012 , 135, 401-410	28
888	Temperature-dependent I-V characteristics for the nanocomposite semiconducting films composed of a thiol end-capped dinuclear macrocyclic complex and Au-NPs bridging 1 fb gap gold electrodes. 2012 , 41, 14309-15	2
887	Stereoselectivity and electrostatics in charge-transfer Mn- and Cs-TCNQIhetworks on Ag(100). 2012 , 3, 940	86
886	Enhancing efficiency with fluorinated interlayers in small molecule organic solar cells. 2012, 22, 22899	18
885	Influence of nanoparticle size to the electrical properties of naphthalenediimide on single-walled carbon nanotube wiring. 2012 , 23, 215701	4
884	Polarization dependence of Schottky barrier heights at interfaces of ferroelectrics determined by photoelectron spectroscopy. 2012 , 86,	66
883	Electronic Properties of Metal/Organic Interfaces. 2012 , 221-241	
882	Tuning the interfacial hole injection barrier between p-type organic materials and Co using a MoO3 buffer layer. 2012 , 112, 033704	12
881	OLED Display Structure. 2012 , 5-35	1
880	Stacking Orientation Mediation of Pentacene and Derivatives for High Open-Circuit Voltage Organic Solar Cells. 2012 , 3, 1079-83	11
879	Conjugated Semiconductors for Organic n-Channel Transistors and Complementary Circuits. 2012 , 137-195	O
878	Stamping transfer of a quantum dot interlayer for organic photovoltaic cells. 2012, 28, 9893-8	19
877	Understanding Interfacial Electronic Structure and Charge Transfer: An Electrostatic Perspective. 2012 , 3, 2342-51	78
876	Understanding the Interface Dipole of Copper Phthalocyanine (CuPc)/C60: Theory and Experiment. 2012 , 3, 2173-7	56
875	Inverted polymer solar cells fabricated by a pre-metered coating process. 2012 , 22, 23022	9

874	Inkjet-Printed Reduced Graphene Oxide/Poly(Vinyl Alcohol) Composite Electrodes for Flexible Transparent Organic Field-Effect Transistors. 2012 , 116, 7520-7525	85
873	Kelvin probe force microscopy in nonpolar liquids. 2012 , 28, 13892-9	32
872	LiF Layer at the Interface of Au Cathode in Organic Light-Emitting Devices: A Nonchemical Induced Carrier Injection Enhancement. 2012 , 116, 2543-2547	24
871	Water-gated charge doping of graphene induced by mica substrates. 2012 , 12, 648-54	146
870	Build-up of symmetry breaking using a titanium suboxide in bulk-heterojunction solar cells. 2012 , 14, 4062-5	10
869	Origins of thermal boundary conductance of interfaces involving organic semiconductors. 2012 , 112, 093503	35
868	Degradation in bulk heterojunction organic solar cells: changes in electrode interface and reduction in the occupation probability of the interface states. 2012 , 19, 1	7
867	Density functional theory for the description of charge-transfer processes at TTF/TCNQ interfaces. 2012 , 131, 1	12
866	Substituent effects on the electronic characteristics of pentacene derivatives for organic electronic devices: dioxolane-substituted pentacene derivatives with triisopropylsilylethynyl functional groups. 2012 , 134, 14185-94	27
865	Modulating semiconductor surface electronic properties by inorganic peptide-binders sequence design. 2012 , 134, 20403-11	13
864	Surface States and Adsorbate-Induced Electronic Structure. 2012 , 115-154	2
863	Interface Electronic Structure of Zinc-Phthalocyanine on the Silver Thin-Film Quantum-Well. 2012 , 10, 149-152	3
862	Changing the Paradigm: Towards Computation with Molecules. 2012 , 37-61	
861	Low-Dimensional Metals and Semiconductors. 2012 , 63-117	
860	Carbon Nanostructures. 2012 , 119-164	
859	Probing Metal/Organic Interfaces Using Doubly-Resonant Sum Frequency Generation Vibrational Spectroscopy. 2012 ,	
858	Metal/organic barrier formation for a C60/Au interface: From the molecular to the monolayer limit. 2012 , 209, 636-646	17
857	Interfacial doping for efficient charge injection in organic semiconductors. 2012 , 209, 1399-1413	41

856	Electronic structure of interfaces with conjugated organic materials. 2012 , 6, 277-293	57
855	Enhanced ambipolar charge injection with semiconducting polymer/carbon nanotube thin films for light-emitting transistors. 2012 , 6, 539-48	60
854	Recent advances in solution-processed interfacial materials for efficient and stable polymer solar cells. 2012 , 5, 5994	903
853	Light-triggered self-construction of supramolecular organic nanowires as metallic interconnects. 2012 , 4, 485-90	151
852	N-Ion-implanted TiO2 photoanodes in quantum dot-sensitized solar cells. 2012 , 4, 2416-22	30
851	End-Group-Induced Charge Transfer in Molecular Junctions: Effect on Electronic-Structure and Thermopower. 2012 , 3, 1962-1967	50
850	Tunability of band gaps in metal-organic frameworks. 2012 , 51, 9039-44	123
849	The application of graphene as electrodes in electrical and optical devices. 2012 , 23, 112001	265
848	Fluorescence of Colloidal Gold Nanoparticles is Controlled by the Surface Adsorbate. 2012 , 22, 1906-1913	49
847	Horizontal Orientation of Disk-like Hole Transport Molecules and Their Application for Organic Light-Emitting Diodes Requiring a Lower Driving Voltage. 2012 , 116, 8699-8706	42
846	Quantitative nanoscale surface voltage measurement on organic semiconductor blends. 2012 , 23, 045703	7
845	Crystalline Organic Heterostructures Engineering Based on Vanadyl Phthalocyanine and Rod-Like Conjugated Organic Semiconductors with Selected Central Groups. 2012 , 22, 4598-4607	21
844	Near-Infrared Electric Power Generation Through Sub-Energy-Gap Absorption in an Organic Inorganic Composite. 2012 , 22, 3035-3042	26
843	Formation Mechanism of Fullerene Cation in Bulk Heterojunction Polymer Solar Cells. 2012 , 22, 3075-3082	9
842	Transition Metal Oxide Work Functions: The Influence of Cation Oxidation State and Oxygen Vacancies. 2012 , 22, 4557-4568	562
841	Optimal Structure for High-Performance and Low-Contact-Resistance Organic Field-Effect Transistors Using Contact-Doped Coplanar and Pseudo-Staggered Device Architectures. 2012 , 22, 4577-4583	48
840	Ideal Energy-Level Alignment at the ZnO/P3HT Photovoltaic Interface. 2012 , 22, 5089-5095	53
839	High-performance and stable organic transistors and circuits with patterned polypyrrole electrodes. <i>Advanced Materials</i> , 2012 , 24, 2159-64	43

838	Electrostatically self-assembled nonconjugated polyelectrolytes as an ideal interfacial layer for inverted polymer solar cells. <i>Advanced Materials</i> , 2012 , 24, 3005-9, 2938	24	252
837	DNA interlayers enhance charge injection in organic field-effect transistors. <i>Advanced Materials</i> , 2012 , 24, 4255-60	24	56
836	Transition metal oxides for organic electronics: energetics, device physics and applications. <i>Advanced Materials</i> , 2012 , 24, 5408-27	24	881
835	Molecular Design of Interfacial Modifiers for Polymer-Inorganic Hybrid Solar Cells. 2012 , 2, 245-252		39
834	Color Tuning in Polymer Light-Emitting Diodes with Lewis Acids. 2012 , 124, 7613-7616		32
833	Color tuning in polymer light-emitting diodes with Lewis acids. 2012 , 51, 7495-8		99
832	The electrode's effect on the stability of organic transistors and circuits. <i>Advanced Materials</i> , 2012 , 24, 3053-8	24	20
831	Interfacial modification of organic photovoltaic devices by molecular self-organization. 2012, 14, 3713-	24	44
830	Universal energy-level alignment of molecules on metal oxides. 2011 , 11, 76-81		751
829	Structural and electronic decoupling of CII rom epitaxial graphene on SiC. 2012, 12, 3018-24		83
828	Electron donor and acceptor spatial distribution in structured bulk heterojunction photovoltaic devices induced by periodic photopolymerization. 2012 , 28, 10305-9		10
827	Energy level alignment at interfaces between 3-(4-biphenylyl)-4-phenyl-5-(4-tert-butyl phenyl)-1, 2, 4-triazole (TAZ) and metals (Ca, Mg, Ag, and Au): experiment and theory. 2012 , 16, 1141-1149		1
826	Weak screening of a large dipolar molecule adsorbed on graphene. 2012 , 50, 1981-1986		16
825	Charge transport characteristics in P3HT:PCBM organic blends under illumination: Influence of metal work functions. 2012 , 529, 64-68		16
824	Effects of UV and white light illuminations on photosensing properties of the 6,13-bis(triisopropylsilylethynyl)pentacene thin film transistor. 2012 , 178, 141-153		27
823	Energy band alignment at interfaces of semiconducting oxides: A review of experimental determination using photoelectron spectroscopy and comparison with theoretical predictions by the electron affinity rule, charge neutrality levels, and the common anion rule. 2012 , 520, 3721-3728		103
822	Intrinsic work function of molecular films. 2012 , 520, 3975-3986		10
821	Organometallic tris(8-hydroxyquinoline)aluminum complexes as buffer layers and dopants in inverted organic solar cells. 2012 , 520, 4475-4481		12

(2016-2012)

820	Surface composition, work function, and electrochemical characteristics of gallium-doped zinc oxide. 2012 , 520, 5652-5663	24
819	Interface electronic structure between organic semiconductor film and electrode metal probed by photoelectron yield spectroscopy. 2012 , 13, 309-319	26
818	Theoretical characterization of the TTF/Au (1 1 1) interface: STM imaging, band alignment and charging energy. 2012 , 13, 399-408	16
817	Self-assembled monolayer modification of silver sourced rain electrodes for high-performance pentacene organic field-effect transistors. 2012 , 13, 593-598	16
816	Coarse-grained kinetic modelling of bilayer heterojunction organic solar cells. 2012, 13, 750-761	13
815	Organic semiconductor heterojunction as charge generation layer in tandem organic light-emitting diodes for high power efficiency. 2012 , 13, 1121-1128	49
814	Organic-organic heterostructures: concepts and applications. 2012 , 13, 628-43	116
813	Versatile hole injection of VO2: Energy level alignment at N,N?-di(1-naphthyl)-N,N?-diphenyl-(1,1?-biphenyl)-4,4?-diamine/VO2/fluorine-doped tin oxide. 2015 , 16, 133-138	10
812	Energetics at Doped Conjugated Polymer/Electrode Interfaces. 2015, 2, 1400403	23
811	Models of charge pair generation in organic solar cells. 2015 , 17, 2311-2325	135
810	Fully solution-processed flexible organic thin film transistor arrays with high mobility and exceptional uniformity. 2014 , 4, 3947	153
809	Vertical phase separation of PSS in organic photovoltaics with a nickel oxide doped PEDOT: PSS interlayer. 2015 , 132, 623-631	18
808	Study of electrical fatigue by defect engineering in organic light-emitting diodes. 2015, 192, 26-51	23
807	A hybrid copper:tungsten suboxide window electrode for organic photovoltaics. <i>Advanced Materials</i> , 2015 , 27, 326-31	27
806	Broad Work-Function Tunability of p-Type Conjugated Polyelectrolytes for Efficient Organic Solar Cells. 2015 , 5, 1401653	50
805	The interplay between interface structure, energy level alignment and chemical bonding strength at organic-metal interfaces. 2015 , 17, 1530-48	88
804	Science and technology roadmap for graphene, related two-dimensional crystals, and hybrid systems. 2015 , 7, 4598-810	2015
803	Optical absorption signature of a self-assembled dye monolayer on graphene. 2016 , 7, 862-8	10

802	Effects of electronic coupling and electrostatic potential on charge transport in carbon-based molecular electronic junctions. 2016 , 7, 32-46		15
801	An Overview of Organic Light-Emitting Diodes and their Applications. 2016 ,		
800	Low-Temperature, Chemically Grown Titanium Oxide Thin Films with a High Hole Tunneling Rate for Si Solar Cells. 2016 , 9, 402		7
799	Band-Tail Transport of CuSCN: Origin of Hole Extraction Enhancement in Organic Photovoltaics. 2016 , 7, 2856-61		27
798	Improved Sensitivity and Durability of Poly(3-Hexylthiophene)-Based Polymeric Photodetectors Using Indium Tin Oxide Modified by Phosphonic Acid B ased Self-Assembled Monolayer Treatment. 2016 , 99, 48-54		2
797	Improving the Charge Injection in Organic Transistors by Covalently Linked Graphene Oxide/Metal Electrodes. 2016 , 2, 1500409		19
796	Theoretical Study on Electronic Structure of Bathocuproine: Renormalization of the Band Gap in the Crystalline State and the Large Exciton Binding Energy. 2016 , 63, 513-520		2
795	Effective Work Function Reduction of Practical Electrodes Using an Organometallic Dimer. 2016 , 26, 2493-2502		25
794	The Swiss-Army-Knife Self-Assembled Monolayer: Improving Electron Injection, Stability, and Wettability of Metal Electrodes with a One-Minute Process. 2016 , 26, 3172-3178		22
793	Multi-Component Organic Layers on Metal Substrates. <i>Advanced Materials</i> , 2016 , 28, 1340-68	24	66
793 792	Multi-Component Organic Layers on Metal Substrates. <i>Advanced Materials</i> , 2016 , 28, 1340-68 The Structural Origin of Electron Injection Enhancements with Fulleropyrrolidine Interlayers. 2016 , 3, 1500852	24	9
	The Structural Origin of Electron Injection Enhancements with Fulleropyrrolidine Interlayers. 2016 ,	24	
792	The Structural Origin of Electron Injection Enhancements with Fulleropyrrolidine Interlayers. 2016 , 3, 1500852	24	9
79 ²	The Structural Origin of Electron Injection Enhancements with Fulleropyrrolidine Interlayers. 2016, 3, 1500852 Semiconductor Heterojunctions. 2016, 223-248 Amide-Functionalized Small Molecules as Solution-Processed Electron Injection Layers in Highly	24	9
79 ² 79 ¹	The Structural Origin of Electron Injection Enhancements with Fulleropyrrolidine Interlayers. 2016, 3, 1500852 Semiconductor Heterojunctions. 2016, 223-248 Amide-Functionalized Small Molecules as Solution-Processed Electron Injection Layers in Highly Efficient Polymer Light-Emitting Diodes. 2016, 3, 1500621 Tailoring the highest occupied molecular orbital level of poly(N-vinylcarbazole) hole transport	24	9 1 4
79 ² 79 ¹ 79 ⁰ 789	The Structural Origin of Electron Injection Enhancements with Fulleropyrrolidine Interlayers. 2016, 3, 1500852 Semiconductor Heterojunctions. 2016, 223-248 Amide-Functionalized Small Molecules as Solution-Processed Electron Injection Layers in Highly Efficient Polymer Light-Emitting Diodes. 2016, 3, 1500621 Tailoring the highest occupied molecular orbital level of poly(N-vinylcarbazole) hole transport layers in organic multilayer heterojunctions. 2016, 108, 023301	24	9 1 4
79 ² 79 ¹ 79 ⁰ 789 788	The Structural Origin of Electron Injection Enhancements with Fulleropyrrolidine Interlayers. 2016, 3, 1500852 Semiconductor Heterojunctions. 2016, 223-248 Amide-Functionalized Small Molecules as Solution-Processed Electron Injection Layers in Highly Efficient Polymer Light-Emitting Diodes. 2016, 3, 1500621 Tailoring the highest occupied molecular orbital level of poly(N-vinylcarbazole) hole transport layers in organic multilayer heterojunctions. 2016, 108, 023301 Investigation of ITO free transparent conducting polymer based electrode. 2016,	24	9 1 4 7

7 ⁸ 4	Submonolayer and multilayer growth of titaniumoxide-phthalocyanine on Ag(111). 2016 , 18, 113022	39
783	On the nature of high field charge transport in reinforced silicone dielectrics: Experiment and simulation. 2016 , 120, 055101	11
782	The effects of nanoparticles and organic additives with controlled dispersion on dielectric properties of polymers: Charge trapping and impact excitation. 2016 , 120, 055102	13
781	Mixture interlayer for high performance organic-inorganic perovskite photodetectors. 2016 , 109, 123301	31
780	Minimizing electrode edge in organic transistors with ultrathin reduced graphene oxide for improving charge injection efficiency. 2016 , 18, 13209-15	10
779	The band-gap enhanced photovoltaic structure. 2016 , 108, 183503	5
778	Influence of steric hindrance on the molecular packing and the anchoring of quinonoid zwitterions on gold surfaces. 2016 , 40, 5782-5796	11
777	Coordination chemistry for information acquisition and processing. 2016 , 325, 135-160	21
776	Charge density at the contacts of symmetric and asymmetric organic diodes. 2016, 35, 74-86	4
775	Work function reduction using 8-hydroxyquinolinolato-lithium for efficient inverted devices. 2016 , 652, 102-105	5
774	Electric Potential Gradient at the Buried Interface between Lithium-Ion Battery Electrodes and the SEI Observed Using Photoelectron Spectroscopy. 2016 , 7, 1775-80	45
773	Non-conjugated water/alcohol soluble polymers with different oxidation states of sulfide as cathode interlayers for high-performance polymer solar cells. 2016 , 4, 4288-4295	14
772	Interface energetics and engineering of organic heterostructures in organic photovoltaic cells. 2016 , 59, 422-435	9
771	Relation between molecule ionization energy, film thickness and morphology of two indandione derivatives thin films. 2016 , 95, 12-18	4
770	Effect of intrinsic polymer properties on the photo sensitive organic field-effect transistors (Photo-OFETs). 2016 , 161, 36-42	9
769	Effect of Al(NO 3) 3 on suppression of the reduction of Ag ions in a poly(vinylpyrrolidone)/AgClO 4 complex membrane. 2016 , 290, 414-417	3
768	Inverted organic photovoltaic cells. 2016 , 45, 2937-75	153
767	Electrochemistry of N4 Macrocyclic Metal Complexes. 2016 ,	25

766	An electrode design rule for high performance top-illuminated organic photovoltaics. 2016, 3, 348-354	2
765	Study of the P3HT/PCBM interface using photoemission yield spectroscopy. 2016 ,	2
764	Determination of charge injection barrier using the displacement current measurement technique. 2016 , 34, 193-199	9
763	Supramolecular vs Electronic Structure: The Effect of the Tilt Angle of the Active Group in the Performance of a Molecular Diode. 2016 , 138, 5769-72	37
762	Functional Interfaces for Transparent Organic Electronic Devices: Consistent Description of Charge Injection by Combining In Situ XPS and Current Voltage Measurements with Self-Consistent Modeling. 2016 , 120, 10466-10475	2
761	Individual and collective modes of surface magnetoplasmon in thiolate-protected silver nanoparticles studied by MCD spectroscopy. 2016 , 8, 11264-74	24
760	Pentacene on Au(1 1 1), Ag(1 1 1) and Cu(1 1 1): From physisorption to chemisorption. 2016 , 28, 094005	32
759	Non-linear photoelectron effect contributes to the formation of negative matrix ions in UV-MALDI. 2016 , 18, 19574-87	7
758	Poly(pyridinium iodide ionic liquid)-based electron injection layers for solution-processed organic light-emitting devices. 2016 , 4, 6713-6719	13
757	Understanding molecular self-assembly of a diol compound by considering competitive interactions. 2016 , 18, 27390-27395	5
756	Tunneling of charge carriers across a goldEquaraine interface. 2016 , 380, 1493-1498	1
755	Highly Conducting In2O3 Nanowire Network with Passivating ZrO2 Thin Film for Solution-Processed Field Effect Transistors. 2016 , 2, 1600218	17
754	Interfacial electronic structure for high performance organic devices. 2016 , 16, 1533-1549	26
753	Doped Organic Transistors. 2016 , 116, 13714-13751	378
75 ²	Electrostatic phenomena in organic semiconductors: fundamentals and implications for photovoltaics. 2016 , 28, 433002	102
75 ¹	Graphene Ink as a Conductive Templating Interlayer for Enhanced Charge Transport of C-Based Devices. 2016 , 8, 29594-29599	3
75°	Interface Engineering of Metal Oxides using Ammonium Anthracene in Inverted Organic Solar Cells. 2016 , 8, 29866-29871	17
749	Energy level alignments at the interface of N,N'-bis-(1-naphthyl)-N,N'-diphenyl-1,1?-biphenyl-4,4?-diamine (NPB)/Ag-doped In2O3 and NPB/Sn-doped In2O3. 2016 , 387, 625-630	6

(2016-2016)

748	Tuning the work function of graphene with the adsorbed organic molecules: first-principles calculations. 2016 , 114, 2993-2998	5
747	Introduction to the Theory of Metal/Organic Interfaces. 2016 , 131-158	2
746	Experimental Characterization of Interfaces of Relevance to Organic Electronics. 2016 , 159-191	2
745	Experimental Characterization of Charge and Exciton Transport in Organic Semiconductors. 2016 , 231-291	3
744	Interface studies of the planar heterojunction perovskite solar cells. 2016 , 157, 783-790	38
743	Dithiocarbamate Self-Assembled Monolayers as Efficient Surface Modifiers for Low Work Function Noble Metals. 2016 , 32, 8812-7	8
742	Organic Semiconducting Materials. 2016 , 11-45	
741	Insights into the effect of donor-acceptor strength modulation on physical properties of phenoxazine-based imine dyes. 2016 , 134, 382-396	19
740	Observation of Charge Separation and Space-Charge Region in Single-Crystal P3HT/C60 Heterojunction Nanowires. 2016 , 55, 10273-7	11
739	Ternary Halide Perovskites for Highly Efficient Solution-Processed Hybrid Solar Cells. 2016 , 1, 712-718	16
738	A Quasi-Free-Standing Single Layer of a B3N3-Doped Nanographene Molecule Deposited on Au(111) Single Crystals. 2016 , 120, 17645-17651	13
737	Employing X-ray Photoelectron Spectroscopy for Determining Layer Homogeneity in Mixed Polar Self-Assembled Monolayers. 2016 , 7, 2994-3000	25
736	Dense Assembly of Soluble Acene Crystal Ribbons and Its Application to Organic Transistors. 2016 , 8, 24753-60	8
735	Radical polymers improve the metal-semiconductor interface in organic field-effect transistors. 2016 , 37, 148-154	13
734	Switching Hole and Electron Transports of Molecules on Metal Oxides by Energy Level Alignment Tuning. 2016 , 8, 22410-7	4
733	The Roles of Structural Order and Intermolecular Interactions in Determining Ionization Energies and Charge-Transfer State Energies in Organic Semiconductors. 2016 , 6, 1601211	37
732	Application to OLED Displays. 2016 , 183-305	
731	Investigation into the Gaussian density of states widths of organic semiconductors. 2016 , 49, 325106	12

730	Poly-3 (hexylthiophene) Hole Transporting Material with Organic Functionalized Carbon Nanostructures. 2016 , 26, 7443-7453	72
729	Squarylium and rubrene based filterless narrowband photodetectors for an all-organic two-channel visible light communication system. 2016 , 37, 346-351	27
728	In situ study of the electronic structure of atomic layer deposited oxide ultrathin films upon oxygen adsorption using ambient pressure XPS. 2016 , 6, 6778-6783	11
727	Charge Transport through Ferrocene 1,1'-Diamine Single-Molecule Junctions. 2016 , 12, 4849-4856	14
726	Resident holes and electrons at organic/conductor and organic/organic interfaces: An electron paramagnetic resonance investigation. 2016 , 37, 379-385	1
725	Direct characterization of the energy level alignments and molecular components in an organic hetero-junction by integrated photoemission spectroscopy and reflection electron energy loss spectroscopy analysis. 2016 , 27, 345704	3
724	Site-Specific Organic/Metal Interaction Revealed from Shockley-Type Interface State. 2016 , 120, 24307-24313	11
723	The origin of high PCE in PTB7 based photovoltaics: proper charge neutrality level and free energy of charge separation at PTB7/PCBM interface. 2016 , 6, 35262	37
722	R6G molecule induced modulation of the optical properties of reduced graphene oxide nanosheets for use in ultrasensitive SPR sensing. 2016 , 6, 21254	14
721	One-step additive crosslinking of conjugated polyelectrolyte interlayers: improved lifetime and performance of solution-processed OLEDs. 2016 , 4, 11150-11156	19
720	Formation of an interphase layer during deposition of cobalt onto tetraphenylporphyrin: a hard X-ray photoelectron spectroscopy (HAXPES) study. 2016 , 18, 30643-30651	7
719	Interface Structure of MoO3 on Organic Semiconductors. 2016 , 6, 21109	56
718	Organic heterojunctions: Contact-induced molecular reorientation, interface states, and charge re-distribution. 2016 , 6, 21291	34
717	Interface-induced face-on orientation of the active layer by self-assembled diblock conjugated polyelectrolytes for efficient organic photovoltaic cells. 2016 , 4, 18478-18489	27
716	Electronic States and Exciton Dynamics in Dicyanovinyl-Sexithiophene on Au(111). 2016 , 120, 27268-27275	17
715	Elucidating the influences of mechanical bending on charge transport at the interfaces of organic light-emitting diodes. 2016 , 619, 281-287	8
714	Improved Performance and Stability of Inverted Planar Perovskite Solar Cells Using Fulleropyrrolidine Layers. 2016 , 8, 31426-31432	52
713	Observation of Charge Separation and Space-Charge Region in Single-Crystal P3HT/C60 Heterojunction Nanowires. 2016 , 128, 10429-10433	1

(2016-2016)

Island shape and electronic structure in diindenoperylene thin films deposited on Au(110) single 712 crystals. 2016, 18, 13693-700 Efficient Charge Injection in Organic Field-Effect Transistors Enabled by Low-Temperature Atomic 28 Layer Deposition of Ultrathin VOx Interlayer. 2016, 26, 4456-4463 Electronic structure and self-organization properties of low band gap polymers: The effect of the 710 5 introduction of additional thiophene moieties. 2016, 157, 286-294 Investigation of Charge Transfer in Ag/N719/TiO2 Interface by Surface-Enhanced Raman 709 34 Spectroscopy. 2016, 120, 13078-13086 Light-responsive spiropyran based polymer thin films for use in organic field-effect transistor 708 35 memories. 2016. 4. 5398-5406 Interfacial electronic structure of C60/ZnPc/AZO on photoemission spectroscopy for organic 707 5 photovoltaic applications. 2016, 478, 145-149 Activated Aq ions and enhanced gas transport by incorporation of KIT-6 for facilitated olefin 706 13 transport membranes. 2016, 513, 95-100 Bis(diphenylamino)naphthalene host materials: careful selection of the substitution pattern for the 705 7 design of fully solution-processed triple-layered electroluminescent devices. 2016, 6, 60565-60577 Charge-Transfer State Energy and Its Relationship with Open-Circuit Voltage in an Organic 704 25 Photovoltaic Device. 2016, 120, 14059-14068 Effect of additional electron acceptor in hybrid P3HT:PCBM:ZnO spin-coated films for photovoltaic 703 application. 2016, 213, 1915-1921 High-resolution core-level photoemission measurements on the pentacene single crystal surface 702 14 assisted by photoconduction. 2016, 28, 094001 Lithium Fluoride Based Electron Contacts for High Efficiency n-Type Crystalline Silicon Solar Cells. 701 95 **2016**, 6, 1600241 Oligothiophene wires: impact of torsional conformation on the electronic structure. 2016, 18, 4842-9 700 10 Irradiation Wavelength-Dependent Photocurrent Sensing Characteristics of AuNPs/P3HT 699 Composites on Volatile Vapor. 2016, 16, 596-602 The incorporation of thermionic emission and work function tuning layer into intermediate 698 21 connecting layer for high performance tandem organic solar cells. 2016, 21, 123-132 697 Nanoscale heterogeniety and workfunction variations in ZnO thin films. 2016, 363, 516-521 18 Far-field and hole injection enhancement by noble metal nanoparticles in organic light emitting 696 21 devices. 2016, 211, 155-160 Degradation of organic light emitting diode: Heat related issues and solutions. 2016, 216, 40-50 695 31

694	Preparation and employment of carbon nanodots to improve electron extraction capacity of polyethylenimine interfacial layer for polymer solar cells. 2016 , 33, 62-70	12
693	(Poly(3,4-ethylenedioxythiophene):Polystyrene Sulfonate):Polytetrafluoroethylene for Use in High-Performance and Stable Bottom-Contact Organic Field-Effect Transistors. 2016 , 120, 956-962	11
692	Extracting the Density of States of Copper Phthalocyanine at the SiO2 Interface with Electronic Sum Frequency Generation. 2016 , 7, 1060-6	15
691	Interfacial engineering for high performance organic photovoltaics. 2016 , 19, 169-177	26
690	A study of the characteristics of indium tin oxide after chlorine electro-chemical treatment. 2016 , 82, 115-121	11
689	Energy-Level Alignment at the Organic/Electrode Interface in Organic Optoelectronic Devices. 2016 , 26, 129-136	53
688	Energy Level Bending in Ultrathin Polymer Layers Obtained through Langmuir Sheer Deposition. 2016 , 26, 1077-1084	33
687	Electronic Structures of Quaterthiophene and Septithiophene on Cu(111): Spatial Distribution of Adsorption-Induced States Studied by STM and DFT Calculation. 2016 , 120, 6681-6688	5
686	Synthesis and characterization of novel polymers containing aminophenylsilole. 2016 , 48, 723-728	5
685	Understanding Chemical versus Electrostatic Shifts in X-ray Photoelectron Spectra of Organic Self-Assembled Monolayers. 2016 , 120, 3428-3437	84
684	Assembly of quantum dots in polymer solar cells driven by orientational switching of mesogens under electric field. 2016 , 129, 184-191	6
683	Seamless growth of a supramolecular carpet. 2016 , 7, 10653	12
682	Substrate-Directed Growth of N-Heteropolycyclic Molecules on a Metal Surface. 2016 , 120, 2866-2873	15
681	The investigation of chemical interaction and energy level alignment at Bepp2/Fe65Co35 interface. 2016 , 370, 169-175	
68o	Molecular-Level Realignment in Donor Acceptor Bilayer Blends on Metals. 2016 , 120, 5997-6005	7
679	Strain-Dependent Dielectric Behavior of Carbon Black Reinforced Natural Rubber. 2016 , 49, 2339-2347	40
678	Electronic Structure Evolution during the Growth of Graphene Nanoribbons on Au(110). 2016 , 120, 7323-7331	14
677	Fluorinated SAMs on Si(001) surface: Surface electronic properties and structural aspects. 2016 , 191, 502-506	4

676	Charge injection barriers at metal/polyethylene interfaces. 2016 , 51, 506-512	42
675	Site-Selection in Single-Molecule Junction for Highly Reproducible Molecular Electronics. 2016 , 138, 1294-300	69
674	Self-assembly of tetracyanonaphtho-quinodimethane (TNAP) based metal®rganic networks on Pb(1 1 1): Structural, electronic, and magnetic properties. 2016 , 373, 2-7	4
673	Charge generation mechanism of tandem organic light emitting diodes with pentacene/C70 organic heterojunction as the connecting layer. 2016 , 4, 376-382	27
672	Hole injection engineering with MoO3 interlayer in organic light-emitting diode revealed by impedance spectroscopy. 2016 , 127, 1424-1428	8
671	Fluorinated and non-fluorinated conjugated polymers showing different photovoltaic properties in polymer solar cells with PFNBr interlayers. 2016 , 28, 178-183	19
670	Energy saving electrochromic windows from bistable low-HOMO level conjugated polymers. 2016 , 9, 117-122	102
669	Barrier modification of Au/n-GaAs Schottky structure by organic interlayer. 2016 , 90, 307-312	4
668	Fermi level, work function and vacuum level. 2016 , 3, 7-10	396
667	Strategies for Tuning Emission Energy in Phosphorescent Ir(III) Complexes. 2017 , 37, 117-145	22
666	Global and local aspects of the surface potential landscape for energy level alignment at organic-ZnO interfaces. 2017 , 485-486, 149-165	16
665	Interfacial electronic structures revealed at the rubrene/CHNHPbI interface. 2017, 19, 6546-6553	41
664	Recent Advances in Energetics of Metal Halide Perovskite Interfaces. 2017 , 4, 1600694	47
663	Interfacial chemical and electronic structure of cobalt deposition on 2,7-dioctyl[1]benzothieno[3,2-b]benzothiophene (C8-BTBT). 2017 , 402, 142-146	5
662	The marriage of AIE and interface engineering: convenient synthesis and enhanced photovoltaic performance. 2017 , 8, 3750-3758	31
661	Electrode buffer layers producing high performance nonvolatile organic write-once-read-many-times memory devices. 2017 , 7, 13171-13176	5
660	Electrostatically self-assembled chitosan derivatives working as efficient cathode interlayers for organic solar cells. 2017 , 34, 164-171	28
659	In-Depth Investigation of the Optical Effects in Rationally Designed Phenoxazine-Based Polyazomethines with Activated Quenched Fluorescence. 2017 , 121, 6300-6313	19

658	On-surface manipulation of atom substitution between cobalt phthalocyanine and the Cu(111) substrate. 2017 , 7, 13827-13835	30
657	Energy level alignment and molecular conformation at rubrene/Ag interfaces: Impact of contact contaminations on the interfaces. 2017 , 409, 22-28	10
656	Simplified Approach to Work Function Modulation in Polyelectrolyte Multilayers. 2017 , 33, 2169-2176	4
655	Understanding the strain-dependent dielectric behavior of carbon black reinforced natural rubber ☐ An interfacial or bulk phenomenon?. 2017 , 142, 91-97	26
654	Magnetization switching in ferromagnets by adsorbed chiral molecules without current or external magnetic field. 2017 , 8, 14567	90
653	Electronic Properties of Optically Switchable Photochromic Diarylethene Molecules at the Interface with Organic Semiconductors. 2017 , 18, 722-727	15
652	OLED Devices. 2017 , 7-59	2
651	Silicon-Quantum-Dot Light-Emitting Diodes With Interlayer-Enhanced Hole Transport. 2017 , 9, 1-10	21
650	Poly(4-vinylpyridine): A New Interface Layer for Organic Solar Cells. 2017, 9, 10929-10936	29
649	Structure-property relationship of D-A type copolymers based on thienylenevinylene for organic electronics. 2017 , 46, 77-87	10
648	Roles of Zeolite Confinement and CuDCu Angle on the Direct Conversion of Methane to Methanol by [Cu2(ED)]2+-Exchanged AEI, CHA, AFX, and MFI Zeolites. 2017 , 7, 3741-3751	97
647	Characterization of charge accumulation on multiple interfaces in phosphorescent organic light-emitting diodes. 2017 , 46, 166-172	3
646	Activating the molecular spinterface. 2017 , 16, 507-515	217
645	Surface Atomic Structure Directs the Fate of Human Mesenchymal Stem Cells. 2017 , 9, 15274-15285	16
644	Fluorinated Reduced Graphene Oxide as an Efficient Hole-Transport Layer for Efficient and Stable Polymer Solar Cells. 2017 , 2, 2010-2016	33
643	Molecular design of interfacial layers based on conjugated polythiophenes for polymer and hybrid solar cells. 2017 , 66, 1333-1348	16
642	Cyano-Functional Group as an Anchoring Tool for Organic Small Molecules on Gold. 2017 , 121, 13660-13665	2
641	Unveiling the Electronic Structure of ZnOI160 CoreBhell Quantum Dots: The Origin of Efficient Electron Transport. 2017 , 121, 12230-12235	5

640	Interface passivation and electron transport improvement of polymer solar cells through embedding a polyfluorene layer. 2017 , 19, 15207-15214	8
639	Improvement of both efficiency and stability in organic photovoltaics by using water-soluble anionic conjugated polyelectrolyte interlayer. 2017 , 5, 66-71	8
638	Dipole formation at organic/metal interfaces with pre-deposited and post-deposited metal. 2017 , 9, e379-e379	21
637	Fermi-level pinning appears upon weak electrode-organic contact without gap states: A universal phenomenon. 2017 , 48, 172-178	19
636	Time resolved resonant photoemission study of energy level alignment at donor/acceptor interfaces. 2017 , 683, 135-139	1
635	Energy Level Alignment at Hybridized OrganicMetal Interfaces: The Role of Many-Electron Effects. 2017 , 121, 13125-13134	19
634	Heterogeneous Integration of Carbon-Nanotube-Graphene for High-Performance, Flexible, and Transparent Photodetectors. 2017 , 13, 1700918	36
633	Electronic Structures of Nucleosides as Promising Functional Materials for Electronic Devices. 2017 , 121, 12750-12756	4
632	Enhancement of Electroluminescent Green Emission by Far-Field Coupling of Au Nanoparticles in Organic Light Emitting Diodes. 2017 , 56, 6952-6961	5
631	Effect of methanol treatment on the performance of P3HT:PC71BM bulk heterojunction solar cells with various cathodes. 2017 , 28, 12909-12915	5
630	Significant reduction in the hole-injection barrier by the charge-transfer state formation: Diindenoperylene contacted with silver and copper electrodes. 2017 , 49, 39-44	5
629	First-principles calculation of electronic energy level alignment at electrochemical interfaces. 2017 , 412, 335-341	4
628	First-principles studies of carrier injection in polyethylene (PE) and ethylene-vinyl acetate copolymer (EVA) oligomers. 2017 , 24, 574-582	15
627	Direct covalent grafting of an organic radical core on gold and silver. 2017 , 7, 20076-20083	7
626	Probing the interplay between geometric and electronic structure in a two-dimensional K-TCNQ charge transfer network. 2017 , 204, 97-110	19
625	Electronic, structural and chemical effects of charge-transfer at organic/inorganic interfaces. 2017 , 72, 105-145	110
624	Interfacial phenomena between conjugated organic molecules and noble metals. 2017, 34, 1281-1293	O
623	Energy Level Alignment at Metal/Solution-Processed Organic Semiconductor Interfaces. <i>Advanced Materials</i> , 2017 , 29, 1606901	. 27

622	C 1s Peak of Adventitious Carbon Aligns to the Vacuum Level: Dire Consequences for Material's Bonding Assignment by Photoelectron Spectroscopy. 2017 , 18, 1507-1512	349
621	Effects of the interfacial charge injection properties of silver nanowire transparent conductive electrodes on the performance of organic light-emitting diodes. 2017 , 121, 105304	9
620	Atomically modified thin interface in metal-dielectric hetero-integrated systems: control of electronic properties. 2017 , 29, 145503	
619	Tuning the Work Function of Printed Polymer Electrodes by Introducing a Fluorinated Polymer To Enhance the Operational Stability in Bottom-Contact Organic Field-Effect Transistors. 2017 , 9, 12637-12646	10
618	C70/C70:pentacene/pentacene organic heterojunction as the connecting layer for high performance tandem organic light-emitting diodes: Mechanism investigation of electron injection and transport. 2017 , 121, 115502	7
617	Easily accessible conjugated pyrene sulfonates as cathode interfacial materials for polymer solar cells. 2017 , 5, 657-662	8
616	Energy level alignment at the interface of NPB/HAT-CN/graphene for flexible organic light-emitting diodes. 2017 , 668, 64-68	15
615	High Brightness Fluorescent White Polymer Light-Emitting Diodes by Promoted Hole Injection via Reduced Barrier by Interfacial Dipole Imparted from Chlorinated Indium Tin Oxide to the Hole Injection Layer PEDOT:PSS. 2017 , 9, 3824-3830	5
614	Elementary Processes in Organic Photovoltaics. 2017,	11
613	Electronic Properties of Interfaces with Oligo- and Polythiophenes. 2017 , 377-399	3
612	Charge Separation at Nanostructured Molecular Donor Acceptor Interfaces. 2017, 77-108	2
611	Highly efficient ITO-free organic light-emitting diodes employing a roughened ultra-thin silver electrode. 2017 , 42, 52-58	16
610	Orientation-Dependent Work-Function Modification Using Substituted Pyrene-Based Acceptors. 2017 , 121, 24657-24668	25
609	Controlled Synthesis of Nickel Encapsulated into Nitrogen-Doped Carbon Nanotubes with Covalent Bonded Interfaces: The Structural and Electronic Modulation Strategy for an Efficient Electrocatalyst in Dye-Sensitized Solar Cells. 2017 , 29, 9680-9694	63
608	Determination of charge transport activation energy and injection barrier in organic semiconductor devices. 2017 , 122, 115502	23
607	Dielectric response of vulcanized natural rubber containing BaTiO3 filler: The role of particle functionalization. 2017 , 97, 57-67	23
606	Size-Dependent Level Alignment between Rutile and Anatase TiO Nanoparticles: Implications for Photocatalysis. 2017 , 8, 5593-5598	62
605	Estimation of hole injection barrier at the poly-3(hexylthiophene)/metal interface using accumulated charge measurement. 2017 , 51, 162-167	3

604	Role of Hybrid Charge Transfer States in the Charge Generation at ZnMgO/P3HT Heterojunctions. 2017 , 121, 21955-21961	9
603	Investigating Working Mechanism of Metallophthalocyanine Derivatives as a Cathode Interlayer in Polymer Solar Cells by Photoemission Spectroscopy. 2017 , 121, 21244-21251	1
602	Sulfur-Capped Germanium Nanocrystals: Facile Inorganic Ligand Exchange. 2017 , 121, 22597-22606	4
601	Voltage Dependence of MoleculeElectrode Coupling in Biased Molecular Junctions. 2017, 121, 21136-21144	16
600	Energy Level Alignment of N-Doping Fullerenes and Fullerene Derivatives Using Air-Stable Dopant. 2017 , 9, 35476-35482	9
599	Self-Bleaching Behaviors in Black-to-Transmissive Electrochromic Polymer Thin Films. 2017 , 9, 34122-34130	20
598	Crystallization Dependent Stability of Perovskite Solar Cells With Different Hole Transporting Layers. 2017 , 1, 1700141	7
597	Controlling Molecular Doping in Organic Semiconductors. <i>Advanced Materials</i> , 2017 , 29, 1703063 24	286
596	Intermixing Effect on Electronic Structures of TQ1:PC71BM Bulk Heterojunction in Organic Photovoltaics. 2017 , 1, 1700142	5
595	Energy band alignment in operando inverted structure P3HT:PCBM organic solar cells. 2017 , 40, 454-461	21
594	Color switching behaviors of organic bistable light-emitting devices fabricated utilizing an aluminum-nanoparticle-embedded tris(8-hydroxyquinoline)aluminum layer and double emitting layers. 2017 , 50, 94-99	7
593	Influence of the Fluorination of CoPc on the Interfacial Electronic Structure of the Coordinated Metal Ion. 2017 , 121, 18564-18574	13
592	Maleic-PEGX-SR3 thin films for polymer light-emitting devices. 2017 ,	
591	Reliable Work Function Determination of Multicomponent Surfaces and Interfaces: The Role of Electrostatic Potentials in Ultraviolet Photoelectron Spectroscopy. 2017 , 4, 1700324	35
590	Electronic Structure of Polyethylene: Role of Chemical, Morphological and Interfacial Complexity. 2017 , 7, 6128	34
589	The effect of organic additives on the intergranular conductivity of Al-doped ZnO. 2017 , 7, 38019-38027	2
588	Triisopropylsilylethynyl-Pentacene on Au(111): Adsorption Properties, Electronic Structure, and Singlet Fission Dynamics. 2017 , 121, 18075-18083	10
587	Symmetry, Shape, and Energy Variations in Frontier Molecular Orbitals at Organic/Metal Interfaces: The Case of F4TCNQ. 2017 , 121, 28412-28419	5

586	Effect of Si on the Energy Band Gap Modulation and Performance of Silicon Indium Zinc Oxide Thin-Film Transistors. 2017 , 7, 15392	21
585	In-situ analysis of microwave conductivity and impedance spectroscopy for evaluation of charge carrier dynamics at interfaces. 2017 , 111, 203302	5
584	Virtual Design in Organic Electronics: Screening of a Large Set of 1,4-Bis(phenylethynyl)benzene Derivatives as Molecular Semiconductors. 2017 , 121, 28249-28261	11
583	Interfacial electronic structure of ClSubPc non-fullerene acceptors in organic photovoltaics using soft X-ray spectroscopies. 2017 , 19, 31628-31633	6
582	Inkjet printing of NiO films and integration as hole transporting layers in polymer solar cells. 2017 , 7, 1775	30
581	On electrode pinning and charge blocking layers in organic solar cells. 2017 , 121, 195502	11
580	n-Doping-induced efficient electron-injection for high efficiency inverted organic light-emitting diodes based on thermally activated delayed fluorescence emitter. 2017 , 5, 8400-8407	21
579	Estimation of the Charge Injection Barrier at a Metal/Organic Semiconductor Interface Based on Accumulated Charge Measurement: The Effect of Offset Bias Voltages. 2017 , 121, 14725-14730	7
578	N-Type Superconductivity in an Organic Mott Insulator Induced by Light-Driven Electron-Doping. Advanced Materials, 2017 , 29, 1606833	17
577	The role of the density of interface states in interfacial energy level alignment of PTCDA. 2017 , 49, 249-254	16
576	Effect of physisorption of inert organic molecules on Au(111) surface electronic states. 2017 , 19, 18646-1865	16
575	Electrical conduction and gas sensing characteristics of P3HT/Au nano-islands composite. 2017 , 241, 1099-1105	6
574	Mixed-dimensional van der Waals heterostructures. 2017 , 16, 170-181	897
573	Unconventional Computing Realized with Hybrid Materials Exhibiting the PhotoElectrochemical Photocurrent Switching (PEPS) Effect. 2017 , 429-467	3
572	Work function mediated by deposition of ultrathin polar FeO on Pt(111). 2017 , 392, 849-853	9
571	Phosphorescent Polymer Light-Emitting Diodes. 2017 , 489-553	
570	Organic Planar Heterojunctions: From Models for Interfaces in Bulk Heterojunctions to High-Performance Solar Cells. <i>Advanced Materials</i> , 2017 , 29, 1603269	85
569	Energy Level Alignment of Organic Molecules with Chemically Modified Alkanethiolate Self-Assembled Monolayers. 2017 , 121, 27399-27405	4

568	High-frequency organic rectifiers through interface engineering. 2017 , 7, 755-769	9
567	Energetic and Nanostructural Design of Small-Molecular-Type Organic Solar Cells. 2017, 137-204	
566	Analytical model of energy level alignment at metal-organic interface facilitating hole injection. 2017 ,	1
565	Adsorption characteristics of ErN@Con W(110) and Au(111) studied via scanning tunneling microscopy and spectroscopy. 2017 , 8, 1127-1134	4
564	Bibliography. 2017 , 195-209	
563	Enhanced Emission by Accumulated Charges at Organic/Metal Interfaces Generated during the Reverse Bias of Organic Light Emitting Diodes. 2017 , 7, 1045	5
562	Adsorption and electronic properties of pentacene on thin dielectric decoupling layers. 2017 , 8, 1388-1395	10
561	Energy-level alignment at interfaces between manganese phthalocyanine and C. 2017 , 8, 927-932	3
560	Introduction to Electronic Properties and Dynamics of Organic Complexes as Self-Assembled Monolayers. 2017 ,	
559	Electronic Level Alignment at an Indium Tin Oxide/PbI Interface and Its Applications for Organic Electronic Devices. 2018 , 10, 8909-8916	8
558	Atomic Nature of the Growth Mechanism of Atomic Layer Deposited High-IYO on GaAs(001)-4 Ib Based on in Situ Synchrotron Radiation Photoelectron Spectroscopy. 2018 , 3, 2111-2118	4
557	Correlation of Device Performance and Fermi Level Shift in the Emitting Layer of Organic Light-Emitting Diodes with Amine-Based Electron Injection Layers. 2018 , 10, 8877-8884	5
556	Fluctuation in Interface and Electronic Structure of Single-Molecule Junctions Investigated by Current versus Bias Voltage Characteristics. 2018 , 140, 3760-3767	29
555	Ordered Growth and Electronic Properties of 1,2:8,9-Dibenzopentacene (trans-DBPen) on Ag(111). 2018 , 122, 8348-8355	7
554	Molecule-Adsorbed Topological Insulator and Metal Surfaces: A Comparative First-Principles Study. 2018 , 30, 1849-1855	6
553	Modification of Gold Work Function upon Adsorption of Mercaptobiphenylcarbonitrile: Experimental Evidence for a Theoretical Prediction. 2018 , 122, 6083-6092	2
552	Organic field-effect transistors integrated with TiCT electrodes. 2018 , 10, 5191-5197	23
551	Energy level alignment of dipolar interface layer in organic and hybrid perovskite solar cells. 2018 , 6, 2915-2924	42

550 Structural Switching of Self-Assembled Monolayer by External Electric Field. **2018**, 16, 76-78

549	An effect of the film texture on high-voltage polarization and local piezoelectric properties of the ferroelectric copolymer of vinylidene fluoride. 2018 , 296, 1057-1070	3
548	Failure of Fermi Level in Referencing Chemical Shift of Molecules on Solid Surfaces. 2018 , 5, 1800150	1
547	The organic-2D transition metal dichalcogenide heterointerface. 2018 , 47, 3241-3264	113
546	Quantitative Femtosecond Charge Transfer Dynamics at Organic/Electrode Interfaces Studied by Core-Hole Clock Spectroscopy. 2018 , 137-178	1
545	. 2018 , 8, 505-511	9
544	Impact of ambient environment on the electronic structure of CuPc/Au sample. 2018, 92, 841-846	1
543	Femtosecond Time-Resolved Transient Absorption Spectroscopy with Sub-Diffraction-Limited Spatial Resolution Reveals Accelerated Exciton Loss at Gold-Poly(3-Hexylthiophene) Interface. 2018 , 122, 3454-3462	5
542	On the Molecular Origin of Charge Separation at the Donor Acceptor Interface. 2018, 8, 1702232	45
541	Large Converse Piezoelectric Effect Measured on a Single Molecule on a Metallic Surface. 2018 , 140, 940-946	25
540	Templating effect of the substrate on the structure of Cu-phthalocyanine thin film. 2018, 669, 176-182	3
539	Emerging Role of the Band-Structure Approach in Biohybrid Photovoltaics: A Path Beyond Bioelectrochemistry. 2018 , 28, 1705305	39
538	Two dimensional simulation of patternable conducting polymer electrode based organic thin film transistor. 2018 , 33, 025006	5
537	Effect of Internal Heteroatoms on Level Alignment at Metal/Molecular Monolayer/Si Interfaces. 2018 , 122, 3312-3325	6
536	Ga-Ti-codoped ZnO embedded silver nanoparticles as an alternative anode in blue and green OLEDs. 2018 , 356, 290-297	2
535	Orbital Control of Photocurrents in Large Area All-Carbon Molecular Junctions. 2018 , 140, 1900-1909	22
534	Copper Phthalocyanine as Contact Layers for Pentacene Films Grown on Coinage Metals. 2018 , 122, 2165-21	72 ₁₄
533	Understanding the Impact of Film Disorder and Local Surface Potential in Ultraviolet Photoelectron Spectroscopy of PEDOT. 2018 , 39, 1700533	20

532	Alcohol-Soluble Conjugated Polymers as Cathode Interlayers for All-Polymer Solar Cells. 2018 , 1, 2176-2182	16
531	Reliable determination of chemical state in x-ray photoelectron spectroscopy based on sample-work-function referencing to adventitious carbon: Resolving the myth of apparent constant binding energy of the C 1s peak. 2018 , 451, 99-103	332
530	Modification of FN tunneling provoking gate-leakage current in ZTO (zinc-tin oxide) TFT by regulating the ZTO/SiO2 area ratio. 2018 , 112, 183502	4
529	Spin Interface and Magnetic Properties of Organic-ferromagnetic Heterojunctions. 2018, 109-135	
528	The adsorption geometry and molecular self-assembly of graphene for 1,3,5-triphenylbenzene on Cu(111). 2018 , 675, 42-46	2
527	Modifying the Surface Properties of Indium Tin Oxide with Alcohol-Based Monolayers for Use in Organic Electronics. 2018 , 1, 2237-2248	9
526	Molecularly Resolved Electronic Landscapes of Differing Acceptor Donor Interface Geometries. 2018 , 122, 8437-8444	9
525	Improved performance of small molecule solar cell by using oblique deposition technique and zinc phthalocyanine cathode buffer layer 2018 , 8, 10999-11005	2
524	Elementary steps in electrical doping of organic semiconductors. 2018 , 9, 1182	133
523	Orbital-specific electronic interaction in crystalline films of iron phthalocyanine grown on Au(111) probed by angle-resolved photoemission spectroscopy. 2018 , 2, 609-614	6
522	Molecular engineering of Rashba spin-charge converter. 2018 , 4, eaar3899	16
521	Air-Stable and High-Performance Solution-Processed Organic Light-Emitting Devices Based on Hydrophobic Polymeric Ionic Liquid Carrier-Injection Layers. <i>Advanced Materials</i> , 2018 , 30, e1705915	26
520	Controlling energy level positions in hole conducting molecular films by additives. 2018 , 224, 100-106	3
519	Organic thin-film transistors with sub-10-micrometer channel length with printed polymer/carbon nanotube electrodes. 2018 , 52, 165-171	8
518	Interface-Assisted Sign Inversion of Magnetoresistance in Spin Valves Based on Novel Lanthanide Quinoline Molecules. 2018 , 28, 1702099	26
517	Charge Carriers at Organic Drganic Interfaces. 2018 , 67-92	
516	Recent progress in interface engineering of organic thin film transistors with self-assembled monolayers. 2018 , 2, 11-21	40
515	Analysis of photon emission induced by light and heavy ions in time-of-flight medium energy ion scattering. 2018 , 417, 75-80	4

514	Negative differential resistance in heterojunction polymeric films. 2018, 114, 15-22	5
513	A study of adventitious contamination layers on technically important substrates by photoemission and NEXAFS spectroscopies. 2018 , 148, 48-53	9
512	Influence of molecular distortion on the exciton quenching for quaterthiophene-terminated self-assembled monolayers on Au(111). 2018 , 669, 160-168	2
511	Organic-inorganic hybrids based on phenanthrene-functionalized gold nanoparticles for OLEDs. 2018 , 31, e3796	O
510	The effect of surfactants on electrohydrodynamic jet printing and the performance of organic field-effect transistors. 2018 , 20, 1210-1220	20
509	Charge transport and prototypical optical absorptions in functionalized zinc phthalocyanine compounds: A density functional study. 2018 , 31, e3785	8
508	Experimental Investigation on Charge Transfer Between Organic Adsorbates and Solid Surfaces. 2018 , 50-67	1
507	Deposition rate related DPA OFET threshold voltage shift and hysteresis variation. 2018 , 6, 12498-12502	3
506	Chemical Functionalization and Photo-Induced Charge Transport. 2018, 573-581	
505	Excitation-Wavelength-Dependent and Substrate-Dependent Photoluminescence From the Nonconjugated Polymeric Thin Film With Self-Assembly Nanoparticles. 2018 , 10, 1-8	1
504	Application of ferroelectric materials for improving output power of energy harvesters. 2018, 5, 30	46
503	Formation of Occupied and Unoccupied Hybrid Bands at Interfaces between Metals and Organic Donors/Acceptors. 2018 , 122, 27554-27560	8
502	In Situ Measurement and Control of the Fermi Level in Colloidal Nanocrystal Thin Films during Their Fabrication. 2018 , 9, 7165-7172	9
501	The Work Function of TiO2. 2018 , 1, 73-89	84
500	Embedded Dipole Self-Assembled Monolayers for Contact Resistance Tuning in p-Type and n-Type Organic Thin Film Transistors and Flexible Electronic Circuits. 2018 , 28, 1804462	48
499	Spectroscopic and microscopic investigations of organic ultrathin films: Correlation between geometrical structures and unoccupied electronic states. 2018 , 93, 108-130	11
498	Photoelectron Angular Distribution Induced by Weak Intermolecular Interaction in Highly Ordered Aromatic Molecules. 2018 , 122, 26472-26479	5
497	Unoccupied States Measurements, Spatial Mapping, and Nanoscale Structures of Organic Ultrathin Films. 2018 , 12, A0098	

496	Facile Synthesis of an Efficient and Robust Cathode Interface Material for Polymer Solar Cells. 2018 , 1, 7130-7139	15
495	Theoretical Insights into Vinyl Derivatives Adsorption on a Cu(100) Surface. 2018 , 122, 27301-27313	5
494	Impact of molecular orientation on energy level alignment at C60/pentacene interfaces. 2018, 113, 163302	8
493	Understanding the effects of the energy band alignment at the donor/acceptor interface on the open circuit voltage of organic photovoltaic devices. 2018 , 711, 113-117	8
492	Oxide-organic heterostructures: a case study of charge transfer disturbance at a SnO-copper phthalocyanine buried interface. 2018 , 20, 16092-16101	7
491	Femtosecond and Attosecond Electron-Transfer Dynamics in PCPDTBT:PCBM Bulk Heterojunctions. 2018 , 122, 12605-12614	11
490	van der Waals Interaction Activated Strong Electronic Coupling at the Interface between Chloro Boron-Subphthalocyanine and Cu(111). 2018 , 122, 14621-14630	5
489	Enhanced diode characteristics of organic solar cell with silanized fluorine doped tin oxide electrode. 2018 ,	1
488	Energy level alignment of blended organic semiconductors and electrodes at the interface. 2018 , 18, 982-992	3
487	Progress in organic molecular/ferromagnet spinterfaces: towards molecular spintronics. 2018 , 6, 6619-6636	25
486	Revealing the influence of hole injection material's molecular orientation on OLED's performance. 2018 , 59, 301-305	9
485	Energy level alignment and hole injection property of poly(9-vinylcarbazole)/indium tin oxide interface. 2018 , 706, 317-322	9
484	Impact of surface states and bulk doping level on hybrid inorganic/organic semiconductor interface energy levels. 2018 , 123, 245501	13
483	Polymer-metal-polymer (PMP) multilayer transparent electrode for organic optoelectronics. 2018 , 156, 135-142	8
482	Visualization of the carrier transport dynamics in layered Organic Light Emitting Diodes by Modulus spectroscopy. 2018 , 61, 10-17	9
481	The influence of ionic radius of interfacial molecule on device performances of polymer solar cells. 2018 , 170, 906-912	3
480	Charge Transfer in Molecular Materials. 2018 , 1-31	3

478	Engineered Nanomaterials for Organic Light-Emitting Diodes (OLEDs). 2018, 312-323	3
477	Electronic Structure of C/Zinc Phthalocyanine/VDIInterfaces Studied Using Photoemission Spectroscopy for Organic Photovoltaic Applications. 2018 , 23,	7
476	Carrier injection in organic electronics: Injection hotspot effect beyond barrier reduction effect. 2018 , 113, 043302	4
475	Light-Induced Interfacial Dynamics Dramatically Improve the Photocurrent in Dye-Sensitized Solar Cells: An Electrolyte Effect. 2018 , 10, 26241-26247	3
474	Correlating the effective work function at buried organic/metal interfaces with organic solar cell characteristics. 2018 , 6, 8060-8068	7
473	Thin film properties and stability of a potential molecular quantum bit based on copper(II). 2018 , 6, 8028-803	4 7
472	Enhanced oxidation power in photoelectrocatalysis based on a micrometer-localized positive potential in a terrace hetero pli junction. 2018 , 10, 630-641	4
471	Organic Semiconductors ?. 2018,	1
470	Influence of Acrylic Polymers Stereoregularity on Interface Interactions in Model Thin Film Systems. 2018 , 219, 1800097	
469	Strategic Design of Vacancy-Enriched FeS Nanoparticles Anchored on FeC-Encapsulated and N-Doped Carbon Nanotube Hybrids for High-Efficiency Triiodide Reduction in Dye-Sensitized Solar Cells. 2018 , 10, 31208-31224	45
468	Fabricating Quasi-Free-Standing Graphene on a SiC(0001) Surface by Steerable Intercalation of Iron. 2018 , 122, 21484-21492	15
467	Interfacial effects on the microstructures and magnetoresistance of Ni80Fe20/P3HT/Fe organic spin valves. 2018 , 769, 991-997	5
466	Modification of the fluorinated tin oxide/electron-transporting material interface by a strong reductant and its effect on perovskite solar cell efficiency. 2018 , 3, 741-747	7
465	Dipole-induced effects on charge transfer and charge transport. Why do molecular electrets matter?. 2018 , 96, 843-858	12
464	Correlation between Chemical and Electronic Properties of Solution-Processed Nickel Oxide. 2018 , 1, 3113-3122	10
463	Direct visualization of diffuse unoccupied molecular orbitals at a rubrene/graphite interface. 2018 , 20, 17415-17422	7
462	A review for polaron dependent charge transport in organic semiconductor. 2018 , 61, 223-234	26
461	A fragment-based approach to evaluate the performance of AMOEBA polarizable force field on charge-carrier electronic polarization. 2019 , 516, 84-91	2

460	Bio-inspired protonic memristor devices based on metal complexes with proton-coupled electron transfer. 2019 , 213, 99-113	8
459	Vacuum-Level Shift at Al/LiF/Alq Interfaces: A First-Principles Study. 2019 , 4, 13426-13434	3
45 ⁸	Efficient Charge Carrier Injection and Balance Achieved by Low Electrochemical Doping in Solution-Processed Polymer Light-Emitting Diodes. 2019 , 29, 1904092	8
457	Interface Behaviour and Work Function Modification of Self-Assembled Monolayers on Sn-Doped In2O3. 2019 , 2, 241-256	1
45 ⁶	Visualizing the Vertical Energetic Landscape in Organic Photovoltaics. 2019 , 3, 2513-2534	16
455	Interfaces in organic electronics. 2019 , 4, 627-650	129
454	A graphene-based hybrid material with quantum bits prepared by the double Langmuir-Schaefer method 2019 , 9, 24066-24073	7
453	Well-Ordered Monolayer Growth of Crown-Ether Ring Molecules on Cu(111) in Ultra-High Vacuum: An STM, UPS, and DFT Study. 2019 , 123, 18939-18950	5
452	Outstanding Energy Exchange between Organic Molecules and Metal Surfaces: Decomposition Kinetics of Excited Vinyl Derivatives Driven by the Interaction with a Cu(111) Surface. 2019 , 123, 19625-19636	5 ⁵
451	Band to Band Tunneling at the Zinc Oxide (ZnO) and Lead Selenide (PbSe) Quantum Dot Contact; Interfacial Charge Transfer at a ZnO/PbSe/ZnO Probe Device. 2019 , 12,	3
45 ⁰	First-principle investigation of the charge injection barriers of polyethylene and polytetrafluoroethylene oligomers. 2019 , 126, 035101	8
449	2 Low-Molecular-Weight Materials: Hole Injection Materials. 2019 , 1-10	
448	The Impact of Dipolar Layers on the Electronic Properties of Organic/Inorganic Hybrid Interfaces. 2019 , 6, 1900581	75
447	Recent Advances in Ambipolar Transistors for Functional Applications. 2019 , 29, 1902105	86
440	Unveiling the origin of performance reduction in perovskite solar cells with TiO2 electron transport layer: Conduction band minimum mismatches and chemical interactions at buried interface. 2019 , 495, 143490	5
445	Organic electrode materials with solid-state battery technology. 2019 , 7, 18735-18758	57
444	Stabilizing Silver Window Electrodes for Organic Photovoltaics Using a Mercaptosilane Monolayer. 2019 , 2, 5198-5205	5
443	Doping of Tetraalkylammonium Salts in Polyethylenimine Ethoxylated for Efficient Electron Injection Layers in Solution-Processed Organic Light-Emitting Devices. 2019 , 11, 25351-25357	10

442	Triphenylene-Derived Electron Acceptors and Donors on Ag(111): Formation of Intermolecular Charge-Transfer Complexes with Common Unoccupied Molecular States. 2019 , 15, e1901741	2
441	Impact of Orbital Hybridization at MoleculeMetal Interface on Carrier Dynamics. 2019, 123, 25877-25882	6
440	A High Efficient FEMD-Based Data Hiding Algorithm. 2019 , 1335, 012014	
439	Vacuum-Deposited Biternary Organic Photovoltaics. 2019 , 141, 18204-18210	14
438	Modulating Photoelectrochemical Water-Splitting Activity by Charge-Storage Capacity of Electrocatalysts. 2019 , 123, 28753-28762	8
437	A generalized Stark effect electromodulation model for extracting excitonic properties in organic semiconductors. 2019 , 10, 5089	5
436	Small-Molecule-Based Organic Field-Effect Transistor for Nonvolatile Memory and Artificial Synapse. 2019 , 29, 1904602	102
435	Energy-Level Alignment at Organic/Inorganic Interfaces from First Principles: Example of Poly(para-phenylene)/Rock-Salt ZnO(100). 2019 , 31, 7143-7150	3
434	Interface and surface properties of oxideBrganic hybrid nanostructures. 2019 , 215-256	2
433	Solvent treatment induced interface dipole and defect passivation for efficient and bright red quantum dot light-emitting diodes. 2019 , 75, 105412	4
432	Direct probing of the effective surface layer thickness during surface electrical breakdown along the solid dielectric and gas interface. 2019 , 498, 143812	5
431	Exfoliated Graphite Electrodes for Organic Single-Crystal Field-Effect Transistor Devices. 2019 , 1, 2174-2183	2
430	Accumulated charge measurement using a substrate with a restricted-bottom-electrode structure. 2019 , 74, 251-257	2
429	Coexisting Charge States in a Unary Organic Monolayer Film on a Metal. 2019 , 10, 6438-6445	15
428	Charge injection and transport properties of large area organic junctions based on aryl thin films covalently attached to a multilayer graphene electrode. 2019 , 1, 414-420	5
427	Study of energy level alignment at weakly interacting small organic molecular thin film interfaces: The validity of classical model from inorganics. 2019 , 125, 035301	2
426	Surface CH3NH3+ to CH3+ Ratio Impacts the Work Function of Solution-Processed and Vacuum-Sublimed CH3NH3PbI3 Thin Films. 2019 , 6, 1801827	8
425	Towards direct enzyme wiring: a theoretical investigation of charge carrier transfer mechanisms between glucose oxidase and organic semiconductors. 2019 , 21, 2968-2976	15

424	Electronic and Optical Excitations at the Pyridine/ZnO(101🛈) Hybrid Interface. 2019 , 2, 1800108	9
423	Interface properties of CoPc and CoPcF on graphene/nickel: influence of germanium intercalation. 2019 , 31, 174004	3
422	Effects of gas cluster ion beam sputtering on the molecular orientation of organic semiconductor films: Ultraviolet photoelectron spectroscopy study of [6]phenacene. 2019 , 114, 231603	4
421	Interface engineering of CdS/CZTSSe heterojunctions for enhancing the Cu2ZnSn(S,Se)4 solar cell efficiency. 2019 , 13, 256-266	12
420	Wafer-scale and patternable synthesis of NbS2 for electrodes of organic transistors and logic gates. 2019 , 7, 8599-8606	5
419	Deviation from Point Dipole Analysis for Exciton Quenching in Quaterthiophene-Terminated Self-Assembled Monolayers on Au(111). 2019 , 123, 16127-16136	1
418	Energy level alignment and interfacial dipole layer formation at the P3HT:PCBM-Electrolyte interface in organic photoelectrochemical cells. 2019 , 200, 110009	
417	Accelerating GW-Based Energy Level Alignment Calculations for Molecule-Metal Interfaces Using a Substrate Screening Approach. 2019 , 15, 4218-4227	16
416	Effects of Energy-Level Alignment on Characteristics of Inverted Organic Light-Emitting Diodes. 2019 , 11, 21749-21755	O
415	Post-treatment of Perovskite Films toward Efficient Solar Cells via Mixed Solvent Annealing. 2019 , 2, 4954-4963	14
414	Imaging of triboelectric charge distribution induced in polyimide film by using optical second-harmonic generation: Electronic charge distribution and dipole alignment. 2019 , 114, 233301	3
413	Introducing pyridyl into electron transport materials plays a key role in improving electron mobility and interface properties for inverted perovskite solar cells. 2019 , 7, 16304-16312	6
412	n-Type Doping of Organic Semiconductors: Immobilization via Covalent Anchoring. 2019 , 31, 4213-4221	17
411	Reversible switching of the Au(111) work function by near infrared irradiation with a bistable SAM based on a radical donor ceptor dyad. 2019 , 7, 7418-7426	1
410	Increasing Quantum Efficiency of Polymer Solar Cells with Efficient Exciton Splitting and Long Carrier Lifetime by Molecular Doping at Heterojunctions. 2019 , 4, 1356-1363	29
409	Promotional effect of silver nanoparticle embedded Ga-Zr-codoped TiO as an alternative anode for efficient blue, green and red PHOLEDs 2019 , 9, 13664-13676	4
408	Polymer Electrolyte Blend Gate Dielectrics for High-Performance Ultrathin Organic Transistors: Toward Favorable Polymer Blend Miscibility and Reliability. 2019 , 11, 17610-17616	20
407	Microscopic View of Tin Phthalocyanine Adsorption on the Rutile TiO2(011) Surface. 2019 , 123, 9209-9216	4

406	Modifying the organic/metal interface via solvent vapor annealing to enhance the performance of blue OLEDs. 2019 , 7, 4784-4790		4
405	A Solvent-Free Solution: Vacuum-Deposited Organic Monolayers Modify Work Functions of Noble Metal Electrodes. 2019 , 29, 1808385		17
404	The role of Dawson Polyoxometalates as interfacial layers on the energy band alignment between indium tin oxide and poly(3-hexylthiophene) films. 2019 , 676, 92-99		1
403	Direct Detection of Local Electric Polarization in the Interfacial Region in Ferroelectric Polymer Nanocomposites. <i>Advanced Materials</i> , 2019 , 31, e1807722	24	47
402	Electronic structure and Fermi-level pinning of indigo for application in environment-friendly devices. 2019 , 484, 808-813		3
401	High-Performance Inverted Perovskite Solar Cells Using Doped Poly(triarylamine) as the Hole Transport Layer. 2019 , 2, 1932-1942		33
400	Direct p-doping of Li-TFSI for efficient hole injection: Role of polaronic level in molecular doping. 2019 , 480, 565-571		4
399	Halide Perovskites: Is It All about the Interfaces?. 2019 , 119, 3349-3417		287
398	How adsorbates alter the metallic behavior of quasi-1D electron systems of the Si(5 5 3)-Au surface. 2019 , 31, 195001		8
397	Redox gated polymer memristive processing memory unit. 2019 , 10, 736		55
396	FePc and FePcF on Rutile TiO(110) and (100): Influence of the Substrate Preparation on the Interaction Strength. 2019 , 24,		6
395	A Comparative Computational Study of the Adsorption of TCNQ and F4-TCNQ on the Coinage Metal Surfaces. 2019 , 4, 16906-16915		4
394	Probing site-dependent decoupling of hexagonal boron nitride with molecular frontier orbitals. 2019 , 37, 061404		6
393	Interfacial charge transfer enhancement via formation of binary molecular assemblies on electronically corrugated boron nitride. 2019 , 21, 26146-26153		3
392	Mobility-Dependent Charge-Transfer Efficiency at the ZnO/MAPbI3 Perovskite Contact: Developing a Novel Test Platform for Probing Electrical Contact Properties. 2019 , 123, 30689-30695		3
391	Simple Interface Modification of Electroactive Polymer Film Electrodes. 2019 , 11, 47131-47142		8
390	Reconfiguration of interfacial energy band structure for high-performance inverted structure perovskite solar cells. 2019 , 10, 4593		130
389	Passivating contacts for crystalline silicon solar cells. 2019 , 4, 914-928		190

388	Current progress in electrode/pentacene interfaces of pentacene-based organic thin films transistors: A review. 2019 , 9, 691-703	1
387	High performance photoanodic catalyst prepared from an active organic photovoltaic cell - high potential gain from visible light. 2019 , 55, 12491-12494	6
386	Surface molecular doping of all-inorganic perovskite using zethrenes molecules. 2019 , 12, 77-84	12
385	Metal-doped organic aerogels for photocatalytic degradation of trimethoprim. 2019, 357, 120-128	12
384	Switchable Schottky Contacts: Simultaneously Enhanced Output Current and Reduced Leakage Current. 2019 , 141, 1628-1635	35
383	A method to discern voltage dependent internal photoemission component from photoconductivity content in spectral response of metal-organic semiconductor-metal devices and evaluate the interface barriers. 2019 , 65, 215-221	1
382	Controlled Enhancement in Hole Injection at Gold-Nanoparticle-on-Organic Electrical Contacts Fabricated by Spark-Discharge Aerosol Technique. 2019 , 11, 6276-6282	1
381	Effect of the Molecular Polarizability of SAMs on the Work Function Modification of Gold: Closedversus Open-Shell DonorAcceptor SAMs. 2019 , 4, 1800152	7
380	Theory of carrier accumulation in organic heterojunctions. 2019 , 65, 26-30	9
379	Exciting vibrons in both frontier orbitals of a single hydrocarbon molecule on graphene. 2019 , 31, 065001	6
378	Electroluminescence and contact formation of 1-(pyridin-2-yl)-3-(quinolin-2-yl)imidazo[1,5-a]quinoline thin films. 2019 , 65, 321-326	16
377	Metal nano-composite as charge transport co-buffer layer in perovskite based solar cell. 2019 , 126, 124-130	14
376	Interfaces of (Ultra)thin Polymer Films in Organic Electronics. 2019 , 6, 1800897	27
375	An ultraviolet photoelectron spectroscopy study on bandgap broadening of epitaxial graphene on SiC with surface doping. 2020 , 157, 340-349	4
374	Ultra-fast measurement circuit for transient space charge limited current in organic semiconductor thin films. 2020 , 31, 015901	
373	X-ray photoelectron spectroscopy: Towards reliable binding energy referencing. 2020 , 107, 100591	597
372	Selective deposition of silver and copper films by condensation coefficient modulation. 2020 , 7, 143-148	7
371	Long noncoding RNA (MEG3) in urinal exosomes functions as a biomarker for the diagnosis of Hunner-type interstitial cystitis (HIC). 2020 , 121, 1227-1237	8

370	Contact Resistance in Organic Field-Effect Transistors: Conquering the Barrier. 2020, 30, 1904576	121
369	Unusual Electrochemical Properties of Low-Doped Boron-Doped Diamond Electrodes Containing sp Carbon. 2020 , 142, 2310-2316	35
368	3D Negative Electronic Compressibility as a New Emergent Phenomenon. 2020 , 33, 229-239	3
367	Plasmonic Hot Hole Transfer in Gold Nanoparticle-Decorated Transition Metal Dichalcogenide Nanosheets. 2020 , 7, 197-202	15
366	Role of Molecular and Interchain Ordering in the Formation of a I-Hole-Transporting Layer in Organic Solar Cells. 2020 , 12, 3806-3814	6
365	Mechanism of Organic Solar Cell Performance Degradation upon Thermal Annealing of MoOx. 2020 , 3, 366-376	10
364	Surface modification of TiO2 layer with phosphonic acid monolayer in perovskite solar cells: Effect of chain length and terminal functional group. 2020 , 78, 105583	14
363	Highly Dispersive Nearly Free Electron Bands at a 2D-Assembled C60 Monolayer. 2020 , 124, 734-741	5
362	Effect of interfacial interaction on spin polarization at organic-cobalt interface. 2020, 78, 105567	6
361	Study on energy level bending at heterojunction of solution-processed phthalocyanine thin film and n-Si by Kelvin probe force microscopy. 2020 , 78, 105599	1
360	Angle-Resolved Photoemission Study on the Band Structure of Organic Single Crystals. 2020, 10, 773	1
359	In-Depth Investigation of the Correlation between Organic Semiconductor Orientation and Energy-Level Alignment Using In Situ Photoelectron Spectroscopy. 2020 , 12, 50628-50637	3
358	Effects of UV-ozone treatment on the electronic structures of F8BT and PFO polymeric thin films. 2020 , 20, 1359-1365	2
357	Non-noble-metal-based organic emitters for OLED applications. 2020 , 142, 100581	24
356	Final-State Simulations of Core-Level Binding Energies at Metal-Organic Hybrid Interfaces: Artifacts Caused by Spurious Collective Electrostatic Effects. 2020 , 5, 25868-25881	3
355	Effect of Electronically Distinct Aromatic Substituents on the Molecular Assembly and Hole Transport of V-Shaped Organic Semiconductors. 2020 , 124, 17503-17511	1
354	Carbon isotope effects in the artificial photosynthesis reactions catalyzed by nanostructured Co/CoO. 2020 , 754, 137731	1
353	Charge Transfer from Organic Molecules to Molybdenum Disulfide: Influence of the Fluorination of Iron Phthalocyanine. 2020 , 124, 16990-16999	13

(2020-2020)

352	The Role of Ag/Al Electrodes in the Improvement of PEDOT:PSS/P3HT:PCBM Solar Cells Performance. 2020 , 10, 1346-1352	2
351	Identifying Atomic-Level Correlation between Geometric and Electronic Structure at a Metal®rganic Interface. 2020 , 124, 17696-17701	2
350	Bottom Contact Metal Oxide Interface Modification Improving the Efficiency of Organic Light Emitting Diodes. 2020 , 13,	2
349	Piezoelectric PVDF-based sensors with high pressure sensitivity induced by chemical modification of electrode surfaces. 2020 , 316, 112424	3
348	Crack-Assisted Charge Injection into Solvent-Free Liquid Organic Semiconductors via Local Electric Field Enhancement. 2020 , 13,	O
347	Understanding coordination reaction for producing stable electrode with various low work functions. 2020 , 11, 3700	13
346	Observation of resistance switching in Vanadyl-phthalocyanine thin films. 2020, 269, 116524	2
345	Stability of radical-functionalized gold surfaces by self-assembly and on-surface chemistry. 2020 , 11, 9162-9172	7
344	Low band-gap polymer brushes: Influence of the end-group on the morphology of core-shell nanoparticles. 2020 , 155, 104700	3
343	Introduction to x-ray photoelectron spectroscopy. 2020 , 38, 063204	40
343	Introduction to x-ray photoelectron spectroscopy. 2020 , 38, 063204 The Potential of X-ray Photoelectron Spectroscopy for Determining Interface Dipoles of Self-Assembled Monolayers. 2020 , 10, 5735	3
	The Potential of X-ray Photoelectron Spectroscopy for Determining Interface Dipoles of	
342	The Potential of X-ray Photoelectron Spectroscopy for Determining Interface Dipoles of Self-Assembled Monolayers. 2020 , 10, 5735	3
342	The Potential of X-ray Photoelectron Spectroscopy for Determining Interface Dipoles of Self-Assembled Monolayers. 2020 , 10, 5735 Interfacial Dipole in Organic and Perovskite Solar Cells. 2020 , 142, 18281-18292	3 70
34 ² 34 ¹ 340	The Potential of X-ray Photoelectron Spectroscopy for Determining Interface Dipoles of Self-Assembled Monolayers. 2020, 10, 5735 Interfacial Dipole in Organic and Perovskite Solar Cells. 2020, 142, 18281-18292 Water/Ethanol Soluble p-Type Conjugated Polymers for the Use in Organic Photovoltaics. 2020, 7, Charge Energetics and Electronic Level Changes At the Copper(II) Phthalocyanine/Fullerene	3 70 1
342 341 340 339	The Potential of X-ray Photoelectron Spectroscopy for Determining Interface Dipoles of Self-Assembled Monolayers. 2020, 10, 5735 Interfacial Dipole in Organic and Perovskite Solar Cells. 2020, 142, 18281-18292 Water/Ethanol Soluble p-Type Conjugated Polymers for the Use in Organic Photovoltaics. 2020, 7, Charge Energetics and Electronic Level Changes At the Copper(II) Phthalocyanine/Fullerene Junction Upon Photoexcitation. 2020, 12, 42992-42996 Conductive Polymer Work Function Changes due to Residual Water: Impact of	3 70 1
342 341 340 339 338	The Potential of X-ray Photoelectron Spectroscopy for Determining Interface Dipoles of Self-Assembled Monolayers. 2020, 10, 5735 Interfacial Dipole in Organic and Perovskite Solar Cells. 2020, 142, 18281-18292 Water/Ethanol Soluble p-Type Conjugated Polymers for the Use in Organic Photovoltaics. 2020, 7, Charge Energetics and Electronic Level Changes At the Copper(II) Phthalocyanine/Fullerene Junction Upon Photoexcitation. 2020, 12, 42992-42996 Conductive Polymer Work Function Changes due to Residual Water: Impact of Temperature-Dependent Dielectric Constant. 2020, 6, 2000408	3 70 1 1 3

334	Solar Energy Harvesting with Photosynthetic Pigment-Protein Complexes. 2020,	О
333	Pump B robe X-ray Photoemission Reveals Light-Induced Carrier Accumulation in Organic Heterojunctions. 2020 , 124, 26603-26612	2
332	Energy-Level Alignment Tuning at Tetracene/c-Si Interfaces. 2020 , 124, 27867-27881	6
331	Substrate-Independent Energy-Level Pinning of an Organic Semiconductor Providing Versatile Hole-Injection Electrodes. 2020 , 2, 3994-4001	1
330	Charge carrier performance of phosphazene-based ionic liquids doped hole transport layer in organic light-emitting diodes. 2020 , 126, 1	7
329	Stacking Interactions of Poly Para-Phenylene Vinylene Oligomers with Graphene and Single-Walled Carbon Nanotubes: A Molecular Dynamics Approach. 2020 , 25,	1
328	The Impact of Atmosphere on Energetics of Lead Halide Perovskites. 2020 , 10, 2000908	8
327	Electric dipole of InN/InGaN quantum dots and holes and giant surface photovoltage directly measured by Kelvin probe force microscopy. 2020 , 10, 5930	6
326	Tuning the electron-deficient core of a non-fullerene acceptor to achieve over 17% efficiency in a single-junction organic solar cell. 2020 , 13, 2459-2466	199
325	Electronic Properties of 6,13-Diazapentacene Adsorbed on Au(111): A Quantitative Determination of Transport, Singlet and Triplet States, and Electronic Spectra. 2020 , 124, 13196-13205	5
324	Over What Length Scale Does an Inorganic Substrate Perturb the Structure of a Glassy Organic Semiconductor?. 2020 , 12, 26717-26726	9
323	Hole transport layers for organic solar cells: recent progress and prospects. 2020 , 8, 11478-11492	52
322	Controlling the Charge Transfer across Thin Dielectric Interlayers. 2020 , 7, 2000592	20
321	Analysis and comparison of total resistance models for accurate static modeling of long- and short-channel OTFTs produced with various organic materials. 2020 , 67, 180-192	2
320	Ion-Activated Greatly Enhanced Conductivity of Thin Organic Semiconducting Films in Two-Terminal Devices. 2020 , 6, 2000238	
319	On the Growth of Evaporated NaF on Phenyl-C61-butyric Acid Methyl Ester and Poly(3-hexylthiophene). 2020 , 124, 15140-15151	O
318	Band structure, work function and interfacial diagrams of oxygen-functionalized carbon nano-onions. 2020 , 266, 116434	5
317	Layer-Dependent Quasiparticle Electronic Structure of the P3HT:PCBM Interface from a First-Principles Substrate Screening GW Approach. 2020 , 124, 13592-13601	2

(2020-2020)

316	Recognition of M2 type tumor-associated macrophages with ultrasensitive and biocompatible photoelectrochemical cytosensor based on Ce doped SnO/SnS nano heterostructure. 2020 , 165, 112367	5
315	The Optical and Microstructural Characterization of the Polymeric Thin Films with Self-Assembly Nanoparticles Prepared by Spin-Coating Techniques. 2020 , 10, 390	1
314	Direct Electrical Measurements of Energy Bands in Organic Semiconductors by Device-Based Ballistic Carrier Emission Spectroscopy. 2020 , 124, 8806-8812	
313	Lightening up a Dark State of a Pentacene Derivative via N-Introduction. 2020 , 124, 7196-7204	4
312	Non-covalent interaction controlled 2D organic semiconductor films: Molecular self-assembly, electronic and optical properties, and electronic devices. 2020 , 75, 100481	14
311	Palladium forms Ohmic contact on hydrogen-terminated diamond down to 4 K. 2020 , 116, 111601	12
310	Improved performance of small molecule organic solar cells by incorporation of a glancing angle deposited donor layer. 2020 , 10, 5766	2
309	Charge Transfer into Organic Thin Films: A Deeper Insight through Machine-Learning-Assisted Structure Search. 2020 , 7, 2000992	17
308	Distinguishing strain, charge and molecular orbital induced effects on the electronic structure: graphene/ammonia system. 2020 , 32, 455501	1
307	Direct Printing of Asymmetric Electrodes for Improving Charge Injection/Extraction in Organic Electronics. 2020 , 12, 33999-34010	9
306	Nanoscale First-Principles Electronic Structure Simulations of Materials Relevant to Organic Electronics. 2020 , 89-131	1
305	Surface Ligands for Methylammonium Lead Iodide Films: Surface Coverage, Energetics, and Photovoltaic Performance. 2020 , 5, 799-806	31
304	Controlling Single Molecule Conductance by a Locally Induced Chemical Reaction on Individual Thiophene Units. 2020 , 132, 6266-6271	
303	Interface Engineering in Organic Field-Effect Transistors: Principles, Applications, and Perspectives. 2020 , 120, 2879-2949	92
302	Technical issues and integration scheme for graphene electrode OLED panels. 2020, 73-98	
301	Charge-Ordered Helical Polypeptide Monolayers on Au(111). 2020 , 124, 5734-5739	8
300	Heteromolecular Bilayers on a Weakly Interacting Substrate: Physisorptive Bonding and Molecular Distortions of Copper-Hexadecafluorophthalocyanine. 2020 , 12, 14542-14551	6
299	Impact of Substrate Rigidity on the Structure of Multilayer Nanoscale ITO Films: Implications for Flexible Electronic Devices. 2020 , 3, 2383-2392	2

298	Towards high-power-efficiency solution-processed OLEDs: Material and device perspectives. 2020 , 140, 100547		93
297	Theoretical exploration of the forces governing the interaction between gold-phthalocyanine and gold surface clusters 2020 , 10, 3895-3901		4
296	Carrier dynamic monitoring of a Econjugated polymer: a surface-enhanced Raman scattering method. 2020 , 56, 2779-2782		8
295	Controlling Single Molecule Conductance by a Locally Induced Chemical Reaction on Individual Thiophene Units. 2020 , 59, 6207-6212		4
294	p-Doping of a Hole Transport Material via a Poly(ionic liquid) for over 20% Efficiency and Hysteresis-Free Perovskite Solar Cells. 2020 , 3, 1393-1401		31
293	Auger Effect Assisted Perovskite Electroluminescence Modulated by Interfacial Minority Carriers. 2020 , 30, 1909222		18
292	Reduced interface energy loss in non-fullerene organic solar cells using room temperature-synthesized SnO2 quantum dots. 2020 , 52, 12-19		6
291	Air-Stable Inverted Organic Light-Emitting Diodes. 2020 ,		О
290	Carrier Injection Mechanism. 2020 , 33-48		
289	Interfacial Interaction of Absorbate Copper Phthalocyanine with PVDF Based Ferroelectric Polymer Substrates: A Spectroscopic Study. 2020 , 36, 4607-4618		3
288	Two-Stage Ultraviolet Degradation of Perovskite Solar Cells Induced by the Oxygen Vacancy-Ti States. 2020 , 23, 101013		34
287	Tuning the Ambipolar Character of Copolymers with Substituents: A Density Functional Theory Study. 2020 , 11, 3928-3933		4
286	Effect of interfacial dipoles on the attraction energy of geminate electron-hole pairs generated at the donor-acceptor interfaces. 2020 , 749, 137448		1
285	Self-Assembled Electret for Vibration-Based Power Generator. 2020 , 10, 6648		11
284	Phenomenological Prediction of the Band Diagram of Organic@rganic and Inorganic@rganic Heterointerfaces. 2021 , 6, 2000110		O
283	Interface Engineering in Organic Electronics: Energy-Level Alignment and Charge Transport. 2021 , 1, 2000015		17
282	Surface Termination of Solution-Processed CHNHPbI Perovskite Film Examined using Electron Spectroscopies. <i>Advanced Materials</i> , 2021 , 33, e2004981	24	15
281	Interface energetics in organic electronic devices. 2021 , 143-164		O

280	Prepare with care: Low contact resistance of pentacene Field-Effect transistors with clean and oxidized gold electrodes. 2021 , 89, 106030	1
279	Metal-organic interfaces in organic and unimolecular electronics. 2021 , 155-178	
278	Accurate vertical ionization energy and work function determinations of liquid water and aqueous solutions. 2021 , 12, 10558-10582	10
277	Doping of the hydrogen-passivated Si(100) electronic structure through carborane adsorption studied using density functional theory. 2021 , 23, 20379-20387	
276	Quantum Nuclei at Weakly Bonded Interfaces: The Case of Cyclohexane on Rh(111). 2021 , 4, 2000241	4
275	Temperature-programmed desorption of large molecules: influence of thin film structure and origin of intermolecular repulsion. 2021 , 13, 13816-13826	1
274	Electronic Tuning of Monolayer Graphene with Polymeric "Zwitterists". 2021 , 15, 2762-2770	11
273	Accumulated Charge Measurement: Control of the Interfacial Depletion Layer by Offset Voltage and Estimation of Band Gap and Electron Injection Barrier. 2021 , 125, 1990-1998	1
272	Light-Promoted Electrostatic Adsorption of High-Density Lewis Base Monolayers as Passivating Electron-Selective Contacts. 2021 , 8, 2003245	5
271	Electrical & Physical Characterization of Silicon-Organic Asymmetrical Metal Insulator Semiconductor Capacitive Test Structure. 1	1
270	Probing Bias-Induced Electron Density Shifts in Metal-Molecule Interfaces via Tip-Enhanced Raman Scattering. 2021 , 143, 1816-1821	2
269	Correlated Energy-Level Alignment Effects Determine Substituent-Tuned Single-Molecule Conductance. 2021 , 13, 4267-4277	5
268	Physically inspired deep learning of molecular excitations and photoemission spectra. 2021 , 12, 10755-10764	9
267	Structure and electronic structure of van der Waals interfaces at a Au(1 1 1) surface covered with a well-ordered molecular layer of n-alkanes. 2021 , 535, 147673	O
266	THE ELECTRONIC STRUCTURE AT ORGANICID MATERIAL HETEROINTERFACES. 2021 , 28, 2140003	
265	First-principles calculations of hybrid inorganic-organic interfaces: from state-of-the-art to best practice. 2021 , 23, 8132-8180	11
264	Review of Interface Passivation of Perovskite Layer. 2021 , 11,	8
263	Influence of Core Halogenation on the Electronic Structure of Naphthothiadiazole Derivatives. 2021 , 125, 6359-6366	1

262	Effect of contact resistance in organic field-effect transistors. 2021 , 2, 1661-1681	6
261	CdS/ZnS nanocomposite: synthesis and utilization in organic light-emitting diodes for a lower turn-on voltage. 2021 , 23, 1	1
260	Nonvolatile Voltage Controlled Molecular Spin-State Switching for Memory Applications. 2021 , 7, 37	7
259	Ambipolar and anti-ambipolar thin-film transistors from edge-on small-molecule heterostructures. 2021 , 542, 148616	2
258	Impact of gamma-ray irradiation on the electronic structures of PCBM and P3HT organic semiconductor films. 2021 , 186, 109518	5
257	References. 2021 , 183-189	
256	Kelvin probe force microscopy studies on the influence of hydrocarbon chain length on 1-alkene self-assembled monolayers on Si (111). 2021 , 60, SE1005	2
255	Effect of waiting time of indium tin oxide electrode in entry chamber on organic light-emitting diodes. 2021 , 78, 810-815	O
254	Perfluorinated Phthalocyanines on Cu(110) and Cu(110)-(2 🗓)O: The Special Role of the Central Cobalt Atom. 2021 , 125, 8803-8814	1
253	Active discovery of organic semiconductors. 2021 , 12, 2422	21
253 252	Active discovery of organic semiconductors. 2021, 12, 2422 Substrate temperature dependence of material, optical, and electronic properties of boron-doped ZnO thin films. 2021, 115, 111052	0
	Substrate temperature dependence of material, optical, and electronic properties of boron-doped	
252	Substrate temperature dependence of material, optical, and electronic properties of boron-doped ZnO thin films. 2021 , 115, 111052 The Impact of UV Photoelectron Spectroscopy on the Field of Organic Optoelectronics A	0
252 251	Substrate temperature dependence of material, optical, and electronic properties of boron-doped ZnO thin films. 2021, 115, 111052 The Impact of UV Photoelectron Spectroscopy on the Field of Organic Optoelectronics Retrospective. 2021, 9, 2100227 Type-I Energy Level Alignment at the PTCDA-Monolayer MoS Interface Promotes Resonance	0 2
252 251 250	Substrate temperature dependence of material, optical, and electronic properties of boron-doped ZnO thin films. 2021, 115, 111052 The Impact of UV Photoelectron Spectroscopy on the Field of Organic Optoelectronics Retrospective. 2021, 9, 2100227 Type-I Energy Level Alignment at the PTCDA-Monolayer MoS Interface Promotes Resonance Energy Transfer and Luminescence Enhancement. 2021, 8, 2100215	0 2 1
252 251 250 249	Substrate temperature dependence of material, optical, and electronic properties of boron-doped ZnO thin films. 2021, 115, 111052 The Impact of UV Photoelectron Spectroscopy on the Field of Organic Optoelectronics Retrospective. 2021, 9, 2100227 Type-I Energy Level Alignment at the PTCDA-Monolayer MoS Interface Promotes Resonance Energy Transfer and Luminescence Enhancement. 2021, 8, 2100215 Enhanced carrier injection hotspot effect by direct and simple ITO surface engineering. 2021, 118, 223301	0 2 1
252 251 250 249 248	Substrate temperature dependence of material, optical, and electronic properties of boron-doped ZnO thin films. 2021, 115, 111052 The Impact of UV Photoelectron Spectroscopy on the Field of Organic Optoelectronics Retrospective. 2021, 9, 2100227 Type-I Energy Level Alignment at the PTCDA-Monolayer MoS Interface Promotes Resonance Energy Transfer and Luminescence Enhancement. 2021, 8, 2100215 Enhanced carrier injection hotspot effect by direct and simple ITO surface engineering. 2021, 118, 223301 From 50 years of OLED Development to the Future. 2021, 141, 266-268	O 2 1 O

244	Reviving the "Schottky" Barrier for Flexible Polymer Dielectrics with a Superior 2D Nanoassembly Coating. <i>Advanced Materials</i> , 2021 , 33, e2101374	16
243	Ultraviolet Photoelectron Spectroscopy [Materials Science Technique. 2021 , 383-403	
242	Hot electron spectroscopy: A novel method to study molecular semiconductor. 2021 , 94, 106164	Ο
241	Spontaneous Orientation Polarization in Organic Light-Emitting Diodes and its Influence on Charge Injection, Accumulation, and Degradation Properties. 2021 , 273-293	
240	Lateral Interactions and Order D isorder Phase Transitions of Metal Phthalocyanines on Ag(111). 2021 , 125, 15623-15635	2
239	High-Performance Flexible Schottky DC Generator via Metal/Conducting Polymer Sliding Contacts. 2021 , 31, 2103132	8
238	Effect of Thermal Annealing on the Charge Carrier Selectivity of Ultra-Thin Organic Interface Dipoles in Silicon Organic Heterojunction Solar Cells. 2021 , 5, 2100466	1
237	Thickness-Insensitive Anode Interface Layer for High-Efficiency Organic Solar Cells. 2021 , 13, 39844-39853	1
236	Electronic structure analysis of nano-lens arrays. 2021 , 56, 17674-17681	
235	Energy-Level Alignment and Orbital-Selective Femtosecond Charge Transfer Dynamics of Redox-Active Molecules on Au, Ag, and Pt Metal Surfaces. 2021 , 125, 18474-18482	O
234	Electronic structures and optical characteristics of fluorescent pyrazinoquinoxaline assemblies and Au interfaces. 2021 , 11, 16978	О
233	The Many Facets of Molecular Orientation in Organic Optoelectronics. 2101004	7
232	On the Origin of Gap States in Molecular Semiconductors Combined UPS, AFM, and X-ray Diffraction Study. 2021 , 125, 17929-17938	О
231	Visualization of Frontier Molecular Orbital Separation of a Single Thermally Activated Delayed Fluorescence Emitter by STM. 2021 , 12, 7512-7518	5
230	Inorganic-organic interfaces in hybrid solar cells.	4
229	Visualization of Interfacial Band Bending in Photomultiplying Organic Photodetectors. 2021 , 21, 8474-8480	5
228	Electronic Properties of Tetraazaperopyrene Derivatives on Au(111): Energy-Level Alignment and Interfacial Band Formation. 2021 , 125, 19969-19979	
227	Effects of two different solvents on Schottky barrier of organic device. 2021 , 5, 095010	Ο

226	Degradation analysis of doped organic p-n heterojunction charge generation layers by impedance and optical spectroscopy. 2021 , 21, 100794	Ο
225	Reduction of Nonradiative Loss in Inverted Perovskite Solar Cells by Donor-EAcceptor Dipoles. 2021 , 13, 44321-44328	10
224	Evolution of the Ionization Energy in Two- and Three-Dimensional Thin Films of Pentacene Grown on Silicon Oxide Surfaces. 2021 , 12, 9407-9412	0
223	Engineering of Printable and Air-Stable Silver Electrodes with High Work Function using Contact Primer Layer: From Organometallic Interphases to Sharp Interfaces. 2106687	6
222	Charge Transfer Screening and Energy Level Alignment at Complex Organic-Inorganic Interfaces: A Tractable GW Approach. 2021 , 12, 8841-8846	1
221	Exploration of Gas-Liquid Interfaces for Liquid Water and Methanol Using Extreme Ultraviolet Laser Photoemission Spectroscopy. 2021 , 125, 10514-10526	2
220	Piezophototronic Effect Enhanced Perovskite Solar Cell Based on P(VDF-TrFE). 2100692	1
219	Quantitative amplitude-modulation scanning Kelvin probe microscopy via the second eigenmode excitation. 2021 , 230, 113399	Ο
218	Ultrasonic spray coating of polyethylenimine (ethoxylated) as electron injection and transport layer for organic light emitting diodes: The influence of layer morphology and thickness on the interface physics between polyethylenimine (ethoxylated) and the Al cathode.	
217	Efficiency of exciton dissociation at the interface between a conjugated polymer and an electron acceptor with consideration for a two-dimensional arrangement of interfacial dipoles. 2021 , 551, 111327	Ο
216	Polymer dielectrics sandwiched by medium-dielectric-constant nanoscale deposition layers for high-temperature capacitive energy storage. 2021 , 42, 445-453	16
215	Electronic structure engineering in organic thermoelectric materials. 2021 , 62, 204-219	8
214	Absolute work function measurement by using photoelectron spectroscopy. 2021 , 31, 52-59	5
213	Outstanding visible trans-to-cis photoinduced isomerization of fac-[Re(CO)3(dcbH2)(trans-stpy)]+ on thin TiO2 film. 2021 , 8, 100061	
212	Adsorption mechanism for tetracycline onto magnetic Fe3O4 nanoparticles: Adsorption isotherm and dynamic behavior, location of adsorption sites and interaction bonds. 2022 , 195, 110634	4
211	Dual interfacial modifications of an organic solar cell by self-assembled monolayers. 2022 , 422, 113554	
210	Confined Hot Electron Relaxation at the Molecular Heterointerface of the Size-Selected Plasmonic Noble Metal Nanocluster and Layered C. 2021 , 15, 1199-1209	5
209	Quantitative electronic structure and work-function changes of liquid water induced by solute. 2021 ,	3

(2001-2021)

208	Tunable built-in electric fields enable high-performance one-dimensional co-axial MoOx/MoON heterojunction nanotube arrays for thin-film pseudocapacitive charge storage devices. 2021 , 9, 13263-13270	2
207	Magnetism of Nanosized Nonmagneticl Materials; the Role of Defects (Review). 2021, 66, 1-24	1
206	High-Efficiency Red-Fluorescent Organic Light-Emitting Diodes with Excellent Color Purity. 2021 , 125, 1980-1989	4
205	Significant enhancement in quantum-dot light emitting device stability via a ZnO:polyethylenimine mixture in the electron transport layer.	2
204	Recent Progress and Challenges toward Highly Stable Nonfullerene Acceptor-Based Organic Solar Cells. 2021 , 11, 2003002	59
203	Electron Flow Through Molecular Structures. 2007 , 715-745	1
202	High-Sensitivity Electric Force Microscopy of Organic Electronic Materials and Devices. 2007, 788-830	9
201	Fabrication and Application of Plasmonic Silver Nanosheet. 2012 , 139-157	1
200	Adsorption of Cysteine on the Au(110)-surface: A Density Functional Theory Study. 2010 , 53-60	1
199	Theoretical Background of Electrochemical Analysis. 2013 , 5-18	13
198	Introduction. 2001 , 215-239	6
197	Semiconductor Aspects of Organic Bulk Heterojunction Solar Cells. 2003, 159-248	7
196	Vertical Bonding Distances Impact Organic-Metal Interface Energetics. 2015, 89-107	5
195	Micro organic light-emitting diodes fabricated through area-selective growth. 2017 , 1, 2606-2612	9
194	Solution-processable, high current efficiency deep-blue organic light-emitting diodes based on novel biphenyl-imidazole derivatives. 2020 , 8, 11239-11251	7
193	ECL Polymers and Devices. 2004 , 445-522	1
192	Energy Level Alignment at Organic-Metal Interfaces. 2001,	3
191	Organic Molecular Interfaces. 2001,	3

190	Photoelectron Spectroscopy of Interfaces for Polymer-Based Electronic Devices. 2001,	1
189	Role of Interfaces in Semiconducting Polymer Optoelectronic Devices. 2001,	3
188	Organic-Metal Interfaces. 2001,	2
187	Charge Transport and Injection in Amorphous Organic Semiconductors. 2009 , 61-109	2
186	Interface in Organic Semiconductor Devices. 2009 , 141-179	1
185	Spin-Polarized Transport in Organic Semiconductors. 2010 , 1-29	1
184	Photoelectron Yield Spectroscopy for Electronic Structures of Organic Electronic Materials and their Interfaces. 2007 , 28, 264-270	21
183	Elucidation and Control of Energy Level Alignment at Organic/Metal Interfaces. 2008, 29, 99-104	2
182	Distributions of Potential and Contact-Induced Charges in Conventional Organic Photovoltaics. 2020 , 13,	2
181	Interface Recombination & mp; Emission Applied to Explain Photosynthetic Mechanisms for (e] h+) Charges Beparation. 2012 , 02, 58-87	3
180	Surface Potential Change Depending on Molecular Orientation of Hexadecanethiol Self-Assembled Monolayers on Au(111). 2009 , 30, 1309-1312	7
179	p-Type Doping of Epitaxial Graphene by p-tert-Butylcalix[4]arene. 2010 , 31, 2809-2812	5
178	The Real Role of 4,4'-Bis[N-[4-{N,N-bis(3-methylphenyl)amino}phenyl]-N-phenylamino] biphenyl (DNTPD) Hole Injection Layer in OLED: Hole Retardation and Carrier Balancing. 2014 , 35, 929-932	5
177	Surface Potential Measurement of Tris(8-hydroxyquinolinato)aluminum and Bis[N-(1-naphthyl)-N-phenyl]benzidine Thin Films Fabricated on IndiumIIin Oxide by Kelvin Probe Force Microscopy. 2011 , 50, 071601	4
176	Adsorption of Phenylphosphonic Acid on Gold and Platinum Surfaces. 2011 , 50, 081606	3
175	Electronic Modification of C60Monolayers via Metal Substrates. 2011 , 50, 08LB06	5
174	Properties of Interface between Organic Hole-Transporting Layer and Indium Tin Oxide Anode Modified by Fluorinated Self-Assembled Monolayer. 2012 , 51, 035701	13
173	Electrostatic Properties of Organic Monolayers on Silicon Oxides Studied by Kelvin Probe Force Microscopy. 2012 , 51, 045702	1

172	Strong Fermi-level pinning at metal contacts to halide perovskites. 2021 , 9, 15212-15220	3
171	Probing polymer brushes with electrochemical impedance spectroscopy: a mini review. 2021 , 9, 7379-7391	5
170	A Critical Outlook for the Pursuit of Lower Contact Resistance in Organic Transistors. <i>Advanced Materials</i> , 2021 , e2104075	12
169	Colloidal Two-Dimensional Metal Chalcogenides: Realization and Application of the Structural Anisotropy. 2021 , 54, 3792-3803	4
168	Visualizing designer quantum states in stable macrocycle quantum corrals. 2021, 12, 5895	1
167	Heterointerface Engineering in Electromagnetic Absorbers: New Insights and Opportunities. Advanced Materials, 2021 , e2106195	43
166	Studies of Organic Thin Films and Interfaces by Various Electron Spectroscopies. 2001,	
165	Organic Light-Emitting Diodes Using Alkaline-Earth Fluorides as an Electron Injection Layer. 2001 ,	
164	Nanometric Electrostatic Phenomena at Molecular Interfaces. 2001,	
163	Molecular Control of Electron and Hole Injection at Electrodes and at Organic Layer Interfaces in Organic Electroluminescent Devices. 2001 ,	
162	A Theoretical Insight into Organic Interfaces in Electro-Optic Devices. 2001,	
161	Electronic Structure of Interfaces Between Organic Molecules and van der Waals Surfaces. 2001,	
160	Organic Electroluminescent Devices Control of Carrier Injection. 2002 , 13-24	
159	Nanoprecise Self-Assembly of Electro-Optic and Electroluminescent Molecular Arrays. 2003 , 241-263	2
158	Adsorption Structure and Work Function of N-Acetylglycine on Cu(110) Surface. 2006, 27, 380-385	
157	Electronic Structure of Organic Device Related Interfaces. 2007 , 50, 716-722	1
156	Interfacial Property of Metal/Nanotube Contacts in Carbon Nanotube Transistors. 2007, 28, 40-45	
155	?????????????. 2008 , 51, 351-356	

154	ULTRAFAST CHARGE TRANSFER ACROSS MOLECULE/METAL INTERFACES BY RESONANT PHOTOEMISSION SPECTROSCOPY. 2008 , 01, 89-104
153	MOLECULAR ORIENTATION AND ENERGY LEVEL ALIGNMENT AT THE CuPc/SAMs INTERFACE. 2008 , 01, 33-45
152	Interfaces in Organic Electronic DevicesNew Insights to Traditional Concepts. 2009 , 181-210
151	Device Physics and Material Science in Organic Transistors. 2010 , 53, 2-7
150	The molecular orientation and electronic structure of 3, 4, 9, 10-perylene tetracarboxylic dianhydride grown on Au(111). 2010 , 59, 1681
149	Implications of Interfacial Electronics to Performance of Organic Photovoltaic Devices. 2010 , 169-197
148	Electronic Structure of MetalMolecule Interfaces. 2010,
147	Organic-Metal Interface: Adsorption of Cysteine on Au(110) from First Principles. 2011 , 119-134
146	Contact Interface Engineering. 185-207
145	Photoelectron Spectroscopic Study of Energy Level Alignment at C12A7:e- / Alq3 Interfaces. 79-84
144	Mobility Improvement in C60-Based Field-Effect Transistors Using LiF/Ag Source/Drain Electrodes. 2011 , 50, 124203
143	Cysteine on Gold: An ab-initio Investigation. 2012 , 105-117
142	Charge Injection Enhanced by Guest Material in Molecularly Doped Liquid Crystalline Thin Films. 2012 , 51, 011701
141	The influence of modified electrodes by V2O5 film on the performance of ambipolar organic field-effect transistors based on C60/Pentacene. 2012 , 61, 218502
140	Observation of n-Type Conduction in Carbon Nanotube Field-Effect Transistors with Au Contacts in Vacuum. 2012 , 51, 02BN06
139	A Study on the Electron Transfer at the Alq3/Ba and Alq3/Au Interfaces by NEXAFS Spectroscopy. 2012 , 45, 15-19
138	Device Simulation of Ditch and Elevated Electrode Structures in Organic Thin-Film Transistors. 2012 , 51, 024303
137	Molecules on Semiconductors. 2012 , 367-396

(2016-2012)

136	Electron Injection Mechanisms Varied by Conjugated Polyelectrolyte Electron Transporting Layers in Polymer Light-Emitting Diodes. 2012 , 36, 519-524
135	Further Developments in IDIS Model. 2013 , 63-93
134	Density functional theory for the description of charge-transfer processes at TTF/TCNQ interfaces. 2014 , 217-224
133	General Introduction. 2013 , 1-16
132	Poly(triphenylamine)-based composites for high-speed photorefractive response time. 2013,
131	Correlating Electronic and Geometric Structures of Organic Films and Interfaces by Means of Synchrotron Radiation Based Techniques. 2013 , 56, 11-17
130	Effect of Switching on Metal-Organic Interface Adhesion Relevant to Organic Electronic Devices. 2013 , 03, 299-306
129	Electrostatic and Thermodynamic Potentials of Electrons in Materials. 2014, 11-44
128	Conductance of a Single Molecule Junction Formed with Ni, Au, and Ag Electrodes. 2014 , 58, 513-516
127	Charge Transport Study of OPV Polymers and Their Bulk Heterojunction Blends by Admittance Spectroscopy. 2015 , 43-65
126	Interface Control of Organic Devices by using Self-Assembled Monolayers. 2015 , 135, 140-145
125	In situ photoemission and inverse photoemission studies on the interfacial electronic structures of organic materials. 2015 , 2, 4-11
124	Probing the Molecular Orientation of ZnPc on AZO Using Soft X-ray Spectroscopies for Organic Photovoltaic Applications. 2015 , 24, 151-155
123	Photoelectrochemical Reactions at Phthalocyanine Electrodes. 2016 , 263-314
122	Chapter 10:Small Molecule Organic Solar Cells. 2016 , 332-366
121	Adsorption Site Recognition in Single Molecular Junctions Spectroscopy. 2016 , 37, 288-293
120	Chapter 11:Modeling Organic Solar Cells: What are the Challenges Ahead?. 2016 , 367-390
119	Organic Semiconductors. 2016 , 311-352

118	Fundamentals. 2017 , 7-45	
117	CHAPTER 8:Applications of Ionic Liquids in Organic Electronic Devices. 2017 , 196-233	
116	Post-Functionalization of Room-Temperature Ferromagnetic Nanoparticle via Surface Modification. 2017 , 38, 30-34	
115	Chemical Functionalization and Charge Carrier Delocalization at a Hybrid Organic/Inorganic Semiconductor Interface. 2018 , 560-572	
114	Future Directions. 2020 , 157-166	
113	How much does surface polymorphism influence the work function of organic/metal interfaces?. 2021 , 575, 151687	1
112	Charge Transfer in Molecular Materials. 2020 , 227-257	1
111	Air Stability for Organic Light-Emitting Diodes. 2020 , 1-4	
110	Role of Band-Structure Approach in Biohybrid Photovoltaics Path Beyond Bioelectrochemistry. 2020 , 79-110	
109	Physics and Design Principles of OLED Devices. 2020 , 1-73	О
109	Physics and Design Principles of OLED Devices. 2020 , 1-73 Plasmonic nanostructures of SnO2:Sb thin film under gamma radiation response. 2020 , 38, 62-72	0
108	Plasmonic nanostructures of SnO2:Sb thin film under gamma radiation response. 2020 , 38, 62-72 Elucidation of hole transport mechanism in efficient energy cascade organic photovoltaics using	1
108	Plasmonic nanostructures of SnO2:Sb thin film under gamma radiation response. 2020 , 38, 62-72 Elucidation of hole transport mechanism in efficient energy cascade organic photovoltaics using triple donor system. 2021 , 151747 Oxygen Plasma Treatment of Rear Multilayered Graphene: A Potential Top Electrode for	0
108 107 106	Plasmonic nanostructures of SnO2:Sb thin film under gamma radiation response. 2020 , 38, 62-72 Elucidation of hole transport mechanism in efficient energy cascade organic photovoltaics using triple donor system. 2021 , 151747 Oxygen Plasma Treatment of Rear Multilayered Graphene: A Potential Top Electrode for Transparent Organic Light-Emitting Diodes. 2021 , 14,	0
108 107 106	Plasmonic nanostructures of SnO2:Sb thin film under gamma radiation response. 2020, 38, 62-72 Elucidation of hole transport mechanism in efficient energy cascade organic photovoltaics using triple donor system. 2021, 151747 Oxygen Plasma Treatment of Rear Multilayered Graphene: A Potential Top Electrode for Transparent Organic Light-Emitting Diodes. 2021, 14, Photoelectrons Spectroscopy of Organized Organic Thin Films. 2004, 69-82	0
108 107 106 105	Plasmonic nanostructures of SnO2:Sb thin film under gamma radiation response. 2020, 38, 62-72 Elucidation of hole transport mechanism in efficient energy cascade organic photovoltaics using triple donor system. 2021, 151747 Oxygen Plasma Treatment of Rear Multilayered Graphene: A Potential Top Electrode for Transparent Organic Light-Emitting Diodes. 2021, 14, Photoelectrons Spectroscopy of Organized Organic Thin Films. 2004, 69-82 NANOSCALE STUDIES ON METAL-ORGANIC INTERFACES. 2007, 9-21 Device-Oriented Studies on Electrical, Optical, and Mechanical Properties of Individual Organic	0

100	Rationalizing energy level alignment by characterizing Lewis acid/base and ionic interactions at printable semiconductor/ionic liquid interfaces. 2021 ,	
99	Understanding the synergistic effect of CO2, H2S and fluid flow towards carbon steel corrosion. 2022 , 196, 110790	1
98	Can We Predict Interface Dipoles Based on Molecular Properties?. 2021 , 6, 32270-32276	3
97	Correlation of Changes in Electronic and Device Properties in Organic Photovoltaic with Exposure to Air. 2101657	1
96	Measuring Energy Gaps of Organic Semiconductors by Electron Energy Loss Spectroscopies. 2022 , 259, 2100459	3
95	Thermal and non-thermal equilibrium processes of charge extraction in accumulated charge measurement (ACM). 2021 , 130, 195501	
94	High Speed Response Organic Photodetectors with Cascade Buffer Layers. 2100539	1
93	Hole injection improvement using ultrathin Li-TFSI layer in organic light-emitting diodes. 2021 , 79, 961-965	
92	Metal oxide charge transfer complex for effective energy band tailoring in multilayer optoelectronics 2022 , 13, 75	Ο
91	A novel energy level detector for molecular semiconductors 2022,	
90	Metal phthalocyanines and their composites with carbon nanostructures for applications in energy generation and storage. 2022 , 401-448	1
89	Influence of N-introduction in pentacene on the electronic structure and excited electronic states 2022 ,	O
88	A review of sodium chloride-based electrolytes and materials for electrochemical energy technology. 2022 , 10, 2637-2671	3
87	Mechanoresistive single-molecule junctions 2022,	2
86	Effects of Surface Contaminants on Interface Dipole Formation of 8-hydroxyquinolinolato-lithium Layer. 2022 , 31, 12-14	
85	Small-molecule ambipolar transistors 2022 ,	3
84	Manipulating Ion Migration and Interfacial Carrier Dynamics via Amino Acid Treatment in Planar Perovskite Solar Cells 2022 ,	1
83	Hexacene on Cu(110) and Ag(110): Influence of the Substrate on Molecular Orientation and Interfacial Charge Transfer 2022 , 126, 5036-5045	1

82	Ligand-Induced Tuning of the Electronic Structure of Rhombus Tetraboron Cluster 2022, e202200060	О
81	Surface potential and local conductivity measurements of micropatterned aromatic monolayers covalently attached to n-Si(111) via Si-C and Si-O bonds.	
80	OrganicIhorganic Hybrid Interfaces for Spin Injection into Carbon Nanotubes and Graphene. 2100166	
79	Perylene-diimide-based cathode interlayer materials for high performance organic solar cells.	6
78	Carrier-selective contacts using metal compounds for crystalline silicon solar cells.	5
77	Electron-assisted deposition and interface control of naphthalenediimide derivative thin films. 2022 , 61, SE1013	
76	Unveiling the Energy Alignment across Ultrathin 4P-NPD Hole Extraction Interlayers in Organic Solar Cells.	1
75	Passivation effect of NTCDA nanofilm on black phosphorus. 2022 , 36, 105466	
74	The effect of carbonyl defect on the electrode injection characteristics of polytetrafluoroethylene film capacitor. 2022 , 8, 599-606	O
73	Optical Imaging of Redox and Molecular Diffusion in 2D van der Waals Space 2021 ,	1
72	Hybrid Organic-2D TMD Heterointerfaces: Towards Devices Using 2D Materials. 2022 , 171-198	
71	Piezoelectricity in Monolayer and Multilayer Ti3C2Tx MXenes: Implications for Piezoelectric Devices. 2022 , 5, 1034-1046	3
70	Thickness-Dependent Energy-Level Alignment at the Organic Interface Induced by Templated Gap States. 2022 , 9, 2101382	1
69	Monolayer-Induced Changes in Metal Penetration and Wetting for Metal-on-Organic Interfaces. 2021 , 33, 9515-9523	
68	Opportunities for energy level tuning at inorganic/organic semiconductor interfaces. 2021 , 119, 260501	2
67	Anomalous Interfacial Electronic Structure of Solid Films of Non-Planar Econjugated Molecule 6-Cycloparaphenylene. 2200242	O
66	Data_Sheet_1.docx. 2020 ,	
65	Resolution of Intramolecular Dipoles and a Push-Back Effect of Individual Molecules on a Metal Surface. 2022 , 126, 7667-7673	

64	Role of Adatoms for the Adsorption of F4TCNQ on Au(111) 2022, 126, 7718-7727	
63	Overall Enhanced Performance of Polymer Photodetectors by Co-Modifying ITO with PEIE and ZnO.	O
62	On the Role of Collective Electrostatic Effects in Electronic Level Pinning and Work Function Changes by Molecular Adlayers: The Case of Partially Fluorinated DNTTs Adsorbed Flat-Lying on Various Metals and Hetero-Structures. 2200361	
61	Electron affinities of small-molecule organic semiconductors: Comparison among cyclic voltammetry, conventional inverse photoelectron spectroscopy, and low-energy inverse photoelectron spectroscopy. 2022 , 106551	О
60	Hole-injection barrier across the intermolecular interaction mediated interfacial DNTT layer. 2022 , 597, 153696	0
59	Structure and electronic states of strongly interacting metal-organic interfaces: CuPc on Cu(100) and Cu(110). 2022 , 723, 122126	1
58	Spontaneous formation of metastable orientation with well-organized permanent dipole moment in organic glassy films.	5
57	Self-Assembly of a Triphenylene-Based Electron Donor Molecule on Graphene: Structural and Electronic Properties.	
56	A transferable prediction model of molecular adsorption on metals based on adsorbate and substrate properties.	1
55	Modeling of thickness-dependent energy level alignment at organic and inorganic semiconductor interfaces. 2022 , 131, 245501	
54	Conductance Switching in Liquid Crystal-Inspired Self-Assembled Monolayer Junctions. 2022, 14, 31044-3105	i 3 o
53	Double Heterojunction Crystalline Silicon Solar Cells: From Doped Silicon to Dopant-Free Passivating Contacts. 2022 , 9, 477	
52	A step-by-step guide to perform x-ray photoelectron spectroscopy. 2022 , 132, 011101	8
51	The Energy Level Conundrum of Organic Semiconductors in Solar Cells. <i>Advanced Materials</i> , 2202575 24	6
50	Substrate roughness influence on the order of nanografted Self-Assembled Monolayers. 2022 , 803, 139819	
49	Ultrafast Exciton Dynamics and Charge Transfer at PTCDA/Metal Interfaces.	
48	Understanding interfacial energy structures in organic solar cells using photoelectron spectroscopy: A review. 2022 , 132, 050701	О
47	Interface energetics make devices. 2022 , 4, 034003	О

46	Directional Manipulation of Electron Transfer by Energy Level Engineering for Efficient Cathodic Oxygen Reduction. 2022 , 22, 6622-6630	O
45	Interface dipole at nickel oxide surface to enhance the photovoltage of perovskite solar cells. 2022 , 652, 129788	O
44	Flexible solar and thermal energy conversion devices: Organic photovoltaics (OPVs), organic thermoelectric generators (OTEGs) and hybrid PV-TEG systems. 2022 , 29, 101614	0
43	Engineered Nanomaterials by designItheoretical studies experimental validations current and future prospects. 301-364	O
42	In situ work function measurements of W, WO3 nanostructured surfaces. 2022 , 447, 128870	O
41	Observation of Hole States at Perylene/Au(110) and Au(111) Interfaces. 2022, 126, 15971-15979	1
40	Polarization-Induced Exciton P olaron Quenching in Organic Light-Emitting Devices and Its Control by Dipolar Doping. 2201348	1
39	Regulation of Interfacial Polarization and Local Electric Field Strength Achieved Highly Energy Storage Performance in Polyetherimide Nanocomposites at Elevated Temperature via 2D Hybrid Structure. 2022 , 9, 2201100	1
38	Injection-limited and space chargeIlmited currents in organic semiconductor devices with nanopatterned metal electrodes.	1
37	Semiconductor Halogenation in Molecular Highly-Oriented Layered pfi (nf) Junctions. 2208507	O
36	Comprehending of the reverse effect of Cliconcentration and fluid flow on pitting corrosion of carbon steel. 2022 , 206, 111547	0
35	Durable flexible direct current generation through the tribovoltaic effect in contact-separation mode.	2
34	Molecular Beam Epitaxy Ibn Organic Semiconductor Single Crystals: Characterization of Well-Defined Molecular Interfaces by Synchrotron Radiation X-ray Diffraction Techniques. 2022 , 15, 7119	0
33	Advanced characterization of organic-metal and organic-organic interfaces: From photoelectron spectroscopy data to energy-level diagrams.	1
32	Selective and moisture-sensitive degradation of bromocresol green for isostructural MOFs assembled with D-camphorate and bipyridine. 2022 , 146, 110044	0
31	Measurement Techniques of Thermoelectric-related Performance. 2022 , 319-366	O
30	Developing a built-in electric field in CdS nanorods by modified MoS2 for highly efficient photocatalytic H2O2 production. 2022 ,	1
29	Significant Lifetime Enhancement in QLEDs by Reducing Interfacial Charge Accumulation via Fluorine Incorporation in the ZnO Electron Transport Layer. 2022 , 14,	1

28	Enhancement of electronic effects at a Biomolecule- Inorganic Interface by Multivalent Interactions.	O
27	On the evolution of oxidative etching of few layer graphene (FLG) in FLG /TiO2 nanocomposites. Interfacial dipole signature and chemical shift in C1s X-ray photoemission spectra. 2023 , 36, 102510	O
26	Chemical approaches for electronic doping in photovoltaic materials beyond crystalline silicon. 2022 , 51, 10016-10063	0
25	Impact of Connectivity on the Electronic Structure of N-Heterotriangulenes.	O
24	Increasing Electrode Work Function Using a Natural Molecule. 2201800	0
23	Topological surface state of Bi2Se3 modified by physisorption of n-alkane.	O
22	Engineered molecular stacking crystallinity of bar-coated TIPS-pentacene/polystyrene films for organic thin-film transistors. 2023 , 13, 2700-2706	0
21	Carbon Nanodots as Electron Transport Materials in Organic Light Emitting Diodes and Solar Cells. 2023 , 13, 169	O
20	A tunable single-molecule light-emitting diode with single-photon precision. 2209750	О
19	Tuning the carrier injection barrier of hybrid metal@rganic interfaces on rare earth-gold surface compounds.	O
18	Self-assembled discotics as molecular semiconductors.	1
17	An Installed Hybrid Direct Expansion Solar Assisted Heat Pump Water Heater to Monitor and Modeled the Energy Factor of a University Students (Accommodation. 2023 , 16, 1159	O
16	Solution-Processed OLEDs for Printing Displays.	О
15	Coverage-Dependent Modulation of Charge Density at the Interface between Ag(001) and Ruthenium Phthalocyanine.	O
14	Lattice-matched heteroepitaxial preparation of InSb/CdTe on Si (111) substrate by magnetron sputtering. 2023 , 212, 112010	О
13	The effect of terminal group of hole injection self-assembled monolayers on the performance of optoelectronic devices on ITO anodes. 2023 , 301, 127666	O
12	On analysis of optical and impedance spectroscopy properties of nickel tetraphenyl porphyrin nanostructure /ITO Schottky diodes. 2023 , 660, 414900	O
11	Enhancement in Power Conversion Efficiency of Perovskite Solar Cells by Reduced Non-Radiative Recombination Using a Brij C10-Mixed PEDOT:PSS Hole Transport Layer. 2023 , 15, 772	O

10	Near-ultraviolet organic light emitting diodes using melem. 2023, 815, 140367	O
9	Structural characterization and electronic properties of Ni/rubrene bilayers with alternative stacking sequences. 2023 , 25, 7927-7936	o
8	Doping in Organic Semiconductors. 2023 , 31-40	o
7	Hole Doping to Perylene on Au(110): Photoelectron Momentum Microscopy. 2023 ,	O
6	Niobium-Carbide MXene Modified Hybrid Hole Transport Layer Enabling High-Performance Organic Solar Cells Over 19%. 2207505	0
5	Chemical Defects and Energetic Disorder Impact the Energy-Level Alignment of Functionalized Hexaazatriphenylene Thin Films.	o
4	Polymorphism mediated by electric fields: a first principles study on organic/inorganic interfaces. 2023 , 5, 2288-2298	0
3	Effect of ground state charge transfer and photoinduced charge separation on the energy level alignment at metal halide perovskite/organic charge transport layer interfaces. 2023 , 129,	o
2	Morphology of Organic/Metal Interface and Photocurrent Multiplication Behaviors. 2023, 49-72	0
1	Probing transport energies and defect states in organic semiconductors using energy resolved electrochemical impedance spectroscopy.	O